BROOD-DEPENDENT MORPHOLOGY, BEHAVIOR, AND BIOPHYSICAL INTERACTIONS AMONG BLUE CRAB (*CALLINECTES SAPIDUS*) ZOEAE

By

JOSEPH CHARLES CARACAPPA JR.

A dissertation submitted to the

School of Graduate Studies

Rutgers, The State University of New Jersey

In partial fulfillment of the requirements

For the degree of

Doctor of Philosophy

Graduate Program in Oceanography

Written under the direction of

Daphne Munroe

And approved by

_____

_____

_____

_____

_____

New Brunswick, New Jersey

October, 2019

ABSTRACT OF THE DISSERTATION

Brood-dependent Morphology, Behavior, and Biophysical Interactions among Blue Crab (*Callinectes sapidus*) Zoeae

By JOSEPH CHARLES CARACAPPA JR.

Dissertation Director:

Daphne Munroe

The goal of this dissertation is to provide a better understanding of the intraspecific variability in morphology and swimming behavior, as well as some of the implications of such variation, in early stage *Callinectes sapidus* zoeae. A long-standing body of work has demonstrated that zoeal morphology is not constant, and morphological features can have an important role in survival and behavior. Additionally, given the presence in brood-dependent morphology in other species and the susceptibility of blue crab life history to generate maternal effects, the presence and magnitude of differences among larval broods should be addressed. In the second chapter, variation in *C. sapidus* zoeal morphology among several larval broods was identified, and used to test whether brood-dependent morphology is present. This experiment involved hatching several broods, making measurements using microscope photography, and image analysis. Simple models of swimming-induced drag and passive sinking velocity were used to create an index of vertical swimming efficiency. Results discussed in Chapter 2 demonstrate that morphology can vary significantly between broods, and these differences can translate to differing

swimming efficiency. In the third chapter, larvae from the same broods described in Chapter 2 were followed further into development to investigate how brood-level morphological differences change over development. By the time of their second molt, broods of zoeae retain most differences in morphological size and shape, but shape difference decrease. These results suggest that over time, brood effects can persist, but there is a detectible morphological convergence, and differences in swimming efficiency are still present. Chapter four tested whether the brood-dependent morphology discussed in the prior chapters translated to similar differences in swimming behavior. Using mesocosm video observations, significant differences in the swimming velocity, orientation, and path straightness of larval broods was confirmed. Despite these differences, distinct modes of behavior that were conserved across broods were observed. These represent differences in swimming behavior within broods either between individuals or over time. In the fifth chapter, simulations were used to test whether the observed brood-dependent behavior and morphology can translate to differences in larval transport. A simplified model of a wind-driven estuarine plume with a sheared current was used, along with observed brood-depending swimming and sinking behaviors, to model larval transport. Model results showed brood-dependent and behaviorally-driven larval transport, where faster-swimming broods of larvae are more able to counter wind-driven vertical mixing and stay in surface waters. Likewise, the type of depth-regulation zoeae use can influence how they are transported. Overall, this dissertation finds that morphological and behavioral traits can differ substantially between larval broods. These results suggest that there may be differential success of larvae from different broods. I recommend that future work could focus on identifying maternal or environmental

predictors of larval condition. Additionally, future models of *C. sapidus* larval dispersal should incorporate observed behavior and its variability.

Acknowledgements

I would like to thank the Department of Marine and Coastal Sciences for continual support and providing opportunities as a Teaching Assistant and Graduate Assistant throughout. Partial funding for this dissertation was also provided by the National Shellfisheries Associations' George R Abbe Student Research Grant and Manasquan River Marlin and Tuna Club's George Burlew Scholarship.

Thanks to the exceptional advisement of Dr. Daphne Munroe, I was able to effectively conduct, analyze, publish, and present my research across several opportunities. I would not have been able to complete this dissertation without her encouragement and guidance. I feel that she has prepared me to be a capable and critical scientist, and I am greatly appreciative.

My committee was central to my ability to formulate my ideas, focus my research, and effectively communicate the results. Thus I would like to thank Dr. Robert Chant, Dr. Heidi Fuchs, Dr. Paul Jivoff, and Dr. Paola López-Duarte for their frequent advice and guidance throughout my dissertation.

I received a tremendous amount of support and assistance from the faculty and staff at the Haskin Shellfish Research Laboratory. This included the use of laboratory space and supplies, as well as organism collection and care. Specifically, I would like to thank Dr. David Bushek, Iris Burt, Nadja DiMartino, Jenn Gius, Emily McGurk, Jenny Shin, Caiti Czaijkowski, and Jared Bianchismak for all of their help. The New Jersey Department of Environmental Protection, specifically Craig Tomlin and Andrew Hassel, were crucial in supplying study organism.

I was lucky enough to work among a fantastic team of graduate students, who helped shape how I approached my research and who provided moral, intellectual, and practical support throughout my time as a graduate student. Thank you to Michael Acquafredda, Sarah Borsetti, Dr. Christopher Free, Dr. Jason Morson, and Jessica Valenti.

Finally, I would not be here today without an amazing family. To my wife, Marta Caracappa, for her support, patience, and sacrifice. To my parents, Joseph and Linda Caracappa for a lifetime of love and encouragement and fostering an early interest in science, and to my siblings Alex and Leanna Caracappa for their help and support.

Dedication

To my parents Joe and Linda and my wife Marta for their unceasing support and encouragement

Table of Contents

List of Tables

List of Figures

Chapter 1: Introduction

1.1 Blue Crab Early Life History

1.1.1 Reproduction and Egg Development

Blue crabs *Callinectes sapidus* inhabit coastal and estuarine waters from the mid-Atlantic, USA to the Gulf of Mexico, to Brazil (McMillen-Jackson and Bert 2004). However, unless stated otherwise, this dissertation will primarily focus on populations in the mid-Atlantic coast, particularly within the Delaware Bay and Chesapeake Bay estuarine system. Here, adult blue crabs mainly live within brackish estuarine waters and are more rarely found offshore. Adult male crabs seek out and guard females just prior to their terminal molt, during the summer (van Engel 1958). Once molted, the male deposit spermatophores into the soft female, where they are stored until egg generation begins (Jivoff et al. 2007). Females will only mate once over their lifetimes, and any subsequent clutches will be fertilized from the stored spermatophores. The majority of females only mate with one male, though up to 12% have been observed to mate with multiple males (Jivoff et al. 2007). Once mating is complete, females will then migrate towards the mouth of their estuaries and bury themselves in the sediment to overwinter (van Engel 1958).

When emerging the following spring, females begin to develop their egg mass (or brood). Eggs are extruded from the female, inseminated on the way, and deposited along hair-like filaments which are attached to swimmerets beneath the abdomen. These young eggs are orange in appearance, as they are mostly yolk at this stage. As the embryos develop and the tissues differentiate, eggs begin to darken towards brown. Once near full-development, eggs are visually black, and large eye-spots are visible under magnification.

Within 24-48 hours of hatching, embryos show signs of movement, and a heart-beat can be seen. The length of egg development varies from 12-17 days and is dependent on temperature, where warmer temperatures accelerate development (Costlow and Bookhout 1959). Temperatures from 26-30 ºC provide reliable hatching rates (Millikin 1978). Low salinities can cause premature hatching and deformation in larvae, so laboratory experiments typically culture eggs at 30 ppt. During egg development, eggs can become unviable due to infections of a fungus *Lagenidium Callinectes* (Umphlett and Mccray 1975) and a nemertean *Carcinonemertes carcinophila* (Millikin 1978), both of which often come along with the adult female.

1.1.2 Larval Development and Culture

Blue crab larvae (zoeae) develop through discrete molt stages with distinct morphological changes. A thorough summary of all larval stages can be found in Costlow and Bookhout's study (1959), which was one of the first to complete larval development for blue crabs in the laboratory and provides a good characterization of each stage. Zoeae generally go through 8 molt stages before metamorphosis into megalopae. Each stage can be identified using particular morphological characteristics, usually by the setation on appendages or the presence of new appendages (Table 1-1). However, molt stages exhibit substantial morphological variability, with some morphologies being combinations of two traditional stages or some intermediate (Costlow 1965). Such variation can make proper identification of zoeal stages in wild sampling particularly difficult.

While larval development is typically characterized as lasting 30 days, it can vary considerably depending on rearing conditions. While Costlow and Bookhout (1959) found zoeae metamorphosing to megalopae in around 45 days, a more recent study by Zmora et

al. (2005) found a substantially abbreviated development, with metamorphosis around 26 days (Figure 1-1). The large difference between both of these laboratory studies was likely due to advancements in rearing methods, nutrition, as well as environmental conditions. Blue crab larvae are cannibalistic in laboratory cultures (Millikin 1978), which is common among other species' zoeae (Anger 2001). However, high density cultures can still reach metamorphosis by maintaining good water quality and proper nutrition (Zmora et al. 2005).

Not much is known about the prey of wild populations of *C. sapidus* zoeae. Early culture studies attempted to identify cost-effective food sources that could sustain zoeal development, but diets on a single species were unlikely to bring zoeae through metamorphosis, with the exception of *Artemia* and *Hydroides* larvae (Sulkin 1975b). The most successful large-scale cultures (~40 % survival to megalopae) use a tiered diet, with the gradual addition of new prey species (Rotifers, *Artemia* nauplii, and copepods) as zoeae develop (Zmora et al. 2005). However, this feeding regimen requires the culturing of additional live animals, increasing the complexity of the overall process.

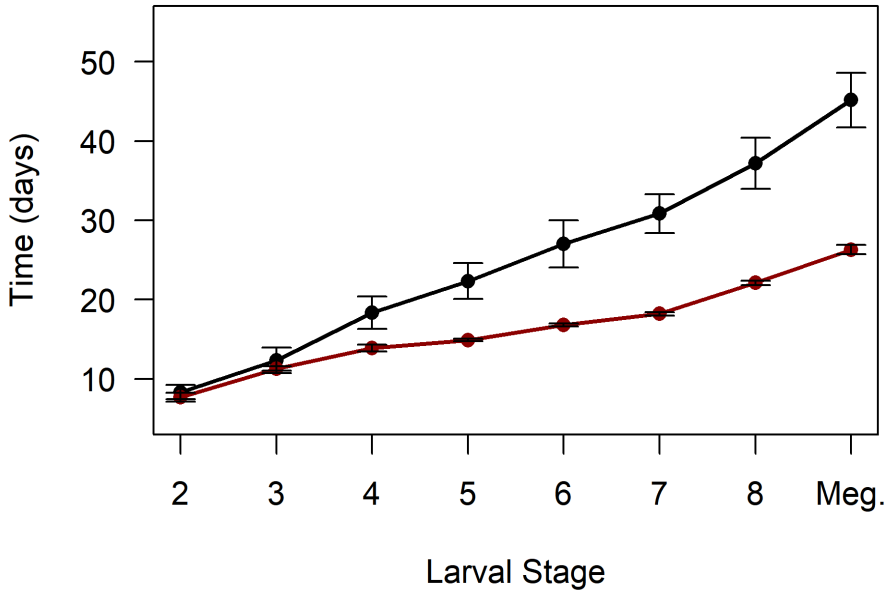

Figure 1-1 *Development time for each larval stage and megalopae as documented by Costlow & Bookhout (1959; black line) and Zmora et al. (2005; red line). Error bars represent one standard error.*

Larval development is also sensitive to environmental conditions. Eggs that develop in low salinity may prematurely hatch into pre-zoeae (Sandoz et al. 1944). Pre-zoeae are an under-developed larvae, and while morphologically distinct from first stage zoeae, they will not molt into one. Optimal salinity for larval rearing is from 26-30 ppt (Millikin 1978), with an optimal temperature of 22-25 ºC (Sulkin and Epifanio 1975; Zmora et al. 2005). Zoeae reared in warmer or lower salinity conditions do not often reach metamorphosis (Costlow and Bookhout 1959).

Table 1-1: Summary of staging criteria from Costlow & Bookhout, 1959. Numbers refer to the setation on each appendage from interior to exterior, except for the telson column, which refers to the number of spines.

Stage	Maxillule	Maxilla	1st Setae	2nd Setae	1st maxilliped	2nd maxilliped	Misc.
Z1	6,5,6	6,8,6,5	4	4	2,2,0,2,5	1,1,4	Eyes Unstalked
Z2	7,7,6,1	6,8,6,7	6	6	2,2,1,2,5	1,1,5	Eyes Stalked
Z3	7,8,6,1	7,9,6,12	8	8	2,2,1,2,6	1,1,5	6th abdominal segment
Z4	8,11,6,1	7,10,6,15	9	9	2,2,1,2,6	1,1,5	Segmented antenna, setae on cephalothorax
Z5	8,11,6,1	8,10,6,20	9	11	2,2,1,2,6	1,1,5	Budding of antenna
Z6	9,11,6,1	8,13,6,25	11	12	2,2,1,2,6	1,1,5	Pleopod buds
Z7	9,17,6,1	10,14,6,29	14	13	2,2,1,2,6	1,1,5	Longer antenna bud, chelae formed
Z8	15,21,7,2	10,15,6,36	12	14	2,2,1,2,6	1,1,5	Chelae, hairy periopods, segmented antenna, 1st maxilliped has new epipodite

1.1.3 Larval Dispersal

Zoeae typically hatch near high tide (López-Duarte and Tankersley 2007) and immediately swim towards the surface. Females' position near the mouths of estuaries allows larvae to be exported within surface waters during ebb tides once at the surface. Field sampling has observed *C. sapidus* zoeae of all stages to primarily inhabit the neuston (Smyth 1980; Provenzano 1983; Epifanio 1995). Provenzano (1983) sampled for zoeae near the mouth of Chesapeake Bay and found that a majority of zoeae were found in the neuston, but nearly 40% were observed within the top 12m. In comparison, more offshore surveys by Epifanio (1995) and Smyth (1980) find a much larger proportion of larvae within the neuston. Since zoeae are negatively buoyant, they must utilize active swimming to achieve this vertical distribution.

Once exported from the estuary, zoeae in the mid-Atlantic are thought to be dispersed in one of two pathways. The first has some retained by these coastal "null zones", regions of dampened coastal currents just north of mid-Atlantic estuaries (Tilburg et al. 2007). These null zones are part of an inshore buoyancy-driven current system, where less dense estuarine waters are driven southward in a relatively narrow (~20 km) band (Garvine 1991). These currents are greatest near the mouths of estuaries but can remain intact for over 100 km, but they are eventually halted by fronts created by adjacent estuarine systems (Yankovsky et al. 2000). In the second pathway, zoeae are exported from the estuary via the along shore current, potentially recruiting to estuaries further south (Epifanio 1995). However, seasonal changes in wind direction can result in Ekman transport offshore, where an offshore counter-current caries them northward (Epifanio and Garvine 2001). This northward transport has been shown in dispersal simulations to enable return to the vicinity

of zoeae's parental estuary (Johnson 1985; Garvine et al. 1997). Whether retained in these "null zones" or advected by coastal currents, eventual intrusion into estuaries is thought to be due to Ekman transport inshore during downwelling circulation (Epifanio and Garvine 2001).

1.2 Blue Crab Larval Morphology

Morphology can play an important function role in many aspects of larval development, including swimming, sinking, feeding, anti-predator defenses, and hydrodynamics. Though zoeae undergo considerable morphological change throughout their development, this section will focus primarily on that of first stage zoeae, as this stage was the focus of most of this dissertation.

C. sapidus zoeae have prominent dorsal spine and rostrum. These spines are of intermediate size across taxa, while not being as large as those of the mud crabs *Rhitrophanopeus spp.* (Sandifer 1972) but substantially larger than that of the pea crabs *Dissodactylus spp.*(Pohle and Telford 1981). These carapace spines can act as antipredatory defenses against larval fish (Morgan 1987; Bollache et al. 2006) and other planktivorous invertebrates (Morgan 1992), where zoeae with longer spines show decreased rates of ingestion by predators (Morgan 1987). Ingestion of prey in larval fish is often limited by their own mouth gape diameter, and the addition of carapace spines can make the apparent size of a zoeae to a fish larvae much larger than its main body. A second method of defense is a physical one, where spines can pierce predators internally once ingested (Morgan 1987).

In addition to their anti-predatory function, zoeal carapace spines can also influence the hydrodynamics of zoeae in motion. *C. sapidus* zoeae typically swim in the direction of their dorsal spine (i.e. "backwards"), with the dorsal spine oriented about 30º from the vertical plane (Sulkin 1984b). In porcelain crab zoeae, carapace spines have been demonstrated to aid in swimming speed and orientation (Smith and Jensen 2015), and presumably have similar functionality for *C. sapidus* zoeae, despite substantial morphological differences. When zoeae passively sink they are oriented with the anterior of their carapace facing downward (Figure 1-2), such that spines are oriented horizontally. In this orientation, spines can increase the cross-sectional area of the zoeae, increase drag, and decrease passive sinking velocities.

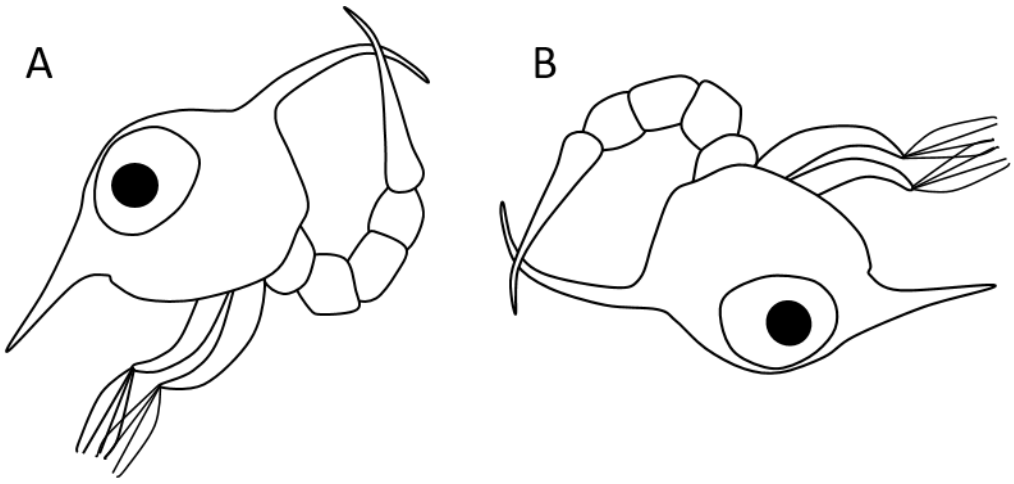

Figure 1-2: *Orientation of zoeae in upward swimming (A) and passive sinking (B) orientations.*

Zoeae swim by either oscillations of their maxillipeds or by abdominal contractions (Chia et al. 1984). In the former case, zoeae beat their maxillipeds, generating thrust on their power stroke proportional to the cross-sectional area of the fanned setae attached. During their recovery stroke, the setae are held together, decreasing their cross-sectional

area and reducing their retrograde motion (Ford et al. 2005; Velazquez 2016). The thrust they are able to produce by these motions is dependent on both the angular velocity and morphology of these appendages. In the latter method, zoeae rapidly contract or straighten their abdomens, resulting in burst of speed that can vary in direction (Chia et al. 1984). Again, the thrust produced by the abdomen should be proportional to the morphology and speed of contraction.

Lastly, the overall morphological characteristics of a zoea can influence its hydrodynamic properties, particularly in the form of drag and Reynolds number (Re). A general equation for the drag force (F_D) is:

$$F_D = \frac{1}{2}\rho A C_d U^2 \quad \textbf{(1.1)}$$

Where ρ is the density of the fluid, *A* is the cross-sectional area in the direction of motion, C_d is a drag coefficient, and *U* is the velocity of the object. Due to the change in orientation of zoeae while swimming and sinking, for *C. sapidus* zoeae, *A* would be the dorsal cross-sectional area while swimming and the anterior cross-sectional area while sinking. This means that while drag will generally increase for larger zoeae, changes in body shape (i.e. morphology) can increase drag even when overall apparent size or volume stays constant.

Additionally, C_d is often parameterized as inversely proportional to Re, where Re takes the form:

$$Re = \frac{lU}{\nu} \quad \textbf{(1.2)}$$

Where l is the object's characteristic length and v is the dynamic viscosity of the fluid. For a zoeae, there is no standard measurement of l, but the straight-line distance between ends of the carapace spines (rostro-dorsal length, RDL) or the carapace diameter are reasonable characterizations of size. Given the same velocity, larger zoeae have a proportionally larger Re, and thus a smaller C_d. Together this produces a tradeoff between larger A and smaller Re for larger zoeae, where changes in shape can determine the ultimate effect on F_D. The amount of drag a zoeae experiences is mainly important from an energetic standpoint. Two zoeae with the same propulsive capability but with different body morphologies will ultimately experience different energetic costs for swimming. As *C. sapidus* zoeae must constantly swim throughout development, these energetic differences have the potential to influence the overall energetic budgets of larvae over development.

In addition to its influence on drag, a zoeae's Reynolds number can have profound influence on its general hydrodynamic qualities. Re represents the balance between viscous and inertial forces acting on an object in a fluid, where a $Re>1$ signifies dominant inertial forces and $Re<1$ dominant viscous forces. *C. sapidus* zoeae exist at an intermediate Re such that their hydrodynamic properties are equally relevant. For instance, organisms with a very low Re ($\ll 1$) move in nearly laminar flow conditions where friction due to viscosity is very high. The lack of inertia means that if the organism were to attempt to swim using purely symmetrical appendage oscillations, they would produce nearly identical thrust during a forward and return stroke and not make substantial forward motion. For *C. sapidus* zoeae, this problem is not as severe, but the morphological and angular velocity changes in appendages during power and recover strokes results in a net forward thrust over the course of the entire movement. In spite of this, significant backward motion is produced

on the recovery stroke, decreasing the efficiency of strokes compared to organisms at a higher Re. Zoeae that are larger, or are shaped such that their Re is larger (e.g. a more streamlined shape), in such a way that doesn't significantly increase drag, can potentially achieve a higher mechanical efficiency while swimming.

1.3 Larval Behavior

1.3.1 Swimming and Sinking

Though a full analysis of swimming mechanics has not been performed, kinematics of green crab (*Carcinus maenas*) has been thoroughly studied (Ford et al. 2005; Velazquez 2016). Directed swimming in zoeae is most commonly achieved by the semi-synchronous oscillations of maxillipeds (i.e. cruise swimming). Maxilliped oscillations of zoeae can be divided into a power and recovery stroke. On the power stroke, natatory setae on the ends of maxillipeds are fanned, and on the recovery stroke, they are closer together (Velazquez 2016). These oscillations are rapid, and for *C. maenas* have a mean frequency of 2.5 Hz (Velazquez 2016). Each set of maxillipeds oscillate in unison, with a slight lag in the rear pair (Ford et al. 2005). As discussed in Section 2, the intermediate Re of zoeae results in negligible inertia and retrograde motion on the recovery stroke. Regardless, the lag in the second pair's oscillations can mitigate this effect and enable net forward motion (Ford et al. 2005). When generating thrust via abdominal contractions, zoeae curl their abdomens inward, reducing loss of velocity during recovery strokes (Velazquez 2016).

For *C. sapidus* zoeae, swimming velocity generally increases over development (Table 1-2; Sulkin et al. 1980), thus outpacing an increase in drag due to growth. As they develop, zoeae can offset this increase in drag with larger maxillipeds, more setae, and the

addition of a third set of maxillipeds for later stages (Costlow and Bookhout 1959). Increases in size for later stages also translate to an increase in sinking velocity (Sulkin et al. 1980), which scales with the volume of particles (Vogel 1994).

Table 1-2: Swimming and sinking velocities of *C. sapidus* zoeae (based on Sulkin et al., 1980)

Stage	Swimming Velocity (cm/s)	Sinking Velocity (cm/s)
1	0.41	0.343
4	1.265	0.463
7	1.885	1.073

1.3.2 Responses to Environment

The swimming behavior of *C. sapidus* zoeae is well documented, and a thorough review is provided by Epifanio and Cohen (2016). Zoeae exhibit negative geotaxis throughout their larval development, and combined with negative buoyancy, zoeae generally swim upward in the absence of other external cues (Sulkin et al. 1980). Barokinetic responses are not as ubiquitous, whereby upward swimming velocity is positively correlated with pressure (i.e. depth) and mid and late stage zoeae have a depressed swimming with depth (Sulkin et al. 1980). Early stage zoeae exhibit a higher response to lower temperature and high salinity than more developed larvae (Sulkin et al. 1980). Together, experiments by Sulkin et al. (1980), imply a surface position of first stage larvae and a deeper depth distribution as zoeae develop. However, this is not necessarily confirmed by observations (Epifanio 1995). There is no evidence of blue crab zoeae demonstrating ontogenetic vertical migrations (Epifanio 1995). They also do not exhibit any endogenous swimming behavior, thus their vertical position is independent of tidal cycles (López-Duarte and Tankersley 2007).

The response of *C. sapidus* zoeae to light is less consistent across experiments. Early work by Sulkin et al. (1980) found that zoeae exhibit positive phototaxis throughout development at 75 W m^{-2} and wavelength of 500 nm. However, the non-diffuse (i.e. collimated) light that was used has been shown to alter phototactic responses on other species (Forward et al. 1984). In fact, at much lower light intensities (10^{-1} to 10^{-7} W m^{-2}) and with a natural light field, first stage zoeae generally exhibit negative phototaxis (Forward and Buswell 1989). As a comparison, full sunlight is on the order of 10^{3} W m^{-2}. It is unclear how changes in phototaxis are attributable to light intensity or the angular distribution of light. Additionally, zoeae response can be dependent on light wavelength, which is confounded by light absorption and scattering with depth (Epifanio and Cohen 2016).

1.3 Maternal Influence and Trait Variation

1.4.1 Maternal Effects

Maternal effects typically refer to genetic and non-genetic influence mothers have on their offspring. Non-genetic effects in marine organism typically take the form of prenatal care and environmental conditions, nutrient provisioning, or spawning or hatching habitat. An important influence mothers can have on their offspring comes in the form of size (i.e. larger eggs). For larvae of non-feeding invertebrates, nutrients provided in eggs are the only source of energy prior to settlement, and thus, egg size can influence larval duration and dispersal potential (Marshall and Keough 2003). Nutrient provisioning in the form of egg size can also influence settlement behavior and gregariousness (Toonen and

Pawlik 1994). However, for planktotrophic larvae, maternal influences on offspring size are still possible (Marshall and Keough 2007).

Blue crab reproductive behavior can facilitate the presence of maternal effects. Since adult females only mate once (van Engel 1958), typically all offspring within a brood are siblings from the same mother and father. This differs from other taxa, such as broadcast spawners, in that the mother is known for all offspring within a brood. Additionally, once the egg mass is extruded, females regularly care for eggs, providing a mechanism for maternal behavior to influence egg quality (van Engel 1958). Up to 7 broods can be produced by a female, and while there are generally few changes in egg quality and larval size, successful development of embryos decreases for later broods (Darnell et al. 2009). Lastly, females migrate prior to hatching and release of eggs, which enables environmental influence on egg development (Carr et al. 2004; Darnell et al. 2012).

Maternal size has been shown to be a predictor of offspring size in several decapod crustaceans, including anomurans (Sato and Suzuki 2010b) and caridieans (González-Ortegón and Giménez 2014). Furthermore, a positive correlation between fecundity and larval size has been documented in carideans (Walsh 1993) and grapsoid crabs (Bas et al. 2007). Egg size can be related to size of zoeae in brachyrans (Bas et al. 2007), and larger zoeae upon hatching can translate to increased sizes of further life stages (Gimenez et al. 2004). However, for *C. sapidus* observations suggest that there is not a relationship with maternal size or fecundity and larval size (Darnell et al. 2009; Koopman and Siders 2013). However, as discussed in previously, there are other traits besides overall size than can influence larval survival and success.

1.4.2 Intraspecific Variation

Intraspecific variation can sometimes be an adaptive trait on its own. In some cases, trait variation can allow for offspring success in spite of variable or uncertain environments (Gotthard and Nylin 1995). In general, morphological traits can depend on a suite of genetic, environmental, and stochastic processes (Monteiro et al. 2000). Recent understanding suggests that intraspecific variation can influence a wide range of ecological processes, including population dynamics and competitive interactions (Bolnick et al. 2011). Morphological variation has been used to identify subpopulations in carideans (Terossi and Mantelatto 2012), as well as a developmental response of morphology to temperature in brachyurans (Shirley et al. 1987). However, to my knowledge, only one study has investigated the morphological variability as it pertains to maternal influences (Tamura et al. 2017).

Maternal influences are not the only causes of intraspecific morphological variation, and a wide range of ecological and environmental factors can influence morphology. Salinity has been shown to influence broad morphometrics in the Chinese mitten crab (*Eriocheir sinensis*), where, as salinity decreased, the ratio of spine length to carapace length decreased (Anger 2003). This effect may be an adaptive response, as lower salinity, more estuarine waters are more likely to contain zooplankton predators, and increased spine lengths may deter predation. Temperature has been shown to influence larval morphology in *Portunus tribuberculatus* (Dan et al. 2013) and *Cancer magister* (Shirley et al. 1987). In both studies, lower temperature results in larger larvae. It is hypothesized that lower temperatures can increase development time, which may be offset by the increased survival created by more pronounced spines (Shirley et al. 1987). Overall,

it is clear that zoeal morphology is plastic, and due to the functionality of morphological features. Better characterization of intra-specific variation is needed to understand processes affecting zoeae over development.

1.4 Outline of Dissertation

The goal of this dissertation is to provide a better understanding of the intraspecific variability in morphology and swimming behavior, as well as some of the implications of such variation, in early stage *Callinectes sapidus* zoeae. In *Chapter 2*, variation in *C. sapidus* zoeal morphology among several larval broods was identified and used to test whether brood-dependent morphology is present. This experiment involved hatching several broods, measuring morphometrics using microscope photography and image analysis. Simple models of swimming-induced drag and passive sinking velocity were also used to create an index of vertical swimming efficiency. In Chapter 3, larvae from the same broods described in Chapter 2 are followed further into development to investigate how brood-level morphological differences change over time. Chapter 4 tested whether the brood-dependent morphology discussed in the prior chapters translated to similar differences in swimming behavior. Using mesocosm video observations, I aimed to characterize swimming velocity, orientation, and path shape both general and within individual broods. I also used mixture models to identify modes of behavior. In Chapter 5, simulations were used to test whether the observed brood-dependent behavior and morphology can translate to differences in larval transport. An idealized model of a wind-driven estuarine plume that utilizes observed brood-depending swimming and sinking behaviors was developed for this purpose. Several model scenarios were used to determine

how physical and behavioral factors can influence transport. Additional analyses aimed to determine how differences in brood behavior alters transport trajectories.

1.6 Literature Cited

Anger K (2001) The biology of decapod crustacean larvae. Crustac Issues 14:417. doi: 10.1651/0278-0372(2005)025

Anger K (2003) Salinity as a key parameter in the larval biology of decapod crustaceans. Invertebr Reprod Dev 43:29–45. doi: 10.1080/07924259.2003.9652520

Bas CC, Spivak ED, Anger K (2007) Seasonal and interpopulational variability in fecundity, egg size, and elemental composition (CHN) of eggs and larvae in a grapsoid crab, *Chasmagnathus granulatus*. Helgol Mar Res 61:225–237. doi: 10.1007/s10152-007-0070-y

Bollache L, Kaldonski N, Troussard JP, Lagrue C, Rigaud T (2006) Spines and behaviour as defenses against fish predators in an invasive freshwater amphipod. Anim Behav 72:627–633. doi: 10.1016/j.anbehav.2005.11.020

Bolnick DI, Amarasekare P, Araújo MS, Bürger R, Levine JM, Novak M, Rudolf VHW, Schreiber SJ, Urban MC, Vasseur DA (2011) Why intraspecific trait variation matters in community ecology. Trends Ecol Evol 26:183–192. doi: 10.1016/j.tree.2011.01.009

Carr SD, Tankersley RA, Hench JL, Forward RB, Luettich RA (2004) Movement patterns and trajectories of ovigerous blue crabs *Callinectes sapidus* during the spawning migration. Estuar Coast Shelf Sci 60:567–579. doi: 10.1016/j.ecss.2004.02.012

Chia F-S, Buckland-Nicks J, Young CM (1984) Locomotion of marine invertebrate larvae: a review. Can J Zool 62:1205–1222.

Costlow JDJ (1965) Variability in larval stages of the blue crab, Callinectes sapidus. Biol Bull 128:58–66.

Costlow JDJ, Bookhout CG (1959) The larval development of *Callinectes Sapidus* Rathbun reared in the laboratory. Biol Bull 116:373–396.

Dan S, Kaneko T, Takeshima S, Ashidate M, Hamasaki K (2013) Variations in larval morphology and their relationships to survival during mass seed production by the swimming crab, *Portunus trituberculatus* (Brachyura, Portunidae). Aquaculture 414:109–118. doi: 10.1016/j.aquaculture.2013.07.029

Darnell MZ, Rittschof D, Darnell KM, McDowell RE (2009) Lifetime reproductive potential of female blue crabs *Callinectes sapidus* in North Carolina, USA. Mar Ecol Prog Ser 394:153–163. doi: 10.3354/meps08295

Darnell MZ, Wolcott TG, Rittschof D (2012) Environmental and endogenous control of selective tidal-stream transport behavior during blue crab *Callinectes sapidus* spawning migrations. Mar Biol 159:621–631. doi: 10.1007/s00227-011-1841-1

Epifanio CE (1995) Transport of blue crab (*Callinectes sapidus*) larvae in the waters off Mid-Atlantic states. Bull Mar Sci 57:713–725.

Epifanio CE, Cohen JH (2016) Behavioral adaptations in larvae of brachyuran crabs: A review. J Exp Mar Bio Ecol 482:85–105. doi: 10.1016/j.jembe.2016.05.006

Epifanio CE, Garvine RW (2001) Larval transport on the Atlantic continental shelf of North America: A review. Estuar Coast Shelf Sci 52:51–77. doi: 10.1006/ecss.2000.0727

Ford MD, Schuegraf MJ, Elkink MS, Edwin DeMont M (2005) A comparison of swimming structures and kinematics in three species of crustacean larvae. Mar Freshw Behav Physiol 38:79–94. doi: 10.1080/10236240500148934

Forward RB, Cronin TW, Stearns DE (1984) Control of diel vertical migration : photoresponses of a larval crustacean '. 29:146–154.

Forward RJB, Buswell CU (1989) A comparative study of behavioral responses of larval decapod crustaceans to light and pressure. Mar Behav Physiol 16:43–56.

Garvine RW (1991) Subtidal frequency estuary-shelf interaction : Observations near Delaware Bay. J Geophys Res 96:7049–7064.

Garvine RW, Epifanio CE, Epifanio CC, Wong K-C (1997) Transport and recruitment of blue crab larvae: A model with advection and mortality. Estuar Coast Shelf Sci 45:99–111. doi: 10.1006/ecss.1996.0161

Gimenez L, Anger K, Torres G (2004) Linking life history traits in successive phases of a complex life cycle: Effects of larval biomass on early juvenile development in an estuarine crab, *Chasmagnathus granulata*. Oikos 104:570–580.

González-Ortegón E, Giménez L (2014) Environmentally mediated phenotypic links and performance in larvae of a marine invertebrate. Mar Ecol Prog Ser 502:185–195. doi: 10.3354/meps10708

Gotthard K, Nylin S (1995) Adaptive plasticity and plasticity as an adaptation: a selective review of plasticity in animal morphology and life history. Oikos 74:3–17.

Jivoff P, Hines AH, Quackenbush LS (2007) Reproduction niology and embryonic development. in: Kennedy VS, Cronin LE (eds) The Blue Crab: *Callinectes sapidus*. Maryland Sea Grant College, pp 255–298

Johnson DR (1985) Wind-forced dispersion of blue crab larvae in the Middle Atlantic Bight. Cont Shelf Res 4:733–745. doi: 10.1016/0278-4343(85)90039-1

Koopman HN, Siders ZA (2013) Variation in egg quality in blue crabs, *Callinectes sapidus*, from North Carolina: Does female size matter? J Crustac Biol 33:481–487. doi: 10.1163/1937240X-00002152

López-Duarte PC, Tankersley R a. (2007) Circatidal swimming behavior of brachyuran crab zoea larvae: Implications for ebb-tide transport. Mar Biol 151:2037–2051. doi: 10.1007/s00227-007-0614-3

Marshall DJ, Keough MJ (2003) Variation in the dispersal potential of non-feeding invertebrate larvae: the desperate larva hypothesis and larval size. Mar Ecol Prog Ser 255:145–153. doi: 10.3354/meps255145

Marshall DJ, Keough MJ (2007) The evolutionary ecology of offspring size in marine invertebrates. Adv Mar Biol 53:1–60.

McMillen-Jackson AL, Bert TM (2004) Mitochondrial DNA variation and population genetic structure of the blue crab *Callinectes sapidus* in the eastern United States. Mar Biol 145:769–777. doi: 10.1007/s00227-004-1353-3

Millikin MR (1978) Blue crab larval culture: Methods and management. Mar Fish Rev 40:10–17.

Monteiro LR, Bordin B, Furtado dos Reis S (2000) Shape distances, shape spaces and the comparison of morphometric methods. Trends Ecol Evol 15:217–220. doi: 10.1016/S0169-5347(99)01775-9

Morgan SG (1987) Morphological and behavioral antipredatory adaptations of decapod zoeae. Oecologia 73:393–400.

Morgan SG (1992) Predation by planktonic and benthic invertebrates on larvae of estuarine crabs. J Exp Mar Bio Ecol 163:91–110. doi: 10.1016/0022-0981(92)90149-5

Pohle G, Telford M (1981) The larval development of *Dissodactylus crinitichelis* Moreira, 1901 (Brachyura: Pinnotheridae) in laboratory culture. Bull Mar Sci 31:753–773.

Provenzano A (1983) Vertical distribution of first stage larvae of the blue crab, *Callinectes sapidus*, at the mouth of Chesapeake Bay. Estuar Coast Shelf Sci 16:489–499.

Sandifer PA (1972) Morphology and ecology of Chesapeake Bay decapod crustacean larvae. College of William and Mary

Sandoz M, Rogers R, Sandoz, Mildred and Rogers R (1944) The effect of environmental factors on hatching , moulting , and survival of zoea larvae of the blue crab *Callinectes Sapidus* Rathbun. Ecology 25:216–228. doi: 10.2307/1930693

Sato T, Suzuki N (2010) Female size as a determinant of larval size, weight, and survival period in the coconut crab, *Birgus latro*. J Crustac Biol 30:624–628. doi: 10.1651/10-3279.1

Shirley SM, Shirley TC, Rice SD (1987) Latitudinal variation in the dungeness crab, *Cancer magister*: Zoeal morphology explained by incubation temperature. Mar Biol 95:371–376.

Smith AE, Jensen GC (2015) The role of carapace spines in the swimming behavior of porcelain crab zoeae (Crustacea: Decapoda: Porcellanidae). J Exp Mar Bio Ecol 471:175–179. doi: 10.1016/j.jembe.2015.06.007

Smyth PO (1980) *Callinectes* (decapoda: portunidae) larvae in the Middle Atlantic Bight, 1975-77. Fish Bull 78:251–265.

Sulkin SD (1975) The significance of diet in the growth and development of larvae of the blue Crab, *Callinectes sapidus* Rathbum, under laboratory conditions. J Exp Mar Bio Ecol 20:119–135.

Sulkin SD (1984) Behavioral basis of depth regulation in the larvae of brachyuran crabs. Mar Ecol Prog Ser 15:181–205. doi: 10.3354/meps015181

Sulkin SD, Epifanio CE (1975) Comparison of rotifers and other diets for rearing larvae of the blue crab, *Callinectes sapidus* Rathbun. Estuar Coast Mar Sci 3:109–113.

Sulkin SD, van Heukelem W, Kelly P, van Heukelem L (1980) The behavioral basis of larval recruitment in the crab *Callinectes sapidus* Rathbun: a laboratory investigation of ontogenetic changes in geotaxis and barokinesis. Biol Bull 159:402–417.

Tamura H, Landeira JM, Goshima S (2017) Morphological and morphometric variability in the zoea I larvae of *Pugettia quadridens* (De Haan, 1839): looking for reliable characters for taxonomic studies on the genus Pugettia Dana, 1851 (Majoidea: Epialtidae). Zootaxa 4226:264–272.

Terossi M, Mantelatto FL (2012) Morphological and genetic variability in *Hippolyte obliquimanus* Dana, 1852 (Decapoda, Caridea, Hippolytidae) from Brazil and the Caribbean Sea. Crustaceana 85:685–712. doi: 10.1163/156854012X643762

Tilburg CE, Dittel AI, Epifanio CE (2007) Retention of crab larvae in a coastal null zone. Estuar Coast Shelf Sci 72:570–578. doi: 10.1016/j.ecss.2006.11.030

Toonen RJ, Pawlik JR (1994) Foundations of gregariousness. Nature 370:511–512.

Umphlett CJ, Mccray EM (1975) A brief review of the involvements of *Lagenidium*, an aquatic fungus parasite, with arthropods. Mar Fish Rev 37:61–64.

van Engel WA (1958) The blue crab and its fishery in Chesapeake Bay: Part 1 - Reproduction, early development, growth, and migration. Commer Fish Rev 20:6–17.

Velazquez CCS (2016) The kinematics and particle image velocimetry of the shore crab larvae *Carcinus maenas*. California State University, Fresno

Vogel S (1994) Life in Moving Fluids: The Physical Biology of Flow, 2nd edn. Princeton University Press

Walsh CJ (1993) Larval development of *Paratya Australiensis* Kemp, 1917 (Decapoda: Caridea: Atyidae), reared in the laboratory, with comparisons of fecundity and egg and larval size between estuarine and riverine environments. J Crustac Biol 13:456–480.

Yankovsky AE, Garvine RW, Münchow A (2000) Mesoscale currents on the inner New Jersey shelf driven by the interaction of buoyancy and wind forcing. J Phys Oceanogr 30:2214–2230. doi: 10.1175/1520-0485(2000)030<2214:MCOTIN>2.0.CO;2

Zmora O, Findiesen A, Stubblefield J, Frenkel V, Zohar Y (2005) Large-scale juvenile production of the blue crab *Callinectes sapidus*. Aquaculture 244:129–139. doi: 10.1016/j.aquaculture.2004.11.012

Chapter 2: Morphological Variability among Broods of First Stage Blue Crab (*Callinectes sapidus*) Zoeae

This chapter appears in its entirety in *The Biological Bulletin* **235** (2018): 123-133. DOI: https://doi.org/10.1086/699922

Abstract

External morphology has been shown to influence predation and locomotion of decapod larvae, and is therefore directly related to their ability to survive and disperse. The first goal of this study was to characterize first stage blue crab zoeal morphology and its variability across larval broods to test whether inter-brood differences in morphology exist. The second was to identify possible correlations between maternal characteristics and zoeal morphology. The offspring of 21 individuals were hatched in the laboratory, photographed, and measured. Zoeae exhibited substantial variability, with all metrics showing significant inter-brood differences. The greatest variability was seen in the zoeal abdomen, rostrum, and dorsal spine length. A principal component analysis, showed no distinct clustering of broods with variation driven by generally larger zoeae. Using observed morphology, models of drag induced by swimming and sinking also showed significant inter-brood differences with a maximum two-fold difference across broods. In contrast to trends in other decapod taxa, maternal characteristics (female carapace width and mass and egg sponge volume and mass) are not significant predictors of zoeal morphology. These results suggest that brood effects are present across a wide range of morphological characteristics and that future experiments involving *C. sapidus* morphology or its functionality should explicitly account for inter-brood variation. Additionally, inter-brood morphological

differences may result in differential predation mortality and locomotory abilities among broods.

2.1 Introduction

Blue crabs (*Callinectes sapidus*) support economically valuable and culturally significant recreational and commercial fisheries in the mid-Atlantic (Rhodes et al. 2001; Paolisso 2007). They are also an important benthic predator and prey in estuarine ecosystems (Millikin and Williams 1984). Historically, adult blue crab population abundance in Delaware Bay and Chesapeake Bay has been volatile (van Engel 1958; Stagg and Whilden 1997), with variation in adult abundance mirrored by juvenile abundance indices (Wong 2010). One potential explanation for highly variable inter-annual adult abundance is changes in larval supply (Johnson and Hess 1990a; Epifanio 1995; Ogburn et al. 2012). Variability in annual larval supply may be the result of declines in the spawning stock (Lipcius and Stockhausen 2002), sperm limitation (Hines et al. 2003), larval predation (Morgan 1992), inter-annual changes in coastal currents (Tilburg et al. 2005; Ogburn et al. 2012), or other complex interactions blue crab larvae have with the environment during development.

Zoeae, the pelagic larval phase of blue crabs, develop in surface waters over the continental shelf from the Mid-Atlantic through the Gulf of Mexico (Epifanio 1988). During their 30 to 40 day development (Costlow and Bookhout 1959), zoea actively feed (Sulkin 1975; McConaugha 1992), constantly swim to counteract passive sinking (Sulkin et al. 1980; Sulkin 1984), and grow to a size at which they can metamorphose into megalopae. Megalopae then re-enter an estuary and metamorphose again into juvenile blue

crabs (van Engel 1958). Identifying factors that improve a zoea's chances of survival and successful dispersal may lead to better understanding of annual variability in larval supply.

Morphological characteristics of zoeae directly relate to their ability to survive and disperse successfully. Carapace spines have been shown to stabilize and orient zoeae while swimming (Smith and Jensen 2015), and longer spines provide anti-predatory defenses against larval fish (Bollache et al. 2006) and reduce predation of zoeae (Morgan 1987, 1992). Zoeae rapidly beat their maxillipeds to swim and generate feeding currents (Foxon 1934), and efficient locomotion relates to the size and cross-sectional area of maxillipeds and attached setae (Chia et al. 1984). Zoeae rapidly contract their abdomens to escape predators (Foxon 1934), generating thrust proportional to the dimensions of the abdomen. A zoea's cross-sectional area and overall size are proportional to the drag force experienced while sinking and swimming (Chia et al. 1984). Lastly, higher drag can cause zoeae to sink slower and require zoeae to use more energy to swim at a given velocity.

Intraspecific morphological variability can be caused by a number of genetic, environmental, or stochastic processes (Monteiro et al. 2000). Variability in morphological traits can also be, in and of itself, an evolutionary adaptation, enabling some individuals to survive in variable environments (Gotthard and Nylin 1995). Variation in zoeal morphology may result in differential predation, energetic costs, behavior, and dispersal across groups of zoeae. Kelp crab (*Pugettia quadridens)* zoeae show significant morphological variability both within and between broods (Tamura et al. 2017). Blue crab zoeae likely also demonstrate some degree of morphological variability both within populations and between broods, and variability in the characteristics of molt stages has

been observed in *C. sapidus* (Costlow 1965). However, there has yet to be a quantitative characterization of those differences.

Variation in decapod larval morphology may be related to maternal effects. Substantial maternal effects have been observed in the caridean *Sclerocrangon boreas* (Guay et al. 2011). Maternal effects on larval morphology have also been seen in some anomurans (Sato and Suzuki 2010) although other species have shown no such relationship (Swiney *et al.,* 2013). Morphological variability has been observed in *Cancer magister* as the result of brooding temperature, not necessarily maternal effects (Shirley et al. 1987). To our knowledge this study is one of the first to investigate relationship between maternal and larval characteristics in brachyurans and specifically in *C. sapidus*. If such a relationship exists for blue crabs, those maternal characteristics could be useful predictors of offspring characteristics. Although no significant relationship between carapace width in mothers and zoeae has been seen in *C. sapidus* (Darnell et al. 2009), we are unaware of a study that has addressed these maternal covariates' relationship to an array of morphological characteristics for blue crab larvae. Maternal characteristics, specifically related to size and fecundity, are more easily measured during existing population surveys than zoeal morphology. Thus, identifying maternal characteristics that could act as predictors of larval features that relate to locomotion and feeding could provide a means for estimating zoeal population's dispersal ability.

The first objective of this study was to characterize first stage blue crab zoeal morphology and its variability across larval broods to test whether inter-brood differences in morphology exist. The second objective was to identify possible correlations between maternal characteristics and zoeal morphology. Morphology is important to *C. sapidus*

early larval survival and dispersal; therefore, understanding the morphological variability may help identify sources of differential success in zoeae. Identifying inter-brood differences in morphology may further our understanding of fitness differences among offspring from different parents. Further, identifying maternal predictors of zoeal morphology could help approximate larval condition from surveys of adult crabs.

2.2 Methods

2.2.1 Animal Collection and Maternal Characteristics

To characterize the morphology of first stage blue crab zoeae, 21 gravid adult female blue crabs were captured via trawling in the summers of 2016 and 2017 in the down-bay portion of Delaware Bay (n=6 in 2016, n=15 in 2017). Crabs were captured opportunistically as part of existing Delaware Bay trawl survey programs, and as such, crabs were caught with an irregular seasonal distribution. Crabs were caught between June and August in 2016, with the majority caught in June (4 of 6). In 2017, crabs were caught from May through August, with the majority also in June (12 of 15). It was assumed that crabs in this region were representative of the bay-wide adult population, as adult females migrate toward the mouth of the estuary prior to spawning (van Engel 1958; Darnell et al. 2010). Crabs were kept individually in 30 L plastic tanks in filtered seawater at 25-28 ºC and a salinity of 30. Crabs were fed *ad libitum* on thawed shucked scallop meat for 6 hours 2-3 times a week; any leftover food was removed. The developmental stage of each crabs eggs was noted upon arrival to the laboratory. One third of the broods arrived with dark, developed eggs in both years, with a mean laboratory duration before spawning of 3.6 ± 0.5 days for orange eggs and 8.2 ± 0.9 SE days for brown eggs. Once egg eye spots

developed (van Engel 1958) female crabs were no longer fed in order to prevent contamination of eggs and zoeae upon hatching.

(V_E) was estimated using measured egg sponge dimensions (Table 2-1) by assuming sponges were ellipsoidal. Eggs remained attached to mothers and were visually monitored daily for color changes (Millikin 1978). When eggs visually darken, zoeal body structures are developed and eggs are 1 to 3 days from hatching (Van Engel 1958). Crab post-spawning weight (M_C) was measured once spawning was complete. The wet weight of crabs before and after spawning was taken, and the difference in weight (pre- minus post-spawning weight) provided an estimate of the mass of each egg sponge (M_E). This method of estimating M_E may be influenced by changes in adult female body mass as well as retained interstitial water prior to spawning. Female crab size (L_C and M_C) has been shown to correlate with fecundity, where larger females produce more offspring (Prager et al. 1990), therefore M_E and V_E are used here as proxies for fecundity.

Table 2-1: Summary of equations and abbreviations used for shape metrics and estimated characteristics of terminal velocity and drag

Abbreviation	Definition	Equation	Definitions
V_E	Egg sponge Volume	$V_E = \pi l_E w_E h_E$	l_E = Egg sponge length w_E = Egg sponge width h_E = Egg sponge height
A_A	Anterior cross-sectional area	$A_A = \pi CW * CH$	CW = Carapace width CH = Carapace height
A_D	Dorsal cross-sectional area	$A_D = \pi CL * CW$	CL = Carapace length
A_B	Abdominal cross-sectional area	$A_B = AL * AW$	AL = Abdominal length AW = Abdominal width
V_C	Carapace volume	$V_C = \frac{4}{3}\pi CL * CW * CH$	
V_A	Abdominal volume	$V_A = \frac{1}{2} AL * AH * AW$	AH = Abdominal height
F_D	Swimming Drag Force	$F_D = \frac{1}{2}\rho_f C_D A_D U^2$	ρ_f = Fluid density (1019 kg/m^3;Siedler and Peters 1986) C_D = Drag coefficient U = Zoea swimming velocity (0.05 m/s; Sulkin1980)
F_B	Buoyant Force	$F_B = g(V_A + V_C)(\rho_z - \rho_f)$	ρ_z = zoea density (1089 kg/m^3; Hamasaki et al. 2013) g = Gravitational acceleration (9.8 m/s)
C_D	Drag Coefficient	$C_D = \frac{24}{Re} + \frac{6}{1+\sqrt{Re}} + 0.4$	Re = Reynolds Number (White 1974)
Re	Reynolds Number	$Re = \frac{l * U}{\nu}$	ν = Kinematic viscosity of seawater (9.5 x 10^{-7} m^2/s; Sharqawy *et al.* 2011) l = CL in sinking orientation and CH in swimming orientation
U_T	Terminal Sinking Velocity	$U_T = \sqrt{\frac{2g(V_A + V_C)(\rho_z - \rho_f)}{\rho_f A_A C_D}}$	

2.2.2 Sample Collection, Photography, and Image Analysis

Once eggs were released and zoeae had hatched, spawning tanks were gently mixed vertically with a flat plunger, and a 1L subsample was drawn randomly from the surface using a small pail. Zoeae in each sample were captured on a 240 μm sieve, then preserved in a borate-buffered 70% ethanol solution. When possible, 26 preserved zoea were digitally photographed under an Olympus SZX10 Stereo Microscope for morphological measurement. For some broods, fewer than 25 larvae were imaged due to damage or loss. Each individual zoea was suspended in glycerin which was diluted with ethanol until the zoea were neutrally buoyant, allowing zoea to be precisely oriented under the microscope. Zoeae were then photographed using an Infinity Lumenera1-3 2Mpx microscope camera with oblique back-lighting from at least two perpendicular perspectives; one perspective was always from the lateral view (Figure 2-1). Images were calibrated using Infinity Analyze 6.5 microscope camera software and a micrometer slide such that a 1000 μm scale bar was present in each image. A total of 14 morphological measurements were made on each zoea using specific landmarks to define each metric (Figure 2-1, Table 2-2). Prior to measurement, each image was calibrated, then all metrics were measured as straight or segmented lines using ImageJ (Rasband, 2016; Figure 2-1).

Table 2-2: Summary of morphometric abbreviations and definitions.

Metric Name	Abbreviation	Description	Number in Figure 2-1
Carapace length	CL	Base of rostrum to posterior end of carapace	1
Carapace width	CW	Between bases of lateral carapace spines; perpendicular to CW	2
Carapace height	CH	from base of dorsal spine to ventral end of carapace; perpendicular to CL	3
Abdomen length	AL	Anterior base of abdomen to midpoint between furca of telson	4
Abdomen width	AW	Average of left to right distance of abdomen segments	5
Abdomen height	AH	Average of dorsal to ventral distance of abdomen segments	6
Rostrum length	RL	Curved distance from base to tip of rostrum	7
Dorsal spine length	DL	Curved distance from base to tip of dorsal spine	8
Rostro-dorsal length	RDL	Straight distance from tip of rostrum to tip of dorsal spine	9
First maxilliped length	ML1	Base of first maxilliped to apical end of exopods; Average of pair	10
Second maxilliped length	ML2	Base of second maxilliped to apical end of exopods; Average of pair	10
First setae length	SL1	Average length of natatory setae of first maxilliped	11
Second setae length	SL2	Average length of natatory setae of second maxilliped	11

2.2.3 Derived Metrics

Additional metrics were derived from measured morphology as either ratios, cross-sectional areas, or volumes. Ratios included carapace length: carapace width (CL:CW), carapace width: carapace height (CW:CH), carapace length: rostro-dorsal length (CL:RDL), and carapace length: abdominal length (CL:AL). CL:CW and CW:CH describe the shape of the carapace in the swimming and sinking orientations, respectively. CL:RDL is a metric used to characterize the relative investment in carapace spines (Anger 2003) and relates to the passive sinking velocity of zoeae. CL:AH relates to propulsive capacity of the zoeae during abdominal contractions to its overall body size. Assuming an ellipsoidal zoeal carapace, cross-sectional areas were estimated for zoeae in both the swimming (dorsal) and sinking (anterior) orientations (A_D and A_A, respectively). A rectangular abdominal cross-sectional area (A_B) was also calculated for the anterior face of the abdomen. An ellipsoidal carapace volume (V_C) was estimated, and abdominal volume (V_A) was estimated by assuming a wedge-shaped abdomen, tapering towards the telson.

Drag influences the resistive forces zoeae experience while sinking and swimming, and was estimated for each zoea based on its morphology and swimming velocity. The parameterization used for the drag coefficient (C_D) assumes a Reynolds number (Re) between 1 and $2x10^5$ for a spherical body (White 1974). Though zoeae are not exactly spherical, this provides a good approximation of their shape. The swimming velocity used for zoeae was 0.5 cm/s, the mean swimming velocity in experiments with first stage zoea (Sulkin 1980).

Terminal sinking velocity (U_T) was also estimated to quantify the effect of morphological differences between broods (Table 2-1), by setting buoyant and drag force

equations equal to each other and numerically solving for U_T. Estimated volumes and cross-sectional areas (described above), as well as published estimates of 1089 kg m^{-3} for the density of zoeae (Hamasaki et al. 2013), were used for this calculation.

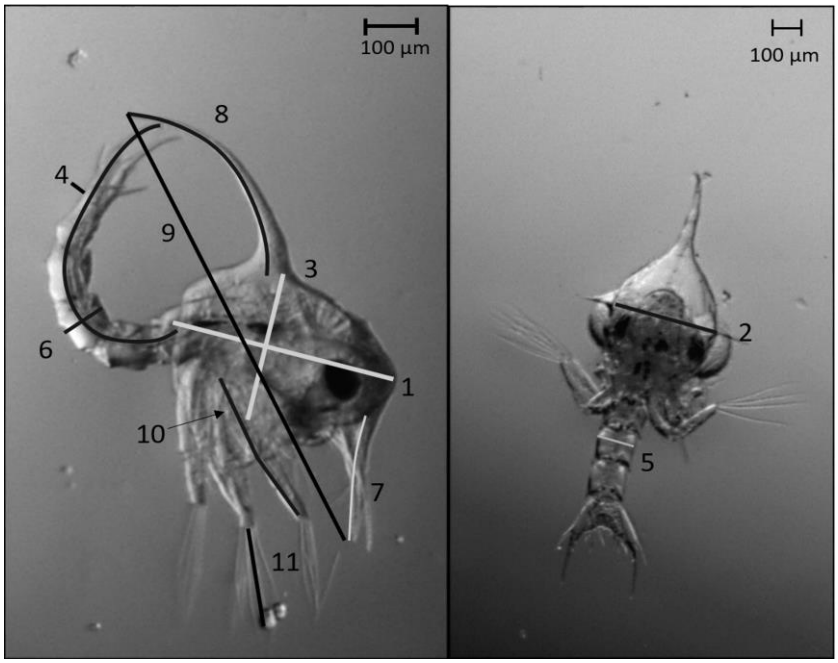

Figure 2-1*: Image of zoea from a side (left) and posterior (right) profile. Numbers correspond to metrics described in the following reference table.*

2.2.4 Statistical Analysis

All statistical analyses were performed in R (R Core Team 2015). Distributions of each metric were calculated by pooling all observed zoeae across all broods. A probability density function was then calculated for each metric using a bandwidth determined by Sheather and Jones' criteria (1991). To quantify morphological variability in the population of first stage zoeae, the distribution of each metric was first tested for normality using the Shapiro-Wilk Test across all larval brood observations. Since metrics were not all normally distributed and were on different scales, the standardized

median absolute deviation (MAD*) was used, to quantify variability across all metrics, where

$$MAD^* = \frac{median|\,X_i - median(X)|}{median(X)} \quad \textbf{(2.1)}$$

MAD* relates the median deviation of all observations from the sample median and is a nonparametric measure of variability that is independent of scale. MAD* was then calculated for each of the measured (Figure 2-1) and derived shape metrics. Bootstrapped 95% confidence intervals were obtained for each metric's MAD* by repeatedly sampling observations with replacement (n=1000), recalculating MAD*, and calculating the 25th and 95th percentiles of the bootstrapped MAD*. Metrics with overlapping confidence intervals were considered to have similar MAD*.

To determine whether morphology differed between broods, a Kruskal-Wallace (K-W) test was performed for each metric with brood as a factor. Then, pairwise K-W comparisons were made using the "*kruskal*" function in the R package "*Agricolae*" (de Mendiburu 2015), to identify statistically similar groups of broods. This was repeated for all of the 14 directly measured metrics.

A principal component analysis (PCA) was used on all measured morphometric data to identify patterns in brood multivariate morphology. PCAs provide a diagnostic tool to investigate overall differences in morphology between groups as well as the drivers of variability (Rohlf and Marcus 1993). Any individual zoea with incomplete morphological data was removed from the analysis. Total length was also excluded from the PCA due to its high correlation with other metrics. 95% data ellipses were calculated for each brood using the "*DataEllipse*" function in the R package "*CAR*" (Fox and

Weisberg 2011). Broods were tested for differences in multivariate morphology using a multivariate analysis of variance (MANOVA).

A linear regression was used to determine whether mean sinking velocity (U_T) and swimming drag (F_D) of each brood were correlated. A MANOVA was used to test for inter-brood differences in zoeal U_T and F_D.

To determine whether maternal characteristics were correlated with zoeal morphology, a regression analysis was performed. Linear regressions were performed on all combinations of maternal characteristics (n=4) and zoeal morphology (n=14), for a total of 56 comparisons. A Bonferroni adjusted alpha of 8.9×10^{-4} (0.05/56) was used, to address the high number of related comparisons.

2.3 Results

2.3.1 Overall Morphological variability

All measured zoeae were combined to characterize the distributions of each morphometric (Figure 2-2). All metrics but the length of the first maxillipeds (ML1) (S-W: p=0.32) were non-normally distributed, and metric medians differed up to an order of magnitude. abdominal width (AW) and abdominal height (AH) had the narrowest distributions, and RDL and AL were the most widely distributed. When standardized by each metric's median, all metrics had similar distributions (K-W: H(12)=6.66, p=0.88).

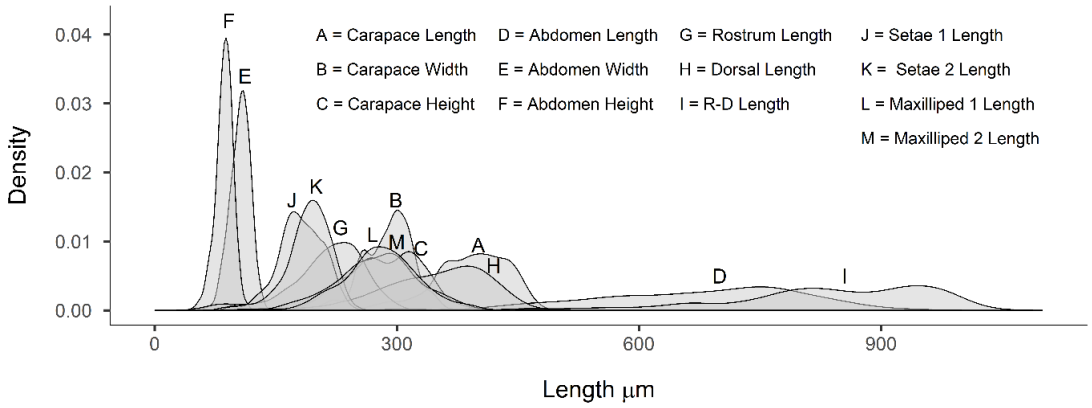

Figure 2-2: *Distribution of a variety of morphological measures across all first stage zoeae collected in 2016 and 2017. Letters indicate metric distributions. Probability density functions were generated using Sheather and Jones criteria (1991).*

MAD* was used to compare variability between metrics for the pooled observations in a way that was independent of scale (Figure 2-3). Across all measured metrics, MAD* ranged from 0.07 to 0.12. Though there were groups of metrics with statistically similar variability, these groups did not necessarily represent anatomical relationships. For example, the group of metrics with the highest amount of variability included spine, carapace, and abdominal metrics. The variability characterized by MAD* did not always correspond to how widely a metric was distributed. While RDL is the most widely distributed metric, in terms of MAD* it has an intermediate variability. The variability of the shape metrics (ratios, surface areas, and volumes) across all observations was also quantified using MAD* (Figure 2-4). Generally, volumes are the most variable (median MAD* = 0.19), cross-sectional areas are intermediately variable (median MAD* = 0.16), and ratios are the least variable (median MAD* = 0.08).

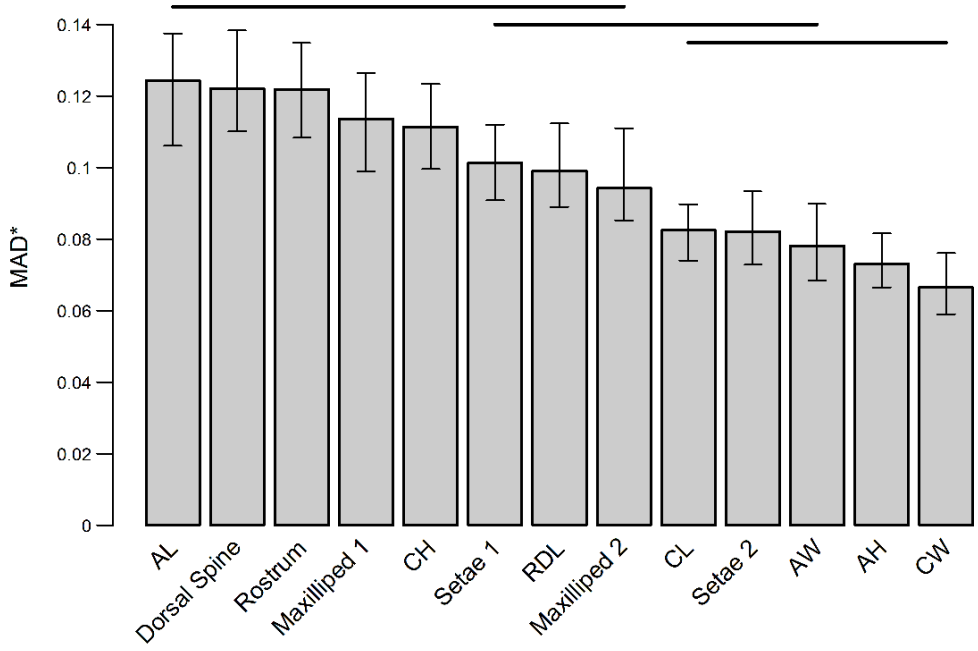

Figure 2-3: *The standardized median absolute deviation (MAD*) was calculated for all metrics of all first stage zoea hatched in 2016 and 2017 experiments. Line ranges represent bootstrapped 95% confidence intervals. MAD* (standardized median absolute deviation) is a non-parametric measure of variation (eq. 2.1).*

2.3.2 Inter-brood Morphological Differences

Morphology of all metrics differed significantly among broods (K-W, all $p<<0.001$), yet pairwise comparisons show that some broods are statistically similar. The distribution of each metric for each brood was examined; however for brevity, only distributions for CL and RDL are shown (Figure 2-5). Broods grouped into 7 to 11 statistically similar groups (pairwise K-W test, $p>0.05$), depending on the metric tested. Though there were statistically different groups of broods for a given metric, brood distributions typically fell along a gradient with only some metrics having distinct breaks between groups. Inter-brood similarities are not consistent across all metrics. While two broods may be similar for one metric, they may differ significantly for another (F25 and F26 in Figures 2-5A and 2-5B, for example).

In terms of multivariate morphology, broods overlap each other with no discrete clustering into groups (Figure 2-6); however, significant differences between broods are present (MANOVA: $F(15,229) = 5.79$, $p<<0.01$, Wilk's $\Lambda = 0.016$). The first two principal components represent 56% of the variation in the multivariate morphology. The first principal component (44% of variation) is driven by an increase in size for all metrics, and the second principal component (11% of the variation) is driven predominantly by CH (positive) and the first and second maxilliped length (negative).

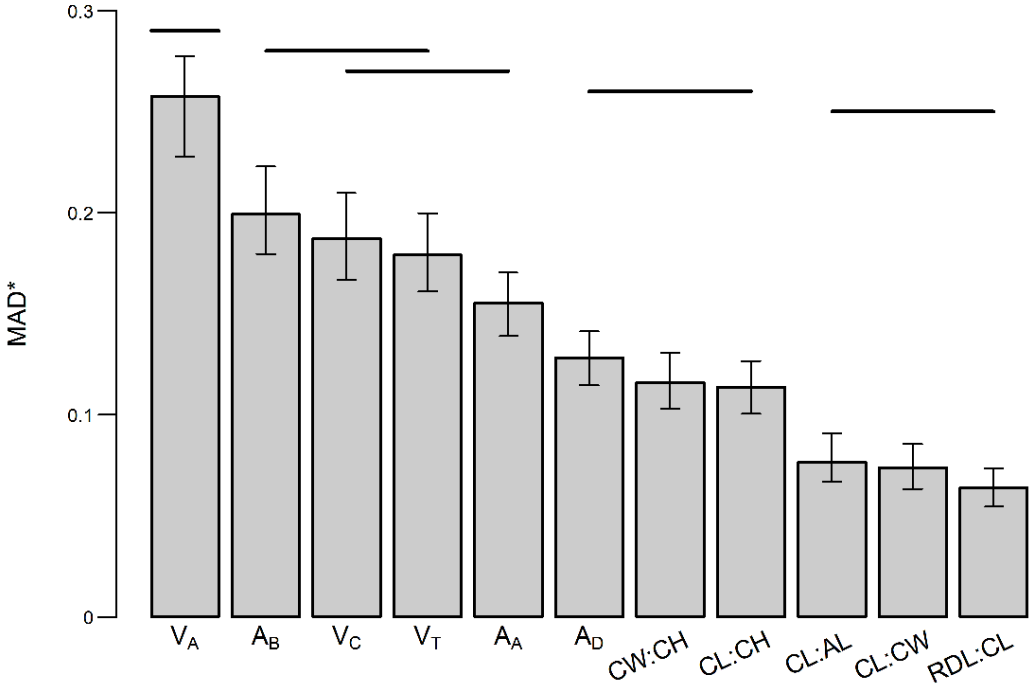

Figure 2-4: *The standardized median absolute deviation (MAD*) was calculated for all derived shape and size metrics (ratios, surface areas, and volume) for all first stage zoeae hatched in 2016 and 2017. Line ranges represent bootstrapped 95% confidence intervals.*

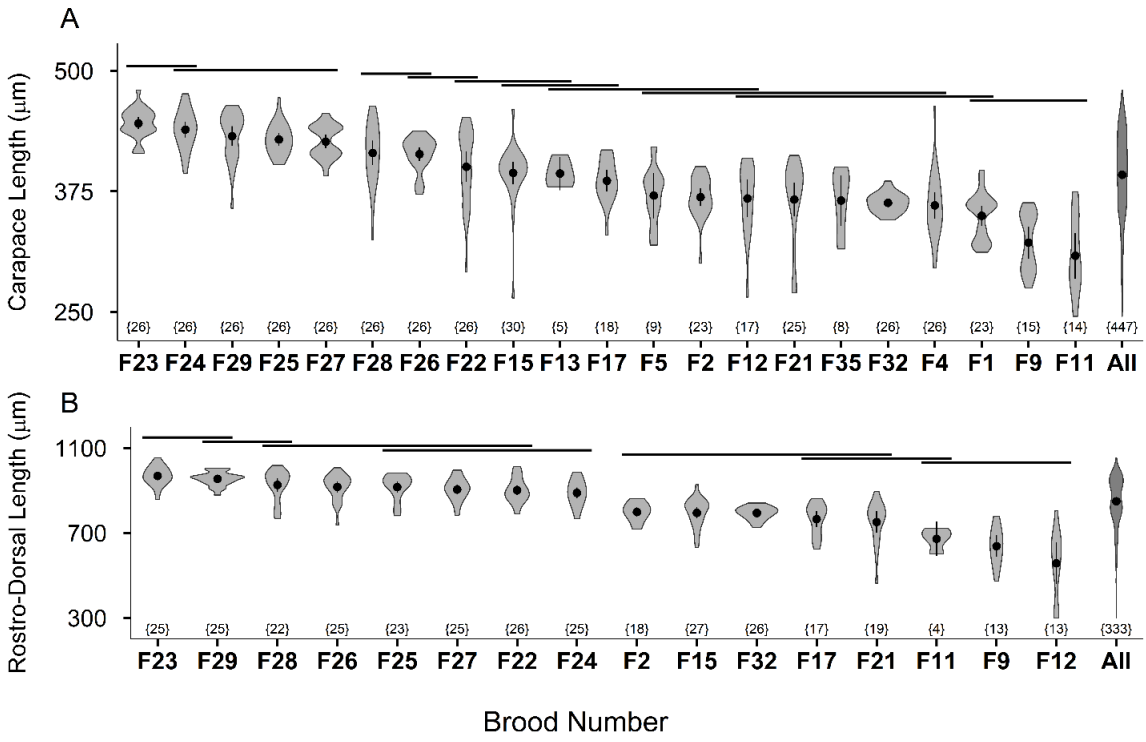

Figure 2-5: *Violin plot of carapace length (A) and rostro-dorsal length (B) for all first stage zoeae of each brood from 2017 experiments. Black dots and vertical bars show mean and 95% confidence intervals for each brood. Numbers in brackets below violins show the number of zoeae measured from each brood. Horizontal black bars above show statistically similar groups (Kruskal-Wallace (K-W) post-hoc test). Zoeal carapace length (K-W: $H(20) = 304.97$, $p << 0.01$) and rostro-dorsal length (K-W: $H(20) = 26.46$, $p << 0.01$) both significantly differed by brood.*

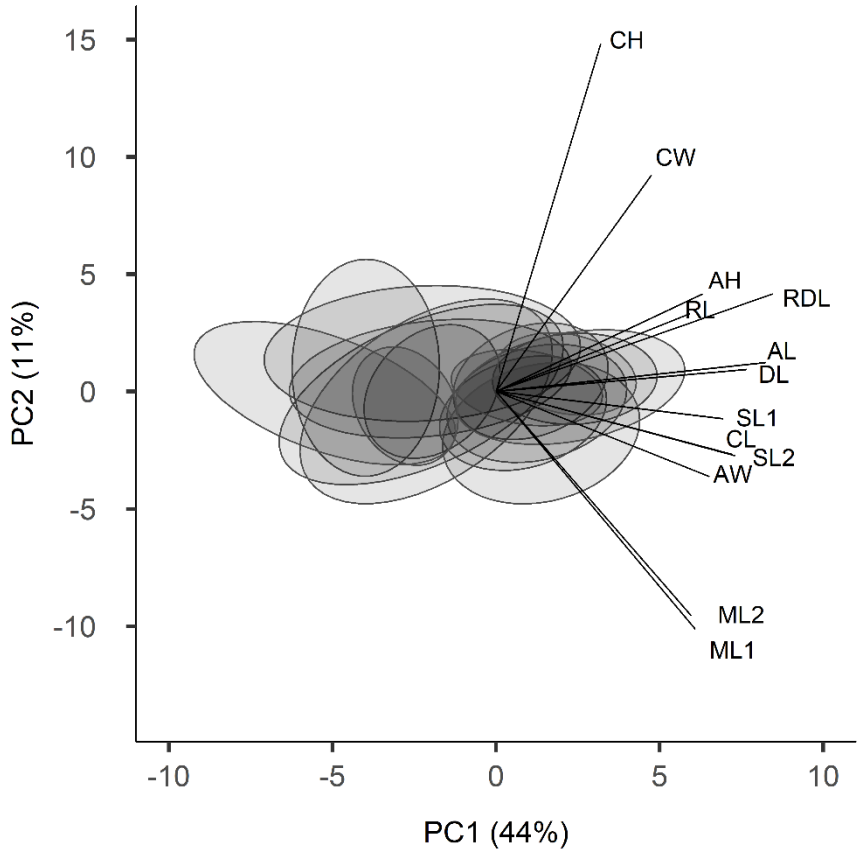

Figure 2-6: *Principal component analysis (PCA) of all first stage zoeal morphometrics from 2016 and 2017. Ellipses cover 95% of the data from each brood. Radiating lines show the eigenvectors associated with each metric in the analysis. The magnitude and direction of these lines show the relative contribution of each principal component.*

Differences in brood-level zoeal morphology result in differences in estimated U_T and F_D (Figure 2-7). Broods located towards the lower-left corner should have a higher swimming efficiency than broods in the upper-right corner. Broods differ significantly for both variables (MANOVA: $F(19,401) = 22.54$, $p<<0.01$, Wilk's $\Lambda = 0.23$). There is a

positive brood-level correlation between U_T and F_D (R^2=0.6, n = 20, p=0.006) and a 2-fold difference in brood means for both variables.

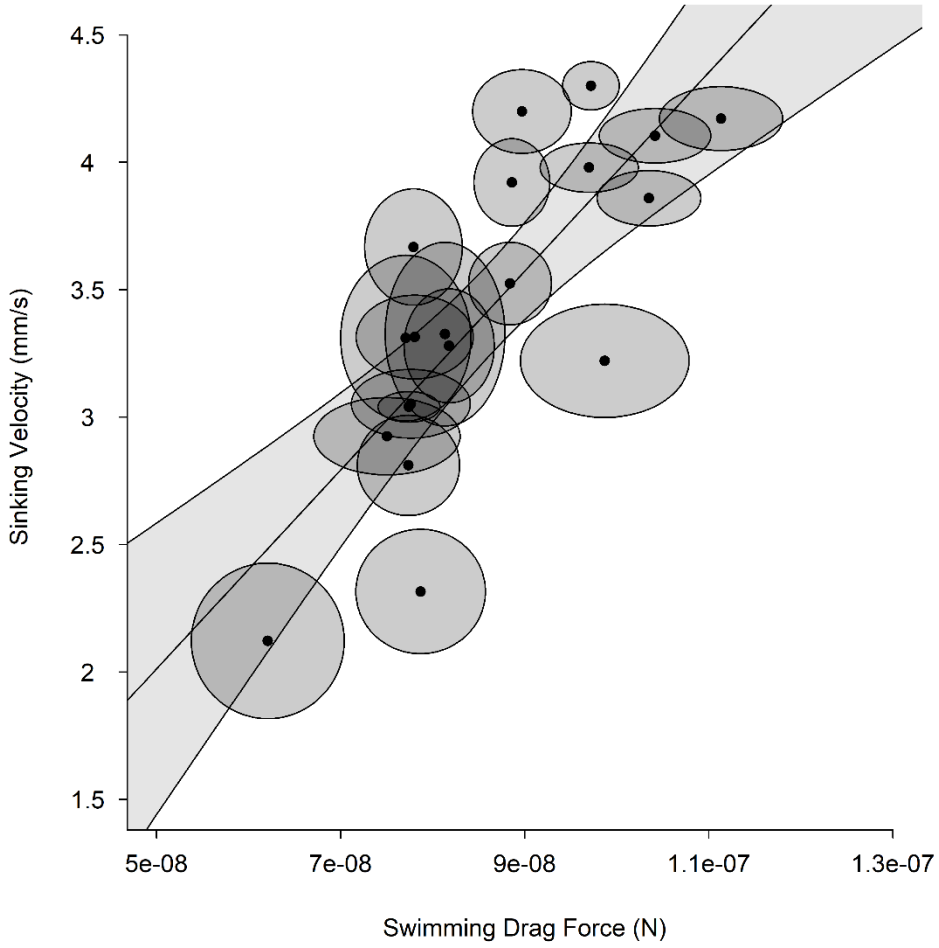

Figure 2-7: *Swimming drag (F_D) and terminal sinking velocity (U_T) were modeled for each brood with observed estimated volumes and cross-sectional areas from observations. A linear regression shows a positive correlation between brood median F_D and U_T (R^2 = 0.60, α = 0.06, β = 3.9 x 10^7, n = 20, p << 0.01). Points represent brood medians and ellipses represent 95% data ellipses. There were significant differences among broods (MANOVA: F(19,401) = 22.54, p<<0.01, Wilk's Λ = 0.23). Data represents observations made in 2016 and 2017.*

2.3.3 Relationship between maternal characteristics and zoeal morphology

Although four combinations of maternal characteristics and zoeal morphometrics appear to be related, regression analysis of all 56 combinations showed no statistically significant correlations after Bonferroni alpha corrections (all $p > 8.9 \times 10^{-4}$). Maternal characteristics thus did not prove to be significant predictors of zoeal morphology.

2.4 Discussion

2.4.1 Overall Morphological variability

Morphological variability is thought to be a product of genetics, an organism's environment, and stochasticity (Monteiro et al. 2000). The degree of variability in certain traits can be the result of evolutionary adaptations or non-adaptive constraints on morphology (Gotthard and Nylin 1995). Intraspecific morphological variability has been observed in larval *C. sapidus* (Costlow 1965) and is well-documented in other larval decapods (DeBrosse et al. 1990; Thatje and Bacardit 2000; Guay et al. 2011; Tamura et al. 2017). In this study, spine lengths are some of the more variable one-dimensional metrics. Longer carapace spines decrease larval fish predation by increasing apparent size and physically damaging predators (Morgan 1987; Bollache et al. 2006). Zoeae of *Rhithropanopeus harrisii* also express differences in spine lengths across broods, and have been observed to develop longer spines when exposed to fish kairomones (Charpentier et al. 2017). The high variability in *C. sapidus* spine lengths may indicate either an adaptation which allows a brood of zoeae to defend against a range of predators or a stochastic response. Conversely, abdominal height (AH) and width (AW) are more constrained metrics, and the narrowness of their distributions and low MAD* may be due to the physics

of abdominal contractions. During these contractions, a wider abdomen, though providing more surface area, produces proportionally higher drag. AH is proportional to the Reynolds number (Re) of the abdomen during contraction. Altering the Re of an abdominal contraction could result in unfavorable changes in the fluid flow during contraction. It is possible that the low variability in AH and AW is a result of an optimization of the mechanics of contraction.

The shape of body structures also influences their functionality. Zoeal carapace shape influences drag while sinking and swimming, by influencing C_D. CL:CW and CW:CH relate to the shape of the zoea in the sinking and swimming orientations, respectively. Though these two ratios express variability, they both have lower MAD* than their one-dimensional components. The relatively low variability for these ratios may be due to selective pressure for a carapace shape that allows minimization of drag forces while in motion (Lagergren et al. 1997; Lord et al. 2006). Drag experienced by zoeae and the degree of optimization may thus show variability within the population. The cumulative effect of suboptimal drag conditions over the span of larval development could result in an increased energy expended to maintain a zoea's vertical position. A difference in the energetic budget of zoeae as a result of altered swimming mechanics could result in compromised growth (Lambert 1989; Power 1989), which has been shown to impact later life-history stages in other species (Bennett and Marshall 2005; Przeslawski and Webb 2009). Swimming ability and energetic considerations may also be important as they relate to environmental variability. Weather events or changes in coastal circulation within a given year may produce situations where zoeae need to swim against stronger turbulence in order to stay in surface waters and where zoeae that are strong swimmers would be

favored. Alternatively, in more mild conditions where vertical currents are relatively weak and it is not necessary for zoeae to be strong swimmers, the development of larger swimming appendages may actually be unfavorable. Larvae with larger swimming appendages are generally larger overall (Figure 2-6) and will likely have increased metabolic costs. In milder conditions, these increased metabolic costs may outweigh the benefits of stronger swimming. The morphological variability of later zoeal stages is outside the scope of this study, but a similar degree of variability may persist throughout zoeal development in order to ensure that some zoeae are equipped to survive in changing environmental conditions.

2.4.2 Inter-brood Morphological Differences

Larval broods express significant morphological differences, yet multivariate morphology is generally similar across all broods. This suggests that differences between broods in that some metrics may be compensated for by others. In terms of all morphometrics, broods generally are part of one large group without distinct clustering, with most of the differences between broods due to larger offspring in all respects. A study by Tamura et al. (2017) found a similar result for *Pugettia quadridens*, though broods in their analysis were more clearly defined along a gradient. The presence of continuity in brood morphology seen here may be an indicator that a full extent, rather than a subset of morphological variability was captured.

Brood morphology lies along a gradient, and there may be notable effects of these differences on zoeae. Terminal sinking velocity (U_T) and swimming drag force (F_D) were used to quantify possible consequences of brood-level morphological differences. Zoeae are found exclusively near the surface of the water column, and due to their negative

buoyancy must actively swim to maintain that position (Sulkin et al. 1980). To optimize their movement, zoeae should have morphologies that maximize their drag while sinking (lower U_T) and minimize their drag while swimming (lower F_D), minimizing of the energy needed to maintain a vertical position. In other species, swimming has been shown to be both a relatively high (Bennett and Marshall 2005) and relatively low (Vlymen 1970) component of zooplankton energy budgets. However, as far as we know, there have been no studies specifically addressing the energetic cost of locomotion in zoeae. U_T is positively correlated with F_D for zoeae in this study, which may be due to the ellipsoidal shape of the blue crab zoeal carapace, where the cross-sectional areas in the sinking and swimming orientation are inversely proportional. Also due to this correlation, the effects of differences in brood morphology are amplified, as broods' zoeae that sink faster will also experience more drag while swimming. While the precise effect of inter-brood differences in swimming dynamics is still unknown, these results suggest that the fitness of larvae between broods might not be equal.

Since all adult crabs were caught from the same wild population and laboratory conditions were kept similar for all females, hatched zoeae from different broods should be comparable. However, it is worth noting that zoeae observed in this study may not be entirely representative of their wild counterparts. Gravid females were kept at constant temperature and salinity without natural diurnal changes. Temperature and salinity have been shown to influence the development of crab zoeae (Costlow and Bookhout 1959); therefore, fluctuations in environmental conditions could result in differences in zoeae morphology that is not represented here. Gravid females were also captured at varying stages of egg development, so their time in laboratory conditions was not constant. Any

laboratory-induced effects related to holding egg-bearing females might have differed between broods as a result.

2.4.3 Relationship between maternal characteristics and zoeal morphology

Among decapod taxa, maternal and offspring size can be either strongly correlated or unrelated (Fox and Czesak 2000; Swiney et al. 2013). Positive correlations between maternal and larval size have been observed in the coconut crab *Birgus latro* (Sato and Suzuki 2010) and the caridean *Palaemon serratus* (González-Ortegón and Giménez 2014). Fecundity is thought to generally be inversely correlated with offspring size, but there is mixed evidence for such a trade-off among crustaceans (Fox and Czesak 2000). A positive relationship between fecundity and larval size has been observed in the grapsoid crab *Chasmagnathus granulatus* (Bas et al. 2007) and the caridean shrimp *Paratya australiensis* (Walsh 1993). For *C. sapidus*, no relationship between maternal size and zoeal size has been observed (Darnell et al. 2009; Koopman and Siders 2013). Darnell et al. (2009) also observed a decrease in progressive clutch sizes in blue crabs with no change in zoeal size. In this study a much broader set of zoeal morphologies was examined and still no correlation to maternal size or fecundity was found, yet there were significant differences in zoeal morphology between broods. These inter-brood differences in morphology may be due to maternal effects, in that differences in zoeae's morphological characteristics are the result of varying maternal behavior or environmental conditions prior to hatching (Marshall et al. 2008). Paternal effects may also be present, but as female crabs mate a year before spawning (van Engel 1958), the mates of the wild-caught females used in this study are unknown.

Salinity and temperature have been shown to alter blue crab egg development time and hatching success (Costlow and Bookhout 1959). Broad environmental conditions that eggs develop in can also result in developmental differences in zoeae (Shirley et al. 1987; Wehrtmann and López 2003). Low salinity has shown to increase RDL:CL of *Eriocher sinensis* over development (Anger 2003), which was hypothesized as a morphological response to lower fluid density by increasing zoeal buoyancy. Maternal nutrition may also influence early larval development by altering the lipid and nutritional content of the eggs (Allen et al. 2008). The elemental composition of eggs has been shown to correlate with larval biomass in *Chasmagnathus granulate* (Giménez and Anger 2001; Bas et al. 2007); however, it is unknown how the composition of *C. sapidus* eggs relates to larval size or morphology. Though it was not possible to control for all pre-hatching environmental variables for wild-captured gravid females, we made observations on zoeae as early upon hatching as possible, with the aim to minimize potential environmentally-induced changes in morphology.

Other potential sources of inter-brood morphological variation in zoeae include seasonal and inter-annual changes in the brooding environment. Seasonal changes in morphology have been documented in megalopae (Ogburn et al. 2011) and zoeae (Stuck et al. 2009). Stuck *et al.* (2009) observed that zoeae were generally larger in the summer and fall. Similarly, laboratory conditions were kept static, and may have altered egg development as a function of time spent in laboratory before hatching. While these factors may be important drivers of variability, the opportunistic nature of our crab collection does not let us adequately differentiate these sources of variability. Egg stage, month, and year are highly conflated in our dataset, as the majority of the crabs (12 of 21) were captured in

June of 2017 and where two-thirds of those arrived into the laboratory with dark eggs. However, even when analyzing the morphology of only zoeae hatched from mothers collected in June of 2017, there are still significant inter-brood morphological differences (MANOVA: $F(11,185) = 5.01$, $p << 0.01$, Wilk's $\Lambda = 0.04$).

Since significant morphological variability was observed among zoeae in this study, there is likely to be differences in their anti-predatory defenses, swimming ability, sinking velocity, and energy expenditures. Identifying ways to characterize the zoeal population in terms of chances of survival and successful dispersal would help predict settlement and possibly recruitment. Though maternal size and fecundity were not significant predictors of zoeal morphology, there may be other means of forecasting zoeal fitness, such as population genetics or environmental conditions during the spawning season. A good predictor of morphology should aim to correlate to multiple morphometrics with similar functionality.

The general morphology of first stage *Callinectes sapidus* zoeae is variable, and larval broods had significant morphological differences. Though laboratory conditions did not entirely mimic natural conditions, these results suggest that inter-brood morphological differences in the wild zoeal population could be significant. The results of this study have important implications in future experimental work with blue crab zoeae. Studies investigating *C. sapidus* zoeal morphology or the functionality derived from morphology (e.g. locomotion, anti-predatory defenses, feeding, etc.) must consider the significant inter-brood morphological differences observed here. Multiple broods should be hatched to encompass a more complete range of morphological traits, otherwise results may not be representative of the entire population. Furthermore, point estimates of

morphological characteristics may inadequately represent zoeal populations. The amount of variation and the shape of distributions of morphologies should be considered when investigating the effects of morphology on zoeal populations, especially with regards to larval dispersal and energetics. Further research should address (1) the effect of morphological variability on predation and behavior, (2) the cumulative effects on survival and dispersal of inter-brood morphological differences over development in blue crab zoeae, and (3) identifying significant maternal or environmental predictors of zoeal morphology.

2.6 Literature Cited

Allen RM, Buckley YM, Marshall DJ (2008) Offspring size plasticity in response to intraspecific competition: an adaptive maternal effect across life-history stages. Am Nat 171:225–237. doi: 10.1086/524952

Anger K (2003) Salinity as a key parameter in the larval biology of decapod crustaceans. Invertebr Reprod Dev 43:29–45. doi: 10.1080/07924259.2003.9652520

Bas CC, Spivak ED, Anger K (2007) Seasonal and interpopulational variability in fecundity, egg size, and elemental composition (CHN) of eggs and larvae in a grapsoid crab, *Chasmagnathus granulatus*. Helgol Mar Res 61:225–237. doi: 10.1007/s10152-007-0070-y

Bennett CE, Marshall DJ (2005) The relative energetic costs of the larval period, larval swimming and metamorphosis for the ascidian *Diplosoma listerianum*. Mar Freshw Behav Physiol 38:21–29. doi: Doi 10.1080/10236240400029333

Bollache L, Kaldonski N, Troussard JP, Lagrue C, Rigaud T (2006) Spines and behaviour as defenses against fish predators in an invasive freshwater amphipod. Anim Behav 72:627–633. doi: 10.1016/j.anbehav.2005.11.020

Charpentier CL, Wright AJ, Cohen JH (2017) Fish kairomones induce spine elongation and reduce predation in marine crab larvae. Ecology 98:1989–1995. doi: 10.1002/ecy.1899

Chia F-S, Buckland-Nicks J, Young CM (1984) Locomotion of marine invertebrate larvae: a review. Can J Zool 62:1205–1222.

Costlow JDJ (1965) Variability in larval stages of the blue crab, *Callinectes sapidus*. Biol Bull 128:58–66.

Costlow JDJ, Bookhout CG (1959) The larval development of *Callinectes sapidus* Rathbun reared in the laboratory. Biol Bull 116:373–396.

Darnell MZ, Rittschof D, Darnell KM, McDowell RE (2009) Lifetime reproductive potential of female blue crabs *Callinectes sapidus* in North Carolina, USA. Mar Ecol Prog Ser 394:153–163. doi: 10.3354/meps08295

Darnell MZ, Rittschof D, Forward RBJ (2010) Endogenous swimming rhythms underlying the spawning migration of the blue crab, *Callinectes sapidus*: ontogeny and variation with ambient tidal regime. Mar Biol 157:2415–2425. doi: 10.1007/s00227-010-1506-5

de Mendiburu F (2015) Agricolae: statistical procedures for agricultural research.

DeBrosse G, Sulkin S, Jamieson G (1990) Intraspecific morphological variability in megalopae of three sympatric species of the genus *Cancer* (Brachyura: Cancridae). J Crustac Biol 10:315–329.

Epifanio CE (1988) Dispersal strategies of two species of swimming crab on the continental shelf adjacent to Delaware Bay. Mar Ecol Prog Ser 49:243–248.

Epifanio CE (1995) Transport of blue crab (*Callinectes sapidus*) larvae in the waters off Mid-Atlantic states. Bull Mar Sci 57:713–725.

Fox CW, Czesak ME (2000) Evolutionary ecology of progeny size in arthropods. Annu Rev Entomol 45:341–369. doi: 10.1146/annurev.ento.45.1.341

Fox J, Weisberg S (2011) An R companion to applied regression, 2nd edn. Sage, Thousand Oaks, CA

Foxon GEH (1934) Notes on the swimming methods and habits of certain crustacean larvae. J Mar Biol Assoc United Kingdom 19:829–850. doi: 10.1017/S0025315400046816

Giménez L, Anger K (2001) Relationships among salinity, egg size, embryonic development, and larval biomass in the estuarine crab *Chasmagnathus granulata* Dana, 1851. J Exp Mar Bio Ecol 260:241–257.

González-Ortegón E, Giménez L (2014) Environmentally mediated phenotypic links and performance in larvae of a marine invertebrate. Mar Ecol Prog Ser 502:185–195. doi: 10.3354/meps10708

Gotthard K, Nylin S (1995) Adaptive plasticity and plasticity as an adaptation: a selective review of plasticity in animal morphology and life history. Oikos 74:3–17.

Guay C, Sainte-Marie B, Brêthes J-C (2011) Strong maternal effects and extreme heterogeneity of progeny development in the caridean shrimp *Sclerocrangon boreas* (Crangonidae). Mar Biol 158:2835–2845. doi: 10.1007/s00227-011-1782-8

Hamasaki K, Sugimoto A, Sugizaki M, Murakami Y, Kitada S (2013) Ontogeny of sinking velocity, body density, and phototactic behaviour in larvae of the coconut crab *Birgus latro*: implications for larval dispersal and recruitment in the sea. J Exp Mar Bio Ecol 442:58–65. doi: 10.1016/j.jembe.2013.02.001

Hines AH, Jivoff PR, Bushmann PJ, van Montfrans J, Reed SA, Wolcott DL, Wolcott TG (2003) Evidence for sperm limitation in the blue crab, *Callinectes sapidus*. Bull Mar Sci 72:287–310.

Johnson DF, Hess KW (1990) Numerical simulations of blue crab larval dispersal and recruitment. Bull Mar Sci 46:195–213.

Koopman HN, Siders ZA (2013) Variation in egg quality in blue crabs, *Callinectes sapidus*, from North Carolina: does female size matter? J Crustac Biol 33:481–487. doi: 10.1163/1937240X-00002152

Lagergren R, Hellsten M, Stenson JAE (1997) Increased drag, and thus lower speed: a cost for morphological defence in *Bosmina* (*Eubosmina*) (Crustacea: Cladocera). Funct Ecol 11:484–488. doi: 10.1046/j.1365-2435.1997.00117.x

Lambert W (1989) The adaptive significance of diel vertical migration of zooplankton. Funct Ecol 3:21–27. doi: 10.2307/2389671

Lipcius RN, Stockhausen WT (2002) Concurrent decline of the spawning stock, recruitment, larval abundance, and size of the blue crab *Callinectes sapidus* in Chesapeake Bay. Mar Ecol Prog Ser 226:45–61.

Lord H, Lagergren R, Svensson J-E, Lundqvist N (2006) Sexual dimorphism in *Bosmina*: the role of morphology, drag, and swimming. Ecology 87:788–795. doi: 10.1890/05-0082

Marshall DJ, Allen RM, Crean AJ (2008) The ecological and evolutionary importance of maternal effects in the sea. In: Gibson RN, Atkinson RJA, Gordon JDM (eds)

Oceanography and Marine Biology: An Annual Review. Taylor & Francis, New York, pp 203–250

McConaugha J (1992) Decapod larvae: dispersal, mortality, and ecology. A working hypothesis. Am Zool 32:512–523.

Millikin MR (1978) Blue crab larval culture: methods and management. Mar Fish Rev 40:10–17.

Millikin MR, Williams AB (1984) Synopsis of biological data on the blue crab, *Callinectes sapidus* Rathbun.

Monteiro LR, Bordin B, Furtado dos Reis S (2000) Shape distances, shape spaces and the comparison of morphometric methods. Trends Ecol Evol 15:217–220. doi: 10.1016/S0169-5347(99)01775-9

Morgan SG (1987) Morphological and behavioral antipredatory adaptations of decapod zoeae. Oecologia 73:393–400.

Morgan SG (1992) Predation by planktonic and benthic invertebrates on larvae of estuarine crabs. J Exp Mar Bio Ecol 163:91–110. doi: 10.1016/0022-0981(92)90149-5

Ogburn MB, Stuck KC, Heard RW, Wang SY, Forward RBJ (2011) Seasonal variability in morphology of Blue Crab, *Callinectes sapidus*, megalopae and early juvenile stage crabs, and Distinguishing characteristics among co-occurring *Portunidae*. J Crustac Biol 31:106–113. doi: 10.1651/09-3241.1

Ogburn MB, Hall M, Forward Jr. RB (2012) Blue crab (*Callinectes sapidus*) larval settlement in North Carolina: environmental forcing, recruit-stock relationships, and numerical modeling. Fish Oceanogr 21:20–32. doi: 10.1111/j.1365-2419.2011.00606.x

Paolisso M (2007) Taste the traditions: Crabs, crab cakes, and the Chesapeake Bay blue crab fishery. Am Anthropol 109:654–665.

Power JH (1989) Sink or swim: Growth dynamics and zooplankton hydromechanics. Am Nat 133:706–721.

Prager MH, McConaugha JR, Jones CM, Geer PJ (1990) Fecundity of blue crab, *Callinectes sapidus*, in Chesapeake Bay: biological, statistical and management considerations. Bull Mar Sci 46:170–179.

Przeslawski R, Webb AR (2009) Natural variation in larval size and developmental rate of the northern quahog Mercenaria mercenaria and associated effects on larval and juvenile fitness. J Shellfish Res 28:505–510. doi: 10.2983/035.028.0312

R Core Team (2015) R: A language and environment for statistical computing.

Rasband WS (2016) ImageJ.

Rhodes A, Lipton D, Shabman L (2001) A socio-economic profile of the Chesapeake Bay commercial blue crab fishery.

Rohlf JF, Marcus LF (1993) A revolution in morphometrics. Trends Ecol Evol 8:129–132. doi: 10.1016/0169-5347(93)90024-J

Sato T, Suzuki N (2010) Female size as a determinant of larval size, weight, and survival period in the coconut crab, *Birgus latro*. J Crustac Biol 30:624–628. doi: 10.1651/10-3279.1

Sharqawy MH, Lienhard V JH, Zubair SM (2011) Thermophysical properties of seawater: A review of existing correlations and data. Desalin Water Treat 29:355–355. doi: 10.5004/dwt.2011.2947

Sheather SJ, Jones MC (1991) A reliable data-based bandwidth selection method for kernal density estimation. J R Stat Soc Ser B 53:683–690.

Shirley SM, Shirley TC, Rice SD (1987) Latitudinal variation in the dungeness crab, Cancer magister: zoeal morphology explained by incubation temperature. Mar Biol 95:371–376.

Siedler G, Peters I (1986) Physical properties (general) of sea water. In: LANDOLT-BÖRNSTEIN, Numerical Data and Functional Relationships in Science and Technology, New Series, Oceanography. Springer, Berlin, pp 233–264

Smith AE, Jensen GC (2015) The role of carapace spines in the swimming behavior of porcelain crab zoeae (Crustacea: Decapoda: Porcellanidae). J Exp Mar Bio Ecol 471:175–179. doi: 10.1016/j.jembe.2015.06.007

Stagg C, Whilden M (1997) The history of Chesapeake Bay's blue crab (*Callinectes sapidus*): fisheries and management. Investig Mar 25:93–104.

Stuck K, Perry H, Graham D, Heard RW (2009) Morphological characterisitics of early life history stages of the blue crab, *Callinectes sapidus* Rathbun, from the Northern Gulf of Mexico with a comparison of studies from the Atlantic seaboard. Gulf Carribean Res 21:37–55. doi: 10.18785/gcr.2101.05

Sulkin S (1975) The significance of diet in the growth and development of larvae of the blue crab, *Callinectes sapidus* Rathbun, under laboratory conditions. J Exp Mar Bio Ecol 20:119–135.

Sulkin SD (1984) Behavioral basis of depth regulation in the larvae of brachyuran crabs. Mar Ecol Prog Ser 15:181–205. doi: 10.3354/meps015181

Sulkin SD, van Heukelem W, Kelly P, van Heukelem L (1980) The behavioral basis of larval recruitment in the crab *Callinectes sapidus* Rathbun: a laboratory investigation of ontogenetic changes in geotaxis and barokinesis. Biol Bull 159:402–417.

Swiney KM, Eckert GL, Kruse GH (2013) Does maternal size affect red king crab, *Paralithodes camtschaticus*, embryo and larval quality? J Crustac Biol 33:470–480. doi: 10.1163/1937240X-00002162

Tamura H, Landeira JM, Goshima S (2017) Morphological and morphometric variability in the zoea I larvae of *Pugettia quadridens* (De Haan, 1839): Looking for reliable characters for taxonomic studies on the genus *Pugettia* Dana, 1851 (Majoidea: Epialtidae). Zootaxa 4226:264–272.

Thatje S, Bacardit R (2000) Morphological variability in larval stages of *Nauticaris magellanica* (A. Milne Edwards, 1891) (Decapoda:Caridea:Hippolytidae) from South American waters. Bull Mar Sci 66:375–398.

Tilburg CE, Reager JT, Whitney MM (2005) The physics of blue crab larval recruitment in Delaware Bay: A model study. J Mar Res 63:471–495. doi: 10.1357/0022240053693699

van Engel WA (1958) The blue crab and its fishery in Chesapeake Bay: part 1 - reproduction, early development, growth, and migration. Commer Fish Rev 20:6–17.

Vlymen WiJ (1970) Energy expenditure of swimming copepods. Limnol Oceanogr 15:348–356.

Walsh CJ (1993) Larval development of *Paratya Australiensis* Kemp, 1917 (Decapoda: Caridea: Atyidae), reared in the laboratory, with comparisons of fecundity and egg and larval size between estuarine and riverine environments. J Crustac Biol 13:456–480.

Wehrtmann IS, López GA (2003) Effects of temperature on the embryonic development and hatchling size of *Betaeus emarginatus* (Decapoda: Caridea: Alpheidae). J Nat Hist 37:2165–2178.

White FM (1974) Viscous Fluid Flow. McGraw-Hill, New York

Wong RA (2010) 2010 assessment of the Delaware Bay blue crab (*Callinectes sapidus*) stock.

Chapter 3: Development and Changes in Blue Crab (Callinectes sapidus) Larval Morphology Across Broods

Abstract

The morphology of brachyuran crab larvae (zoeae) can influence a wide range of processes, including anti-predatory defenses, energetics, and swimming behavior. A previous study (Caracappa and Munroe 2018) has identified brood-dependent morphological differences in blue crab (*Callinectes sapidus*) zoeae, and models indicated that these morphological differences may result in differences in swimming-induced drag and sinking velocity. However, that study only addressed the morphology of newly-hatched (first stage) zoeae. In this study, I cultured zoeae from 11 broods further into development (8 days) in order to (1) identify the amount of change in morphology and its variability over time, (2) determine whether brood-dependent morphology persists in older zoeae, and (3) investigate how inter-brood morphological relationships change over time. Within broods, there was significant morphological change by day 8, yet variability did not change for the majority of broods. I provide a new application of network models and profile analysis to investigate changes in zoeal morphology both within and between broods and over time, which allowed an examination of size and shape changes separately. Results showed that morphological shape differences decrease over time, suggesting a trend towards convergence in morphological shape. However, there was no change in the amount of size differences over time, and there were still morphological differences between broods at both times. Models also identified brood-level differences in drag and sinking velocity. Change in drag could not be explained by an increase in swimming velocity alone, where brood-level morphological differences were capable of amplifying

or dampening changes in drag. These results suggest that brood-dependent morphological differences can persist further into development and that these may result in brood-specific larval performance. I recommend future studies aim to quantify brood-level effects on swimming, energetics, and survival.

3.1 Introduction

Blue crabs (*Callinectes sapidus*) support economically valuable fisheries in the eastern Unites States, especially in mid-Atlantic states (Rhodes et al. 2001). Their pelagic larval stage (zoeae) develop over the continental shelf for up to 40 days, where successful recruitment involves export and return to estuarine waters (Epifanio 1988). In the mid-Atlantic, zoeae utilize wind-driven surface currents and rely on seasonal changes in wind-patterns to successfully disperse and recruit to estuaries (Epifanio 1995). During their larval phase, zoeae are presumed to undergo extremely high mortality (McConaugha 1992) and must actively swim and feed. One characteristic of zoeae that can influence their success is their morphology.

Zoeal morphology affects several aspects of survival and behavior. Carapace spines function as defensive structures that can deter and defend against predators (Bollache et al. 2006), slow their passive sinking velocity, and hydrodynamically stabilize zoeae while swimming (Smith and Jensen 2015). As *C. sapidus* larval dispersal requires zoeae to maintain a near-surface position, they must constantly swim upwards to counter their negative buoyancy. Zoeae swim by either maxilliped oscillations or by abdominal contractions (Velazquez 2016). Thrust produced by maxilliped oscillations is proportional to the cross-sectional area of both maxillipeds and fanned setae during their power stroke,

as well as the angular velocity and frequency of strokes (Ford et al. 2005). Similarly, thrust produced during abdominal contractions is related to the anterior cross-sectional area of their abdomens as well as the velocity and frequency of contractions.

In addition to the size of morphological features, the shape of appendages and the zoea as a whole can influence several aspects of performance and energetics. The overall shape of the zoeal carapace can influence the drag larvae experience, where drag is proportional to the cross-sectional area of the zoea in the direction of motion. More oblong carapaces can also reduce drag through streamlining effects. Increased resistance due to drag can make it energetically more costly to swim, and it can decrease the passive sinking velocity of zoeae, reducing the swimming time required to stay near the surface. However, these effects are not necessarily the same magnitude due to asymmetry of zoeal carapaces and changes in swimming and sinking orientations. Shape can also show the dominant processes influencing aspects of larval development. The relative length of carapace spines to body size represents tradeoffs between anti-predator defenses, investment in tissue growth, and swimming behaviors.

Morphological characteristics are not always constant across a population, and previous studies in *C. sapidus* (Caracappa and Munroe 2018) and *Pugettia quadridens* (Tamura et al. 2017) have shown that the morphology of first stage zoeae can vary considerably both within a population and between larval broods. Female blue crabs only mate once, (van Engel 1958) and provide substantial care to their broods, which can both create a mechanism for maternal influences (Jivoff et al. 2007). Brood-dependent morphology may also result in brood-dependent swimming ability, anti-predatory defenses, and energetics. Although the cause for brood-dependent morphology is not yet

known, it may have an origin in genetics, maternal brood care, or natal environments (Caracappa and Munroe 2018). However, these studies only addressed morphological variability for first stage zoeae, and it has not yet been demonstrated whether brood-dependent morphology persists further into development.

For this study, I build off of the observations by Caracappa and Munroe (2018), and investigate zoeal morphology for more developed larvae in three different cases. In the first case, I observed how the morphology of larvae *within* broods change over time. This change can occur via growth (molting) as well as mortality. In the second case, I addressed morphological changes between broods at a given point in time. This is akin to the type of analysis done by Caracappa and Munroe (2018) to investigate inter-brood differences in morphology. In this case, changes represent results of multivariate analyses, and changes in individual morphometrics cannot be inferred from this analysis. In the third case, I investigated how the relationship between broods changes over time. This was to assess whether broods converged or diverged morphologically over time. In all three cases I investigated changes in morphological size, shape, and variability.

3.2 Methods

3.2.1 Organism Collection and Adult Rearing

Eleven ovigerous female blue crabs were obtained via trawling in the southern portion of Delaware Bay, New Jersey between May and August of 2016 (N=4) and 2017 (N=7). Crabs were then placed in 30 L individual static, aerated containers (25±2° C, salinity of 30±2) with 2 cm of sand as substrate and were fed twice a week on oyster meat. Eggs were monitored daily for developmental stage and water was changed three times per

week. Crabs were no longer fed once eggs were within 48 hours of hatching and visible darkening and movement was observed within (Millikin 1978).

3.2.2 Larval Rearing

When eggs hatched, 1000 to 2000 zoeae from each brood were transferred into 15 L aerated static cultures (25±2° C, salinity of 30±2). Cultures received water changes and were cleaned every other day. Zoeae were fed rotifers (*Brachionus plicatilis)* daily as per Zmora et al. (2005). Rotifers were grown in separate cultures fed on *Nannocloropsis spp.* at a salinity of 15. Up to 20 zoeae were sampled from each culture on days 1 and 8, if possible, by pipetting them individually from cultures and preserving them in 70% borate buffered ethanol. Only zoeae that were alive and active were sampled. However, due to preservation issues, some of the sampled zoeae degraded and were not able to be measured.

3.2.3 Morphological Measurements

Morphological analysis for 8 day-old zoeae follows the methods described by Caracappa and Munroe (2018). Preserved zoeae were suspended in a glycerin-ethanol mixture, then photographed using an Olympus SZX10 stereomicroscope camera with an Infinity Lumenera-3 2 Mpx microscope camera. Photographs of each larvae were taken from a lateral perspective and at least one other perpendicular perspective (dorsal or anterior). This allowed for estimates of 3-dimensional shape. The camera was calibrated with a micrometer, and morphology was measured from photographs using imageJ (Rasband 2016).

A subset of morphometrics used by Caracappa and Munroe (2018) was used in this study to reduce the co-linearity between measurements, as well as reduce the number of

possible statistical comparisons. These included the length, width, and height of the zoeal carapace (CL, CW, and CH) and abdomen (AL, AW, and AH). The rostrum length (RL) was used instead of the more common rostro-dorsal length as many zoeae had damaged dorsal spines after collection and preservation. The mean swimming appendage length (SA) was also calculated as the mean length of both pairs of maxillipeds (including setae).

The drag force induced while swimming (F_D) as well as terminal sinking velocity (U_T) was modeled using measured morphological measurements in addition to literature values for other physical and behavioral parameters (Table 1). The models used were based on those in Caracappa and Munroe (2018), and allowed comparison of swimming efficiency between broods across multiple points in development. First stage swimming velocity was 2.5 mm s^{-1} (Caracappa and Munroe 2019). The swimming velocity of older zoeae was estimated to be 5 mm s^{-1}, which was an extrapolated value between stages 1 and 4 zoeae reported by Sulkin et al. (1980). The mass density of individual zoeae was estimated as 1066 kg m^{-3} (Fuchs and Low, unpublished data).

Table 3-1: Description of models of drag force while swimming (F_D) and passive sinking velocity (U_T), based on Caracappa and Munroe (2018).

Metric	Definition	Equation	Details
A_D	Dorsal Cross-sectional Area	$A_D = \pi$ CL × CW	
A_A	Anterior Cross-Sectional Area	$A_A = \pi$ CL × CH	
F_D	Swimming Drag Force	$F_D = \frac{1}{2}\rho_f C_D A_D U^2$	ρ_f = fluid density (1019 kg m^{-3})
C_D	Drag Coefficient	$C_D = \frac{24}{Re} + \frac{6}{1+\sqrt{Re}} + 0.4$	(White 1974)
Re	Reynolds Number	$Re = \frac{AH \times U}{\upsilon}$	ν = 9.5 x 10^{-7} m^2 s^{-1}
U_T	Terminal Sinking Velocity	$U_T = \sqrt{\frac{2g(V_A + V_C)(\rho_z - \rho_f)}{\rho_f A_A C_D}}$	V_A = abdominal volume ($\frac{1}{2}AL \times AW \times AH$), V_C = carapace volume ($\frac{4}{3}\pi CL \times CW \times CH$), ρ_z = zoeal density (1066 kg m^{-3})

3.2.4 Statistical Analysis

Kruskal-Wallace tests were performed to determine both whether morphology differed between broods on the same observation day or between day 1 and day 8 zoeae of the same brood. Profile analysis was used to investigate inter-brood differences in morphology at both ages. Profile analysis is a multivariate method analogous to a repeated-measures ANOVA that tests whether two sets of observations differ in equality and parallelism (Davison and Davenport 2002).

The distinction between changes in morphological shape and size is a crucial component to this study. In the context of morphology, two groups can be said to differ in equality if the magnitude of morphometrics (size) differs between them. A change in size in this study was thus defined as a uniform a shift in magnitude (positive or negative) across

all measured morphologies. Alternatively, two groups would differ in parallelism if the relative relationship between morphometrics (shape) differs between groups. These shape changes are a multivariate measure and do not constitute any single ratio of metrics. Thus it is possible to detect uniform changes in size across metrics, while there may be no changes in the relationship among metrics (and *vice versa*).

A profile analysis, using all measured morphometrics, was performed on all pairwise combinations of broods, testing for equality and parallelism between day 1 and 8. Morphological data was modeled as a network with brood morphology as nodes and the results of profile analyses as connections. This approach allowed for the visualization of patterns and relationships between all broods as well as how those relationships change over time. I then calculated the percentage of inter-brood comparisons that were statistically similar or different, as well as the proportion of inter-brood comparisons that changed their relationship by day 8.

The geometric median absolute deviation (gMAD) was used as a measurement of multivariate morphological variability:

$$gMAD = \sqrt{\sum_{j=1}^{n} median(\left|X_{ij} - \tilde{X}_j\right|)^2} \qquad \textbf{(3.1)}$$

where for each larvae i and variable j, $\tilde{X}_j$ is the median of each variable and X_{ij} are individual observations. gMAD was calculated for each brood at each age, and a bootstrapping routine was used to generate confidence intervals and test for differences in gMAD between groups. Sets of larval morphometrics were randomly drawn, with

replacement, from each brood such that the generated broods contained the same number of larvae as was originally sampled. gMAD was calculated for each generated brood and this process was repeated (N=1,000), and a 95% confidence interval was generated from the distribution of each broods' gMAD. If the gMAD for one brood fell outside the interval for another, the broods were said to have different morphological variabilities. Using this method, I tested for changes in gMAD between day 1 and day 8 within individual broods and whether those relationships changed over time. I also tested whether broods were similar within a given observation day.

A standardized median absolute deviation (MAD*) was used as a measure of variability for individual metrics that is independent of scale, thus allowing for comparisons between metrics. MAD* was calculated as

$$\boldsymbol{MAD^{*}} = \frac{\boldsymbol{median}(\left|\boldsymbol{X_i} - \widetilde{\boldsymbol{X}}\right|)}{\widetilde{\boldsymbol{X}}} \quad \textbf{(3.2)}$$

This allowed us to make comparisons to Caracappa and Munroe (2018) as well as identify the contributions of individual metrics to potential changes in variability. All statistical analyses were performed in R (R Core Team 2015), and profile analyses were performed with the *profileR* package (Bulut and Desjardins 2018).

3.3 Results

Table 3-2: Results of MANOVA testing for multivariate morphological differences between broods and age groups.

	Df	Wilks' λ	F	P
Brood	10	0.11	10.73	$\ll 0.001$
Age	1	0.52	36.84	$\ll 0.001$
Brood × Age	10	0.19	7.45	$\ll 0.001$
Residuals	324			

Upon hatching, one day old zoeae exhibited significant inter-brood differences for all individual morphometrics (K-W, $p<0.05$), and K-W post-hoc comparisons showed 4-7 statistically different groups, where the membership of groups varied by metric (Caracappa and Munroe 2019). In this study, morphological differences between broods were also present for 8 day old zoeae (K-W, all $p<0.05$), with 2-7 statistical groups, depending on the metric. MANOVA results showed significant differences in multivariate morphology between broods, age, and the interaction between the two (Table 3-2).

I also tested whether individual morphometrics changed over time while combining all zoeae and disregarding brood identity. I found that all metrics, except for AH, significantly differed between observation times (K-W, $p<0.05$; Table 3-3). All individual morphometrics increased over time, where CL, CH, AL, and RL each increased by over 10 % (Table 3-4).

Table 3-3: Results of Kruskal-Wallace tests comparing individual morphometrics between day 1 and day 8 across all broods.

Metric	Chi	df	p
CL*	7.1	1	0.01
CW*	6.5	1	0.01
CH*	22.0	1	$\ll$0.001
AL*	11.6	1	0.001
AW*	4.9	1	0.03
AH	1.7	1	0.19
RL*	6.6	1	0.01
SA*	6.4	1	0.01

3.3.1 Profile Analysis and Multivariate Variability

Despite changes in individual morphometrics over time, results of profile analyses showed that multivariate morphology did not always change both in size and shape (Table 3-5). However, all but one brood did change in at least one respect over this time. Brood differences in morphology was present for both age groups (Table 3-6), and there were significant changes in the relationships between broods over that time. The majority of inter-brood comparisons showed differences in shape (parallelism) and size (equality) at both times, and in all cases, broods differed from at least one other brood (Figure 3-1). This indicates a persistence of brood-dependent morphology over time. Profile analyses showed that, there became less shape differences among broods (71% to 53%) and nearly one half of brood comparisons (56%) did not change their relationship. Though this is indicative of some degree of convergence in morphological shape (i.e. an increase in trait similarity over time), broods still maintained statistically significant shape differences. Similarly, a majority of brood comparisons differed in size (58%), but this only increased slightly for older larvae (60%). About one half of comparisons did not change their relationship in terms of size (55%). However, unlike for shape characteristics, there was no appreciable

bias in direction for those relationships that changed, indicating neither convergence nor divergence in morphological size.

Table 3-4: Medians and median absolute deviations (MAD) of 1 and 8 day-old zoeae, as well as the percent change between observations. Median values are in μm.

	CL	CW	CH	AL	AW	AH	RL	SA
Day 1 Median	384.9	284.9	273.9	657.5	104.5	83.8	211.8	220.5
Day 8 Median	412.7	286.7	314.7	727.9	109.4	89.9	231.8	238.9
% Change Median	15.23	3.35	17.35	13.14	9.63	8.47	15.81	9.94
Day 1 MAD	0.07	0.06	0.12	0.11	0.07	0.08	0.11	0.06
Day 8 MAD	0.09	0.11	0.1	0.08	0.06	0.07	0.11	0.08
% Change MAD	22.8	74.4	-13.4	-25.4	-12.8	-14.8	5.6	22.7

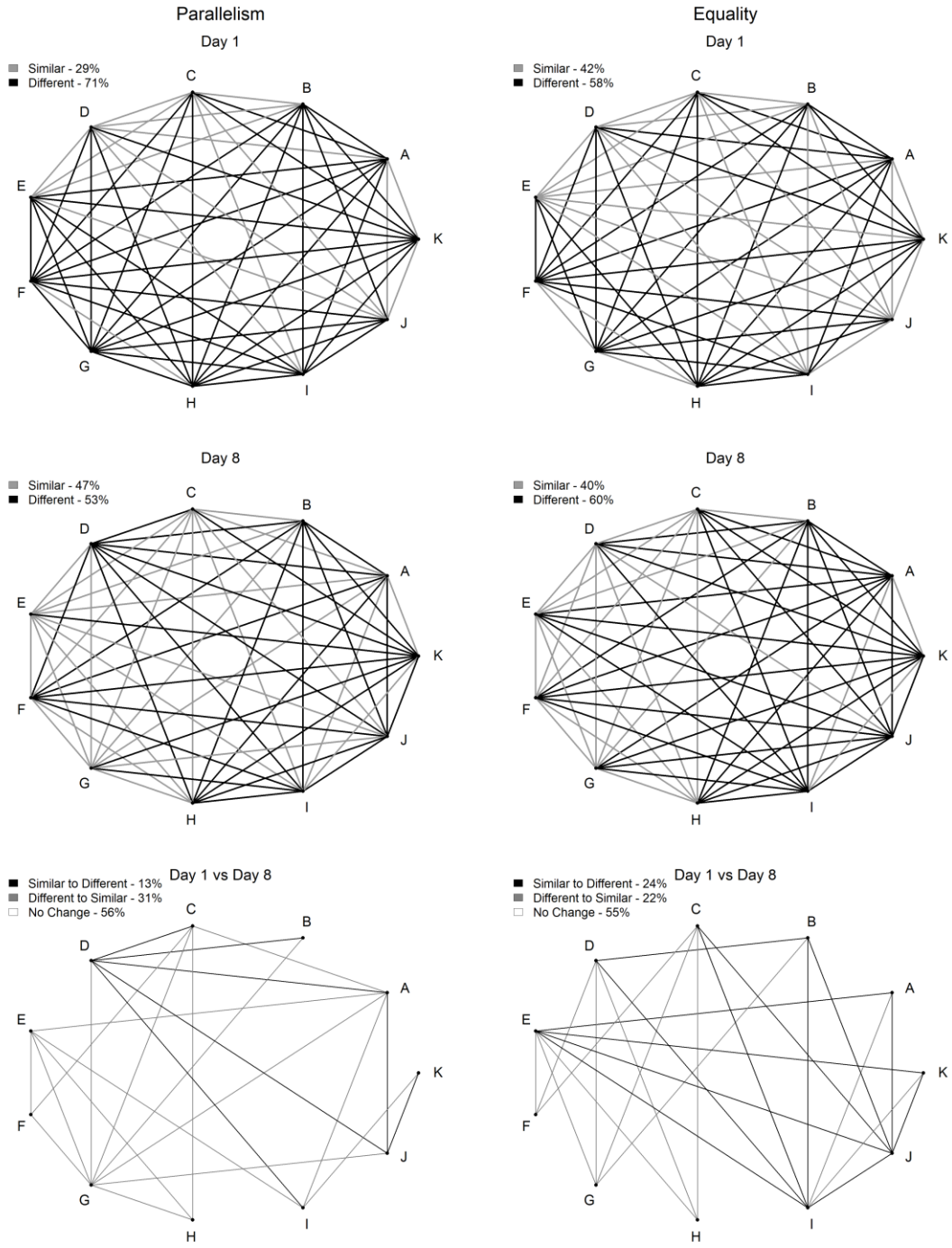

Figure 3-1: *Network models of inter-brood comparisons of morphology based on profile analyses on pair-wise combinations of broods. The first row shows comparisons for one day-old zoeae, the second row shows comparisons for 8 day-old zoeae, and the third row shows the change in relationships between the two observation times. The left column shows the results of tests of equality of means (size), and the right column shows test of parallelism of means (shape).*

Table 3-5: Results of profile analysis comparing age groups within each brood. Asterisks denote statistically significant differences between both times.

Brood	Equality (Size) P value	Parallelism (Shape) P value
A	0.102	≪0.001*
B	<0.001*	0.001*
C	0.846	0.577
D	0.025*	0.054
E	0.053	0.022*
F	<0.001*	0.079
G	0.033*	0.087
H	0.711	0.031*
I	0.216	≪0.001*

Broods exhibited similar amounts of morphological variability (gMAD) at both ages (Table 5). For day 1 zoeae, a strong majority (76%) of brood comparisons showed different degrees of variability. While brood differences in variability decreased by day 8 (64%), 73% of comparisons had no change in their relationship. I also tested whether gMAD changes over time within individual broods. With the exception of two broods, which decreased in variability by day 8, generally gMAD did not change within broods over time.

Table 3-6: Results of profile analysis on 1 and 8 day-old broods. Percentages reflect the proportion of inter-brood comparisons within each comparison category. Shape and size refer to profile analysis tests for parallelism and equality, respectively. The gMAD column shows the changes in the variability (geometric median absolute deviation). "Day 1 vs 8" shows describes the comparison between Day 1 and Day 8 comparisons.

	Comparison	Shape (%)	Size (%)	gMAD (%)
Day 1	Similar	29.1	41.8	23.6
	Different	70.9	58.2	76.4
Day 8	Similar	47.3	40.0	36.4
	Different	52.7	60.0	63.6
Day 1 vs 8	Similar to Different	12.7	23.6	7.3
	Different to Similar	30.9	21.8	20.0
	No Change	56.4	54.5	72.7

3.3.2 Models of Drag and Sinking Velocity

There were significant differences in modeled drag (F_D) and sinking velocity (U_T) between broods at both day 1 and 8 (MANOVA $F(8,125)$, $p \ll 0.001$, Wilk's $\Lambda = 0.41$; Figure 2). Drag increased for all broods as they developed. The majority of the change in drag was due to a constant increase in swimming velocity with age, since drag scales with the square of velocity. Without any changes in morphology an increase in swimming velocity from 2.5 to 5 mm s^{-1} would increase drag 12%. For each brood, the effect of the predetermined increase in swimming velocity was subtracted from the difference in F_D across both points in time. The remainder then was the change in F_D attributable to morphological changes. On average, morphology decreased F_D by 15%, meaning that morphological changes typically dampened the increase in drag one would expect from an increase in swimming velocity. However, morphological effects were capable of dampening this velocity effect by as much as 49%, or increasing them by up to 49%.

Changes in sinking velocity (U_T) were much less pronounced than changes in F_D (Figure 2). There was an average increase in U_T by about 10% across broods, but this was

mostly driven by large increases in three broods. These broods showed large increases in larval volume or decreases in A_A. F_D was positively correlated with U_T (R^2 = 0.70, p = 0.001) for older as well as younger zoeae (R^2=0.60, p = 0.005). However, the slope of these relationships is similar (ANCOVA: p = 0.26). Broods generally fell along a gradient from low F_D and low U_T, to high F_D and U_T. Brood's F_D varied by a factor of 1.8 at day 1 which decreased to a factor of 1.4 by day 8. Similarly, U_T changed from varying by a factor of 1.9 to 1.5. Overall, these results indicate that vertical swimming efficiency remains brood-dependent for older zoeae.

3.4 Discussion

Results of this study suggest that larval broods trend towards a convergence in shape but maintain similar degrees of size differences over a portion of their larval development. Since shape comparisons were multivariate measures, a convergence in shape could be interpreted as a growing similarity in broad morphological features (e.g. a body-plan). However, significant brood-level differences in morphological size and shape were detectible at both observation times, meaning that any convergence is gradual and would likely occur over several molt cycles. Additionally, when comparing gMAD between broods, there seems to be a slight convergence in variability. This indicates that convergence in morphological shape may be related to the changes in the shape of metric distributions rather than simply a convergence in means. Lastly, I find that these morphological changes result in a similar pattern in swimming efficiency indices as for day 1 zoeae, where broods experience differing degrees of swimming efficiency depending on their morphology. Furthermore, depending on the particular nature of broods' morphological changes, these changes can either amplify or dampen the effects of drag.

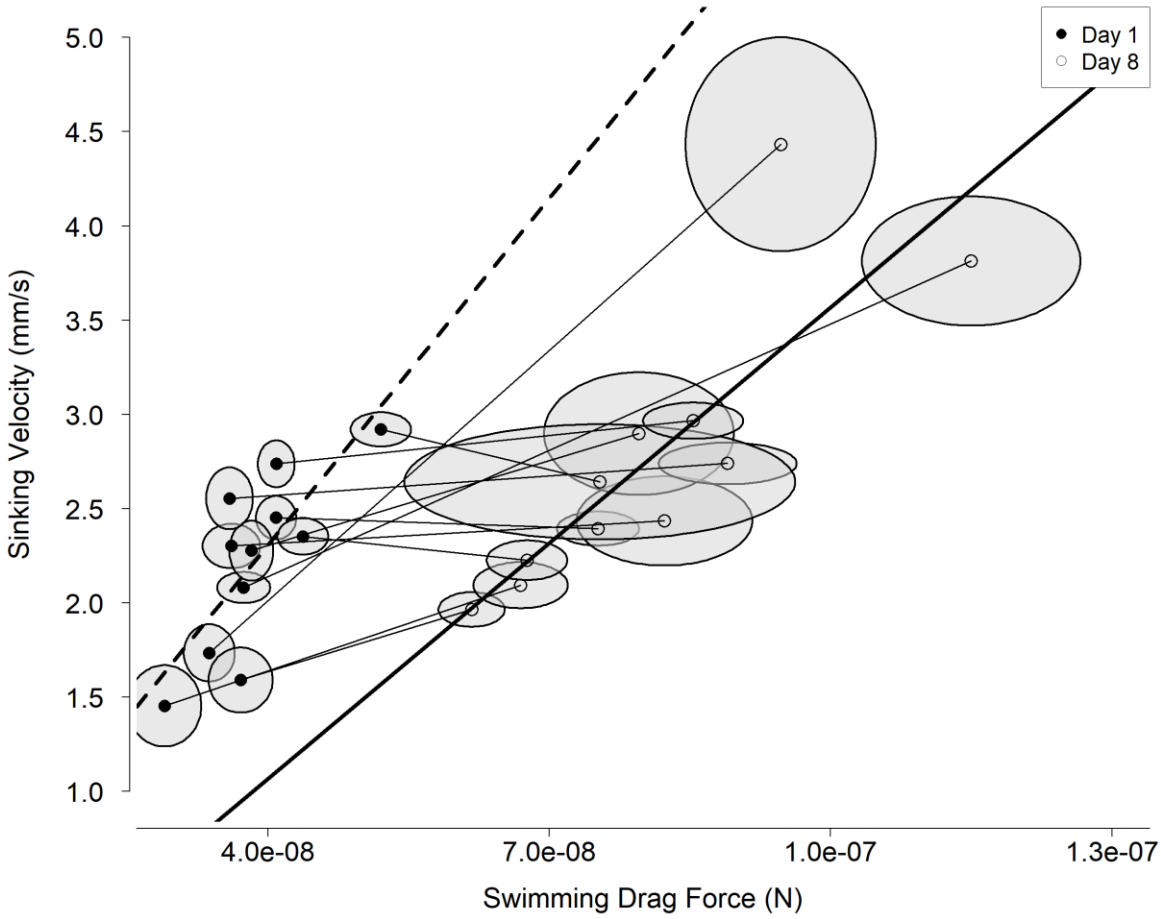

Figure 3-2: *Estimates of modeled swimming drag force and sinking velocity are shown for individual broods at day 1 (solid points) and day 8 (open points). Thin solid lines indicate the trajectories of broods between observations. Ellipses represent the 95% confidence intervals of model estimates. Thicker dashed and solid lines show the results of linear regressions between drag force and sinking velocity for younger and older broods, respectively.*

The fact that broods converge in shape but relationships in size persist indicates that not only can brood-dependent morphology persist into development, but that brood morphology does not change uniformly over time between broods. Day 1 broods do not form consistent groups among one another with respect to individual metrics. In that, while two broods may be similar in one trait, they may differ for another. Since the measure of morphological shape in this study relates to the relative values of morphometrics, it is not

surprising to see changes in shape that did not match changes in size over time. Furthermore, this indicates that there were not unilateral changes across all metrics over time.

The relatively short observation interval in this study, while long enough to detect morphological changes, only represents about one third of the *C. sapidus* zoeal development period. Complications with larval cultures past 8 days led to too few samples of older larvae for statistical significance. Though there are several morphological features that can be used to distinguish the first two larval stages (Costlow and Bookhout 1959), differences between them are not as dramatic as that of later stages. If brood-dependent morphological differences are detectible between successive molt stages, future studies should be able to identify them further into development. However, I am unable to conclude how long or to what degree these differences persist for later stage zoeae.

One caveat of this study was that mortality estimates were not made on broods as they developed. Thus it is not possible to say with certainty whether changes in inter-brood morphological comparisons were due to differential mortality, to growth during molting, or both. In the first case, mortality may differ between broods depending on the particular characteristics (morphological or otherwise) of zoeae. For instance, zoeae with longer spines may sink more slowly and require less energy to stay near the surface, and over time, zoeae with shorter spines may experience higher mortality due to high energetic costs. However, mortality-driven changes in morphology can be related to shape characteristics as well. In the presence of predators, longer spines may deter predation, yet there may be some spine length to body size ratio that optimizes predation and energetic costs. Then, when predators are removed, it may some optimal shape that become dominant over

development. In the second case, broods could become similar or different over time due to differences in growth, whereby upon molting, zoeae change their morphology dependent on environmental cues, available resources, or genetics. I make the case that it was changes due to growth that were observed and not mortality.

Cultures were all kept in similar conditions with the same water sources, food supply, and feeding schedules. There were also no predators present in cultures to create a selective pressure. Given that conditions were similar between broods, differences in growth rates could be attributed to differences in metabolism or maternal influences on the original nutrient content of eggs. Although, environmental conditions (Anger 2003) and predators (Charpentier et al. 2017) can influences morphological traits, it is still unknown how different broods would respond to the same cues. Since there was only a convergence in larval shape, a potential selective pressure would need to act on larval shape characteristics, not necessarily size. Since brood cultures were isolated, in ideal conditions, and without food limitations, a broad shape characteristic that would result in mortality is not obvious to us. If there was some variant on swimming appendage or body morphology that did not allow zoeae to swim against gravity or feed properly, it could experience mortality over this time. This type of phenomenon might also necessitate that the way in which morphology influences mortality changes between broods, such that some broods became more similar and others more different.

An absence of differential mortality is also supported by the fact that broods maintained similar degrees of morphological variability. Presumably, directional mortality within broods should decrease the amount of morphological variability within a brood as unfavorable shapes remove themselves for cultures over time. However, this assumes that

there is some optimal form, and that it was captured by the metrics used in this study. When I analyzed the changes in variability with broods over time, I found that only two broods decreased in variability and the others did not change. Thus, while the precise nature of the convergence in morphological shape cannot be determined, it is likely due to growth.

The ability for zoeae to stay in near-surface waters is crucial for effective larval dispersal. Larval transport and successful reinvasion of estuaries is dependent on their ability to remain within wind-driven surface currents in *C. sapidus*. Zoeae's negative buoyancy necessitates that they must constantly swim to stay afloat, which has the potential to be energetically costly over larval development. One way to estimate a zoea's ability to stay near the surface is to compare how fast it would passively sink (U_T) and the resistance it needs to overcome in order to swim (F_D). Broods whose zoeae experience low drag and slow sinking velocities could be categorized as having a high swimming efficiency as they lose less vertical distance upon resting and need to spend less energy to swim. Caracappa and Munroe (2018) found that F_D and U_T were positively correlated for first stage zoeae, and broods were separated across this efficiency gradient. Similarly, in this study broods at 8 days also lie along a similar gradient, and significant differences were still present for both F_D and U_T among broods. Though much of the change in F_D was due to an increase in swimming velocity, and all broods increased in F_D, morphology acted to either amplify or dampen this velocity effect, depending on brood. The non-uniform increase in F_D and U_T between broods was likely due to the increase in shape differences over time, whereby changes in zoeal carapace shape can increase drag in either orientation. Since size differences between broods did not increase, it follows that there would be an unequal change in F_D and U_T.

It is worth noting that the models of drag and sinking velocity used here make simplifying assumptions regarding the shape of zoeae, where zoeae's carapaces and abdomens are assumed to be ellipsoids and wedges respectively. Additionally, more precise models could incorporate the contribution of spines and swimming appendages, which are not incorporated into the model. More accurate estimates of drag and the energetic costs of swimming may be necessary for other applications, but the purpose of the models in this study were to provide broad comparisons of the influence of morphology between larval broods. Furthermore, drag is not the only factor in determining the energetic expenditure of swimming, and other terms such as acceleration reaction, as well as muscular and mechanical efficiencies would need to be estimated, requiring a more mechanistic model of zoeal swimming.

In conclusion, brood-level morphological differences persist further into development, and broods differences in shape decrease but remain similar in size. Viewing inter-brood comparisons as a network of relationships, in combination with profile analysis, provides a useful way to determine changes in traits over time. Zoeal morphological changes are not uniform across metrics, and changes in shape characteristics occur in a way that minimizes changes in variability. I suggest that changes in morphological relationships signify a slight convergence in morphological shape due to growth. These morphological changes have the potential to result in a decrease in swimming efficiency in the form of a slight increase in sinking velocity and a larger increase in drag. Though changes in drag are very sensitive to changes in swimming velocity, morphological changes increase drag more than an increase in velocity alone. Future studies should focus on analyzing morphological relationships over the entire zoeal

development, coupled with behavior observations of individuals, in order to determine how brood-level variation influences swimming ability.

3.6 Literature Cited

Anger K (2003) Salinity as a key parameter in the larval biology of decapod crustaceans. Invertebr Reprod Dev 43:29–45. doi: 10.1080/07924259.2003.9652520

Bollache L, Kaldonski N, Troussard JP, Lagrue C, Rigaud T (2006) Spines and behaviour as defenses against fish predators in an invasive freshwater amphipod. Anim Behav 72:627–633. doi: 10.1016/j.anbehav.2005.11.020

Bulut O, Desjardins CD (2018) ProfileR: Profile analysis of multivariate data in R.

Caracappa JC, Munroe DM (2018) Morphological variability among broods of first-stage blue crab (*Callinectes sapidus*) zoeae. Biol Bull 235:123–133.

Caracappa JC, Munroe DM (2019) Variability in swimming behavior among broods of blue crab (*Callinectes sapidus*) zoeae. J Exp Mar Bio Ecol 518:151176. doi: 10.1016/j.jembe.2019.151176

Charpentier CL, Wright AJ, Cohen JH (2017) Fish kairomones induce spine elongation and reduce predation in marine crab larvae. Ecology 98:1989–1995. doi: 10.1002/ecy.1899

Costlow JDJ, Bookhout CG (1959) The larval development of *Callinectes sapidus* Rathbun reared in the laboratory. Biol Bull 116:373–396.

Davison ML, Davenport EC Jr. (2002) Identifying criterion-related patterns of predictor scores Using Multiple Regression. Psychol Methods 7:468–484. doi: 10.1037//1082-989X.7.4.468

Epifanio CE (1988) Dispersal strategies of two species of swimming crab on the continental shelf adjacent to Delaware Bay. Mar Ecol Prog Ser 49:243–248.

Epifanio CE (1995) Transport of blue crab (*Callinectes sapidus*) larvae in the waters off Mid-Atlantic states. Bull Mar Sci 57:713–725.

Ford MD, Schuegraf MJ, Elkink MS, Edwin DeMont M (2005) A comparison of swimming structures and kinematics in three species of crustacean larvae. Mar Freshw Behav Physiol 38:79–94. doi: 10.1080/10236240500148934

Jivoff P, Hines AH, Quackenbush LS (2007) Reproduction biology and embryonic development. In: Kennedy VS, Cronin LE (eds) The Blue Crab: Callinectes sapidus. Maryland Sea Grant College, pp 255–298

McConaugha J (1992) Decapod larvae: dispersal, mortality, and ecology. A working hypothesis. Am Zool 32:512–523.

Millikin MR (1978) Blue crab larval culture: methods and management. Mar Fish Rev 40:10–17.

R Core Team (2015) R: A language and environment for statistical computing.

Rasband WS (2016) ImageJ.

Rhodes A, Lipton D, Shabman L (2001) A socio-economic profile of the Chesapeake Bay commercial blue crab fishery.

Smith AE, Jensen GC (2015) The role of carapace spines in the swimming behavior of porcelain crab zoeae (Crustacea: Decapoda: Porcellanidae). J Exp Mar Bio Ecol 471:175–179. doi: 10.1016/j.jembe.2015.06.007

Sulkin SD, van Heukelem W, Kelly P, van Heukelem L (1980) The behavioral basis of larval recruitment in the crab *Callinectes sapidus* Rathbun: a laboratory investigation of ontogenetic changes in geotaxis and barokinesis. Biol Bull 159:402–417.

Tamura H, Landeira JM, Goshima S (2017) Morphological and morphometric variability in the zoea I larvae of *Pugettia quadridens* (De Haan, 1839): looking for reliable characters for taxonomic studies on the genus *Pugettia* Dana, 1851 (Majoidea: Epialtidae). Zootaxa 4226:264–272.

van Engel WA (1958) The blue crab and its fishery in Chesapeake Bay: part 1 - reproduction, early development, growth, and migration. Commer Fish Rev 20:6–17.

Velazquez CCS (2016) The kinematics and particle image velocimetry of the shore crab larvae *Carcinus maenas*. California State University, Fresno

Zmora O, Findiesen A, Stubblefield J, Frenkel V, Zohar Y (2005) Large-scale juvenile production of the blue crab *Callinectes sapidus*. Aquaculture 244:129–139. doi: 10.1016/j.aquaculture.2004.11.012

Chapter 4: Variability in Swimming Behavior among Broods of Blue Crab (*Callinectes sapidus*) Zoeae

This chapter appears in its entirety in *The Journal of Experimental Marine Biology and Ecology* **518** (2019): 151176. DOI: https://doi.org/10.1016/j.jembe.2019.151176

Abstract

Blue crabs (*Callinectes sapidus*) support economically important fisheries across the eastern United States, which have exhibited historical variability in recruitment. Blue crab zoeae develop in surface waters over the continental shelf, where they need to constantly swim upward in order to stay within surface currents to successfully disperse. Morphology influences the drag zoeae experience and their ability to produce thrust, and morphological traits can vary across the population, especially between larval broods. The objectives of this study were to characterize the swimming behavior of first stage *C. sapidus* zoeae, determine whether there were inter-brood differences in swimming behavior, and identify morphological traits that are correlated with swimming behavior. The swimming behavior of zoeae from nine blue crab broods were observed within 24 hours of hatching using video recordings, and metrics relating to velocity, orientation, and path straightness were calculated. Individual zoeae exhibited substantial variability in behavior, and broods significantly differed for all behavioral metrics measured. A mixture model analysis identified two modes of behavior each for velocity, orientation, and path straightness. These behavioral modes exist within individual broods, but the proportions exhibiting each behavior varied. Some morphometrics were significantly correlated with behavior, though some hypotheses based on the theoretical mechanics of zoeal swimming were not confirmed. Zoeal swimming ability, in terms of velocity and path straightness,

varies among individuals within broods, yet across broods patterns of behavior were somewhat similar. The behavioral groups observed may result in inequality in the energetic costs of swimming for zoeae within a given brood, as well as varying optimization of vertical swimming. These results highlight the importance of individual and brood variation in swimming behavior and demonstrate the relationship of morphology in determining swimming behavior. Future work investigating zoeal swimming mechanics and behavior should incorporate this population-level variation.

4.1 Introduction

Blue crabs (*Callinectes sapidus*) are an economically and ecologically important species along the United States Atlantic and Gulf coasts (Rhodes et al. 2001). While adults predominantly inhabit estuarine waters, their larvae (zoeae) are released at the mouths of estuaries and develop in surface waters over the continental shelf (Epifanio 1988). Inter-annual fluctuations in adult crab population have led to investigations of factors that might influence the successful dispersal of zoeae and recruitment of juveniles (Johnson and Hess 1990a; Epifanio 1995; Ogburn et al. 2012). One important aspect of blue crab larval dispersal is their ability to swim, specifically vertical swimming allows larvae to counter negative buoyancy and stay within surface waters.

Coastal surveys have found blue crab zoeae to primarily inhabiting surface waters throughout their larval development (Provenzano 1983; Epifanio 1995). Though the precise dispersal mechanism may vary between systems, the contemporary understanding is that in riverine estuaries, such as the Delaware and Chesapeake bays, zoeae utilize wind-driven surface currents for dispersal. For instance, in Delaware Bay, it is hypothesized that

along shore currents and offshore counter-currents transport zoeae southward then northward, respectively, and they are carried offshore and inshore during upwelling and downwelling events via Ekman transport (Epifanio and Tilburg 2008). This pathway necessitates that zoeae are located within the surface mixed layer, as current regimes can change dramatically at different depths. *C. sapidus* zoeae are negatively buoyant (Sulkin et al. 1980), and must actively swim upwards to maintain this surface position, meaning that upward swimming is near-constant and potentially energetically costly.

General aspects of blue crab zoeal swimming behavior have been well-documented. In laboratory experiments, early stage zoeae exhibit negative geotaxis, positive phototaxis, and tend to swim faster in higher salinities (Sulkin et al. 1980). Zoeae also do not exhibit any endogenous vertical migration (diurnal or otherwise) in the laboratory, unlike other crab species with similar larval dispersal patterns (López-Duarte and Tankersley 2007). There is some evidence that *C. sapidus* zoeae employ predator avoidance behaviors by swimming (Morgan 1987), but it remains unknown which swimming methods are used. Studies modeling swimming mechanics in other zooplankton crustaceans have shown the importance of appendage morphology in propulsion (Morris et al. 1985; Wilkin and Jeffs 2011).

There are two main methods of swimming in zoeae, which we are denoting as "cruise" and "burst" swimming. During cruise swimming, thrust is produced via near-synchronous oscillations of both maxilliped pairs (Ford et al. 2005; Velazquez 2016), and zoeae typically swim in the direction of their dorsal spine (Sulkin 1984). Zoeae's intermediate Reynolds number and multiphase strokes result in an unsteady velocity, but zoeae can swim at relatively constant velocities averaged over longer time periods. Setae

are fanned during the thrust-producing power stroke, increasing their surface-area, and they are retracted during the recovery stroke, decreasing backward motion. The thrust produced during these maxilliped oscillations, should be proportional to the morphology of the appendages (length and cross-sectional area) as well as maxilliped's angular velocity and beat frequency. Alternatively, during burst swimming, zoeae rapidly contract their abdomens for a sharp increase in velocity or changes in direction (Chia et al. 1984; Velazquez 2016). During these motions, thrust is produced based on the contraction velocity of the abdomens as well as their cross-sectional area. Zoeae are quickly slowed by viscous forces during burst swimming, which in turn has a brief duration. When sinking passively, zoeae are oriented with rostrum and dorsal spine horizontal (Sulkin 1984), and drag being produced primarily by the carapace spines and anterior cross-section of the carapace.

Morphology has been shown to vary significantly within and between larval broods in at least two brachyuran crabs, *C. sapidus* (Caracappa and Munroe 2018) and *Pugettia quadridens* (Tamura et al. 2017). Since morphology is an integral component of zoeal swimming ability, we hypothesize that swimming behaviors may vary similarly. To our knowledge, for *C. sapidus*, no study has investigated either the swimming trajectories across multiple larval broods, nor the relationship between zoeae's morphology and swimming behavior. Presumably, across a larval population, some zoeae are better swimmers than others, potentially to the degree that some zoeae are less able to maintain a surface position that will facilitate effective dispersal or do so but with a less efficiency. Potential differences in swimming behavior could also influence the energetic cost of

swimming, a substantial component of crustacean zooplankton energy budgets (Mootz and Epifanio 1974; Levine and Sulkin 1979; Torres 1984).

This study had three main objectives: (1) characterize the swimming behavior of individual first stage blue crab zoeae, (2) determine whether there are inter-brood differences in swimming behavior, and (3) test whether zoeal morphology is correlated to swimming behaviors.

4.2 Methods

4.2.1 Organism Collection and Larval Hatching

Gravid blue crabs were collected in New Jersey estuaries by trawling during the summer of 2018. Nine ovigerous *C. sapidus* were collected: 7 from the lower Delaware Bay and 2 from Barnegat Bay. Crabs were housed in individual 30L plastic bins containing water at salinity of 30 ppt and 2 cm of sand substrate. Water was changed every other day, and crabs were fed oyster meat three times per week. Feedings were suspended when embryos reached late stages of development. After hatching, zoeae from each brood were transferred to separate 20L containers with a salinity of 30 ppt.

4.2.2 Experimental Setup

To record swimming behavior, recently-hatched zoeae (within 24 hours) were placed in a half-gallon plastic aquarium (24cm length x 8cm width x 10cm depth) fixed to a fiberglass base (Figure 4-1). An overhead LED light source (color temperature of 7000 ± 1000 K and intensity of 2250 ± 250 mcd) was fixed 6 cm above the observation region. Thus lighting in this study was slightly cooler than overhead sunlight, and intensity was an order of magnitude greater than similar studies (Forward and Buswell 1989) but still two

orders of magnitude lower than full daylight. The LED light source minimized heat transfer and convection during observations, helping to maintain still-water conditions. Though a full-spectrum light source was used, it was not diffuse. No other light sources were present during observations, and the flat black surface beneath the experimental unit minimized reflection from below. A mm-scale ruler was fixed in the center of the aquarium and within frame of the camera, for scale. The aquarium and camera rig were completely submerged in a water bath (55cm length x 38cm width x 30cm depth), stabilizing the temperature and minimizing refraction during recording. An Olympus Tough TG-5 waterproof digital camera (focal length 4.5-18 mm) was mounted onto the plate at 5 cm from the scale at the center of the aquarium. This corresponded to a field of view 5.6cm wide by 3.2cm tall, located 1 cm above the bottom of the aquarium.

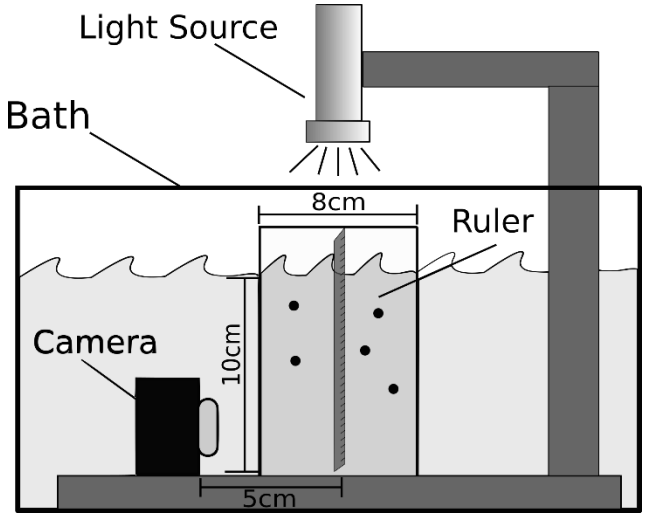

Figure 4-1: *Schematic of video system setup. Aquarium and camera rig were completely submerged in a water bath up to water level in the aquarium.*

Zoeae were all recorded within 24 hours of hatching, were not fed prior to experiments, and no food was present during video observations. Water in the aquarium

was 23 ± 1°C, salinity of 30 ppt, and was passed through a 1 μm filter and UV sterilizer prior to experiments. For each of nine broods, three videos were recorded (1080p resolution, 60 fps) under the digital "super macro" setting, using different groups of zoeae (~100-200) for each video. Zoeae were removed from their hatching containers using a 250 μm sieve, then gently poured into the aquarium using a small beaker. Larvae were allowed to acclimate to aquariums for 10 minutes with only the overhead LED as a light source. This allowed any mixing produced by the introduction of zoeae to dissipate. All observations occurred in the afternoons between 12:00 and 5:00 pm local time, though the precise time varied. Video observations had a duration of 17 minutes with the first 2 minutes excluded due to potential movements generated by starting the recordings.

4.2.3 Swimming Behavior

Videos were analyzed using the open-source software, *Kinovea* (Charmant 2018). For each video, 10 random 5 second periods were selected from the 15 minute experimental recording. Videos were calibrated using the ruler in frame. Up to 5 zoeae were tracked in each 5 second period as long as they remained in frame for up to 5 seconds. If less than 5 zoeae were visible at the start of each 5 second period, additional 5 second periods were selected until swimming tracks of 50 random zoeae were measured per video. *Kinovea*'s auto-tracking tool and some manual adjustments were used to create and export position and time data for each zoea.

Table 4-1: Summary of morphological metrics, abbreviations, and results of Kruskal-Wallace (K-W) tests. P values are adjusted using a Bonferroni correction, and the *Groups* column shows the number of statistically distinct groups from pairwise K-W tests.

Metric	Full Name	Median	P Value	Groups
CL	Carapace Length	376 μm	<0.01	5
CW	Carapace Width	271 μm	<0.01	7
AL	Abdominal Length	684 μm	<0.01	6
AW	Abdominal Width	100 μm	<0.01	5
RDL	Rostro-Dorsal Length	788 μm	<0.01	4
SA	Swimming Appendage Length	460 μm	<0.01	5
A_D	Dorsal Cross-Sectional Area	0.032 mm^2	<0.01	6
A_B	Abdominal Cross-Sectional Area	6.80E-02 mm^2	<0.01	7

Eight metrics were calculated from exported position-time data (Table 4-1). Artefacts in the position data from the auto-tracking tool were removed during post-processing and prior to calculations. These included smoothing over both sharp changes in direction and movements smaller than the precision of the software, which were the result of the angular nature of single pixel movements between frames. Median speed (*s*) was calculated as the median of all non-zero speed increments, in order to characterize *s* only when zoeae were in motion. The median vertical velocity (*w*) was calculated as the median of the vertical components of velocity increments. Maximum speed (s_{max}) and maximum vertical velocity (w_{max}) were both calculated as the 95th percentile of all speed and velocity increments for an individual, respectively. The mean swimming angle (θ) was a measure of the general orientation of zoeae and was calculated as

$$\theta = \tan^{-1} \frac{mean(\sin \theta_i)}{mean(\cos \theta_i)} \quad \textbf{(4.1)}$$

where θ_i is the angle of motion between the timesteps t_i and t_{i-1}. This calculation was used because values for θ_i span from 0 to 360, and an arithmetic mean would poorly describe the motion of zoeae with angles near 0. The proportion of time swimming upward (*P*) was also a metric of orientation and was defined by the time increments where $0<\theta<180$. The net-to-gross displacement ratio (NGDR; *sensu* Buskey, 1984) was calculated both irrespective of direction (NGDR) and for only the vertical component of motion ($NGDR_y$). NGDR has been used as a metric of path efficiency in several zooplankton species including octopus larvae (Villanueva et al. 1996) and copepods (Buskey 1984; Doall et al. 1998) and serves as a measure of general and vertical path straightness, respectively. Simulations showed that the NGDR for random motion would be about 0.03. Lastly, the proportion of time that zoeae were in motion (*M*) was also calculated.

4.2.4 Morphological Observations

After each video was complete, 10 zoeae from each video were sampled at random for morphological analysis (total of 30 zoeae measured per brood). Morphological analysis from Caracappa & Munroe (2018) show that this sample size is sufficient to detect brood-level differences in morphology. Zoeae were suspended in a glcyerine and ethanol solution and photographed using an Olympus SZX10 stereo microscope (Olympus Life Science, MA) with an Infinity 1-3 2-megapixel microscope camera (Ottawa, Ontario, Canada). At least two photos were taken for each zoea with perpendicular perspectives.

Eight morphological metrics were measured on each zoea. The length and width of zoeal carapaces (CL and CW) and abdomens (AL and AW) were measured, where lengths were anterior to posterior, widths were left to right, and heights were ventral to dorsal. Carapace and abdominal dimensions were all perpendicular. Rostro-dorsal length (RDL)

was the straight tip-to-tip spine length of zoeae, and swimming appendage length (SA) was measured as the average length of the first and second maxillipeds plus the mean length of all setae. The dorsal and abdominal cross-sectional area (A_D and A_B) were derived from measured metrics. A_D was estimated using the elliptical area of the carapace from a dorsal perspective ($A_D = \pi CL*CW$). Drag is proportional to the cross-sectional area in the direction of motion and should thus be proportional to A_D while swimming. A_B was calculated as the rectangular ventral area of the abdomen ($A_B = AL*AW$) and is should be proportional to the thrust produced by zoeae during abdominal contractions.

4.2.5 Statistical Analysis

All statistical analyses were performed in R (R Core Team 2015). Since both behavioral and morphological variables, individually, were not normally distributed, a Kruskal-Wallace Test was used to determine whether variables differed between broods. A multivariate analysis of variance (MANOVA) was used to test for multivariate differences in morphology between broods.

4.2.5.1 MIXTURE MODEL

The distributions of swimming variables for individual broods showed visual differences in behavior. Mixture models were used on a subset of swimming variables (*w*, θ, NGDR, $NGDR_y$, and *P*) to identify potentially distinct behavior modes, using the *mixtools* R package (Benaglia et al. 2009). This analysis uses an expectation-maximization algorithm to identify univariate normal distributions that will best sum to the observed overall distribution (component distributions). Mixture model analysis has been used to evaluate modes of behavior in larval gastropods (Fuchs et al. 2004), mussels (Fuchs and Dibacco 2011), and barnacles (DiBacco et al. 2011). Two component distributions were

specified for each analysis, and a bootstrapping routine was used to confirm that two components were sufficient. Mixture model results provide an estimation of the proportion of observations (λ_1 and λ_2) as well as the means (μ_1 and μ_2) of each component distribution.

It was possible that modes of behavior, as described by component distributions, were present across the population and not specific to particular larval broods. Conversely, larvae from particular broods may exhibit different modes of behavior than others, and thus differ in component distributions. To test this, separate mixture models were performed for the distributions of each behavioral metric for each brood. A bootstrapping analysis was used to repeat brood-level mixture models for each variable by repeating random drawings of brood observations for each variable (N=1000) and determining whether the parameters for the overall distribution model (all broods) fell within the credible interval (2.5^{th} and 97.5^{th} percentiles) of the individual brood models. If the component means of the full model fell within the credible interval of the brood-level model parameters, broods were said to have similar modes of behavior. If the proportions within each component were similar to the overall distribution, broods were said to have similar representation in each behavior mode.

4.2.5.2 Regression Analysis

Multiple regressions analysis was used to determine whether correlations were present between zoeal morphology and swimming behavior. Since it was not possible to have corresponding one-to-one measurements for individual zoea's morphology and swimming behavior due to practical constraints, regressions were performed using individual broods as units of observation (N=9). Mean values of for each metric were calculated for zoeae across all three videos per brood. Swimming metrics were tested as a

function of morphological metrics in all instances. In the case of response variables *S*, S_{max}, *w*, and w_{max}, linear regressions were used, while for NGDR, $NGRY_y$, *P*, and *M*, beta regressions were used (Ferrari and Cribari-Neto 2008). Beta regressions can be used to model proportions data (0,1) and assumes that values are described by a beta-distribution. In this regression model, coefficients are estimated that describe each variable's contribution to the model's mean and precision.

While 13 morphometrics were measured, multiple collinearities were present, so a subset of morphologies was used as independent variables in all models, such that collinearity was minimized and metrics represented functional morphology. This subset of morphometrics was chosen *a priori* based on hypothesized relationships to swimming-related functionality. These included RDL, A_D, A_B, and SA, which relate to a one-dimensional measure of size, drag-inducing cross-sectional area, a cross-sectional area related to burst swimming, and overall size of swimming appendages, respectively. Regressions were weighted by the standard deviation of the response variable (behaviors) for each brood. Beta regressions were performed using the *betareg* package in R (Cribari-Neto and Zeileis 2010), and likelihood ratio test was performed on each (Zeileis 2002) to test for significance. The final model for the linear regressions was selected using a stepwise elimination of variables and choosing the model with the lowest AIC. For the beta regression models, all possible combinations of variables (for both mean and precision terms) was calculated, and the model with the lowest AIC was selected.

It was hypothesized that maximum speed and velocity would be positively correlated with A_B, as zoeae that can produce greater thrust during abdominal contractions should reach higher maximum velocities. We also hypothesized that A_D would be

negatively correlated with all speed and velocity metrics, as the increase in drag should inhibit zoeal movement. Similarly, SA should be positively correlated with speed and velocity metrics, as longer appendages should produce more thrust during maxilliped oscillations. Lastly, we hypothesized that RDL would be positively correlated with NGDR, as spines help stabilize zoeae while swimming and may minimize erratic changes in direction.

4.3 Results

4.3.1 Morphological Observations

Morphological measurements were made on 270 zoeae (30 from each of 9 broods). Multivariate morphology varied significantly between broods (MANOVA $F(8,234)$, $P<<0.01$, Wilk's $\Lambda = 0.15$). Individual morphometrics were not normally distributed (Shapiro-Wilk $p<0.05$), and brood morphology differed for all metrics measured (K-W, $p<0.05$; Table 4-1). Broods were divided into 4 to 7 statistically similar groups depending on the metric, but there were no obvious patterns in how broods grouped across metrics. These morphological differences were comparable to those seen by Caracappa and Munroe (2018).

4.3.2 Swimming Behavior

4.3.2.1 General Characteristics

A total of 1,350 zoeae (150 from each of 9 broods) were measured in video observations. Individual swimming tracks varied visually in terms of direction and pattern of motion. While some zoeae traveled in relatively straight trajectories, others moved erratically, and others barely moved at all (Figure 4-2). No behavioral metrics were

normally distributed (Shapiro-Wilk, $p<0.05$). K-W tests showed significant differences between broods for all behavioral metrics, with broods being split in 4 to 8 distinct groups (Table 4-2). Similar to the morphological differences between broods, a pair of broods may have been similar for one behavioral metric while differing for another (Figure 4-3).

Table 4-2: Summary of behavioral metrics, abbreviations, and results of Kruskal-Wallace (K-W) tests. *s*, s_{max}, *w*, and w_{max} were measured in mm s^{-1}. NGDR, $NGDR_y$, *P*, and *M* were measured as ratios from 0 to 1. P values are adjusted using a Bonferroni correction. The G*roups* column shows the number of statistically distinct groups from pairwise K-W tests.

Metric	Description	Median	Min	Max	P Value	Groups
s	Median Speed	2.50	0.86	13.96	<0.01	6
s_{max}	Maximum Speed	5.81	0.22	27.06	<0.01	4
w	Median Vertical Velocity	0.00	-9.96	9.83	<0.01	6
w_{max}	Maximum Vertical Velocity	0.00	-3.59	23.97	<0.01	4
NGDR	Net-to-Gross Displacement Ratio	0.62	0.02	0.99	<0.01	5
$NGDR_y$	Vertical Net-to-gross displacement ratio	0.67	0.00	1.00	<0.01	7
P	Proportion of time moving upward	0.37	0.00	1.00	<0.01	8
M	Proportion of time in motion	0.92	0.24	1.00	<0.01	6

All speed and velocity metrics exhibited negatively skewed distributions, with *s*, s_{max},and w_{max} having distributions with long tails and extending into high values. The median vertical velocity was 0 mm s^{-1} and showed much less skew (Figure 4-3). We observed a wide range of speeds, where *s* varied from 0.86 to 13.96 mm s^{-1} and the fastest speed observed was over an order of magnitude higher than the median at 27.06 mm s^{-1} (Table 4-2).

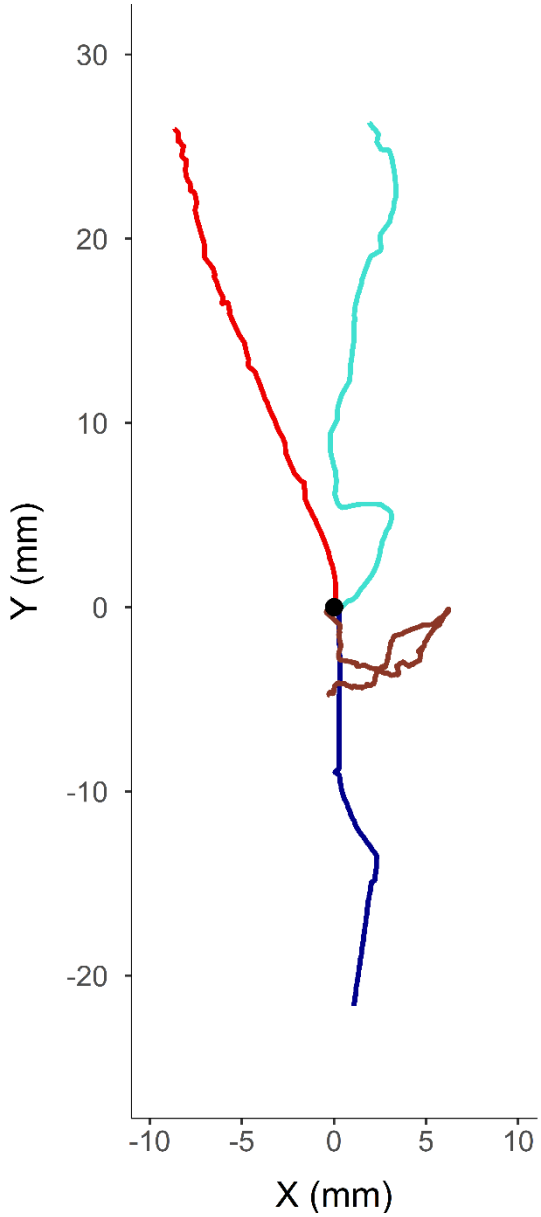

Figure 4-2: *Four example tracks of zoeae with the same relative starting position. Tracks show examples of zoeae that moved primarily upward (light blue) and downward (dark blue), as well as those that move with a high path efficiency (red) and low path efficienty (brown).*

Zoeae exhibited a bimodal distribution in swimming direction (θ), with peaks about ±10° from vertically upward or downward (Figure 4-3). Similarly, the proportion of time zoeae spent swimming upward (*P*) also had a bimodal distribution with peaks at relatively low (0.21) and high (0.81) proportions. Zoeae's swimming paths were moderately straight with a unimodal distribution of NGDR and a median of 0.67, which is substantially straighter than random motion (~0.03). In comparison, the distribution of NGDRy was bimodal with a large peak at 0.87 and a smaller peak at 0.24 (Figure 4-3 and Figure 4-4). This closer to the NGDR described by random motion, but still attains some net direction. Zoeae that swam with the highest NGDR were moving either directly upward or downward. Those that were swimming more horizontally tended to have a much lower NGDR. Zoeae spent a high proportion of time in motion (*M*), resting little during observations, with a strong peak at 0.97 (Table 4-2).

4.3.2.2 Mixture Model

The mixture model showed two significant component distributions for each behavioral metric (θ, *P*, NGDR, $NGDR_y$, *w*, and *s*; Figure 4-4), corresponding to two modes of behavior for each metric. The overall distributions of swimming angle (θ) and the proportion of time upward (*P*) showed very similar components (Table 4-3). Zoeae grouped into nearly equally proportioned orientations, swimming either nearly straight upward (89°) or downward (254°) with slightly more zoeae in the downward mode. The majority of zoeae (60%) spent most of their time swimming downward (P=0.2), while the other group (40%) spent most of their time swimming upward (P=0.8; Table 4-3). Mixture models for individual broods showed that broods had component distributions for θ and *P* with similar means, but the proportion exhibiting each behavior varied between broods

(Table 4-4). The upward oriented component varied from 23% to 78% across broods, and the downward component ranged from 22% to 77%.

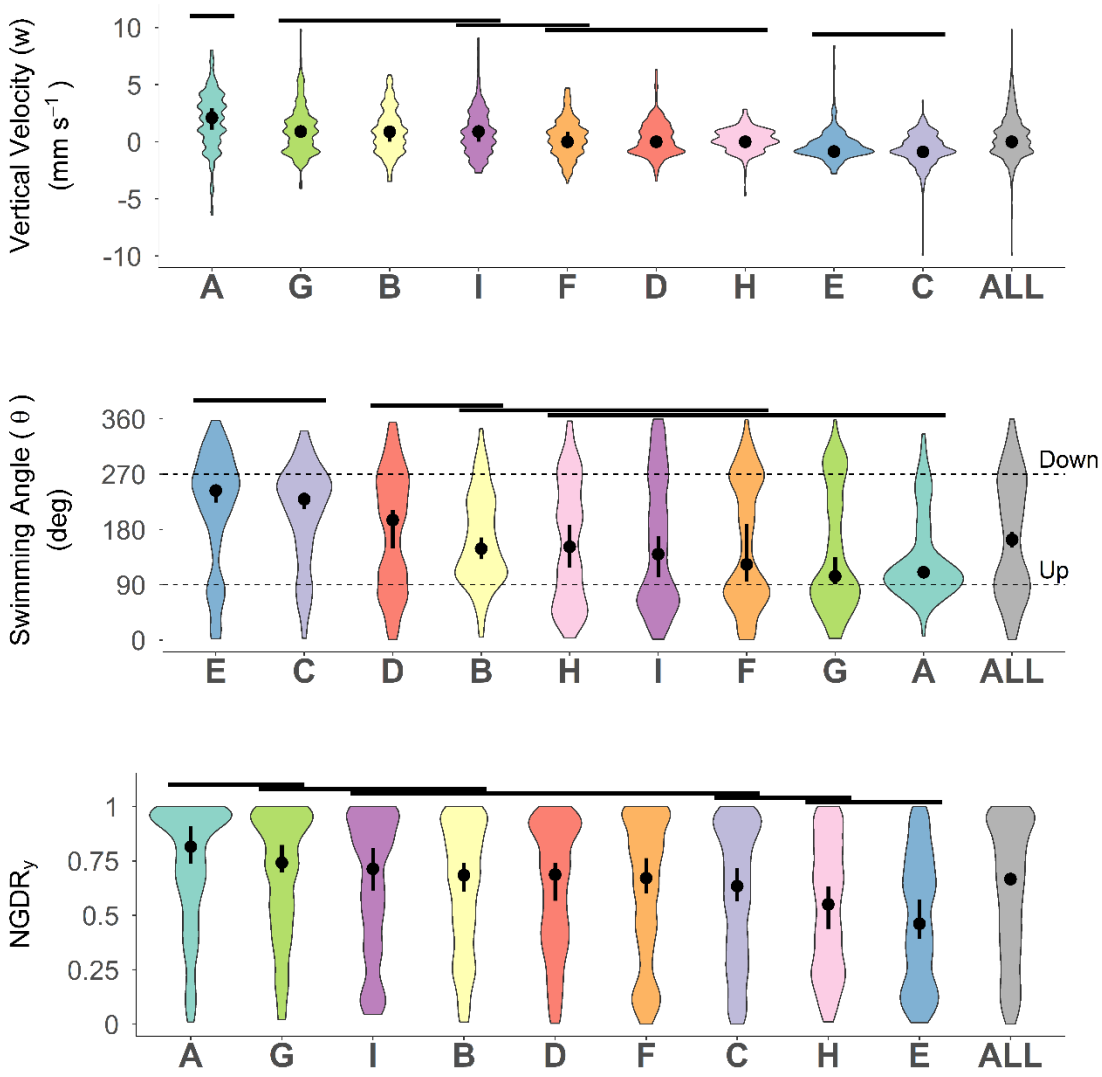

Figure 4-3: *Violin plots showing the distribution of w, θ, and $NGDR_y$ for all nine broods (A through I) observed in this study as well as the overall distribution (ALL). Points and line ranges within violins show the median and bootsrapped confidence intervals for each brood. Horizontal bars above violins show statistically similar groups of broods from Kruskal-Wallace tests. 150 zoeae were observed for each brood.*

Regarding the path straightness of trajectories for all larvae, both NGDR and $NGDR_y$ had similar component distributions, both in the proportions and means for each group (Table 4-3). In both cases a slight minority (38%) of zoeae swam with less straight paths (low NGDR), which again are closer to random motion but with some directionality. However, the majority of zoeae (62%) swam straighter paths with much higher NGDR (Table 4-3). Individual broods had similar low and high NGDR components, both in the means and proportions within each group.

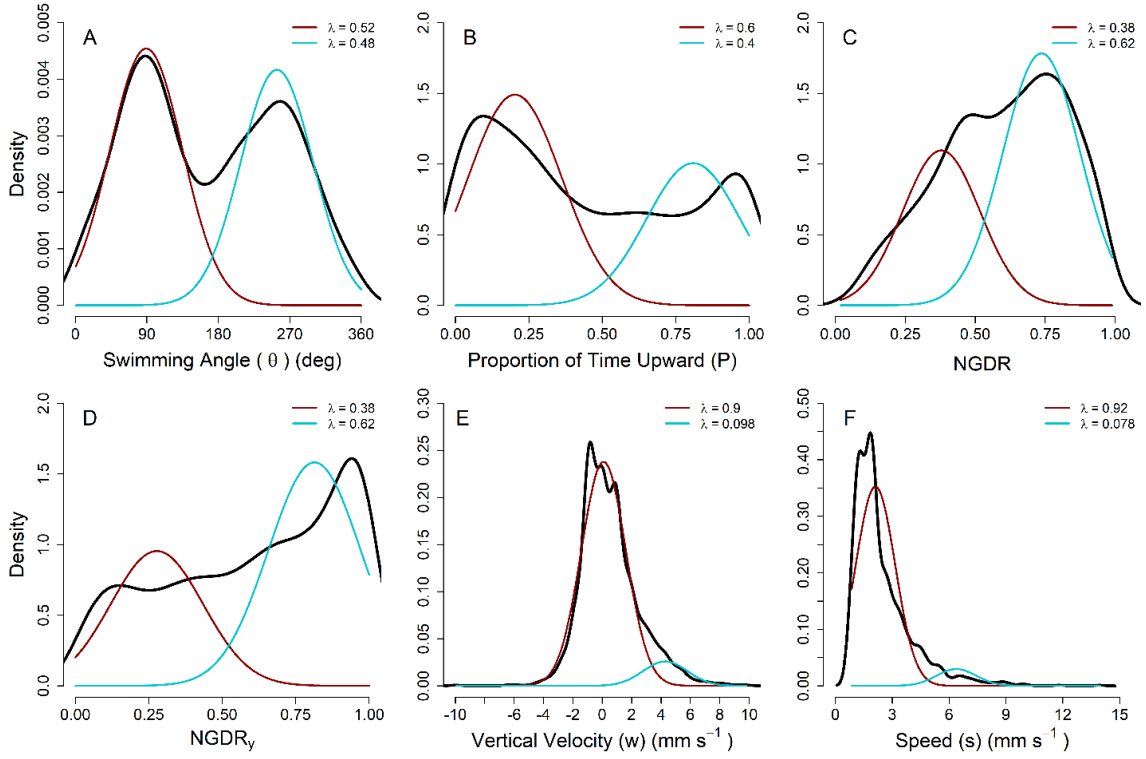

Figure 4-4: *Results of mixture model analysis on θ, P, NGDR, $NGDR_y$, w, and s. Solid lines show the distribution of each metric for all zoeae observed in this study (N=1350). The first (λ_1, dashed lines) and second (λ_2. dotted lines) components are shown as well as the proportion of observations within each component.*

There was less agreement between behavioral groups when analyzing speed (*s*) and vertical velocity (*w*). Across all broods, a large majority of zoeae (90%) had a very low vertical velocity (0.09 mm s^{-1}), where zoeae are effectively hovering in place (Table 4-3). This is in contrast to a much smaller component of zoeae (10%) that swam substantially faster (4.28 mm s^{-1}). The proportions within each component group were similar for *s* and *w*, but zoeae swam generally faster in regards to speed, with component means of 2.11 and 6.38 mm s^{-1}. The analysis for individual broods showed that the proportions within each component were similar to the overall distribution of both *s* and *w* (Table 4-4), but the means of each component were only similar for *w* (Table 4-4). There was brood-level variation in mixture model results for *s* and *w*, such that one brood exhibited the opposite proportionality of each component for the overall distribution with 87% of zoeae swimming at higher velocities. Additionally, the faster swimming component had a mean varying from 3.25 to 8.21 mm s^{-1} across broods. Thus, although individual broods did show some similarity to the overall distribution, between broods there was much less consistency in component parameters for *s* and *w* than for the other variables.

Table 4-3: Results of the mixture model on all zoeal observations showing the proportions (λ_1 and λ_2) and means (μ_1 and μ_2) of each component distribution. Means for median speed (*s*) and median vertical velocity (*w*) were measured in mm s^{-1}, mean angle of motion (θ) was measured in degrees, and net-gross displacement ratio (NGDR), vertical NGDR ($NGDR_y$), and proportion of time moving upward (*P*) were measured as ratios.

Metric	**λ_1**	**λ_2**	**μ_1**	**μ_2**
s	0.92	0.08	6.38	6.38
w	0.90	0.10	0.09	4.28
θ	0.52	0.48	89.20	254.00
NGDR	0.38	0.62	0.38	0.74
$NGDR_y$	0.38	0.62	0.28	0.81
P	0.60	0.4	0.20	0.81

Table 4-4: Results from bootstrapped mixture model analysis on brood-level distributions of swimming variables. Ratios show the proportion of broods that have similar component parameters to the mixture model of the overall distribution. Since λ_2 is the reciprocal of λ_1, it was excluded from this analysis.

Metric	λ_1	μ_1	μ_2
s	0.78	0	0.56
w	0.67	0.56	0.56
θ	0.44	0.56	0.89
NGDR	0.78	0.89	0.78
$NGDR_y$	0.67	0.89	0.78
P	0.33	0.89	0.56

4.3.3 Morphology and Behavior

Morphological metrics generally showed some degree of correlation with observed behavioral characteristics (Table 4-5). Overall, zoeal morphometrics showed high collinearity, as many relate to the absolute size of zoeae. By a step-wise removal of highly correlated variables, four morphometrics were chosen as the independent variables for the regression analysis (RDL, SA, A_D, and A_B). Since it was not possible to have paired observations for swimming and morphology of individual zoeae, the regressions in this study represent trends across groups of zoeae from the same brood.

A_D was hypothesized to be negatively correlated with all speed and velocity metrics, but the opposite was found. A_D was positively correlated with *s*, s_{max}, w_{max}, NGDR, and $NGDR_y$, such that zoeae, that should be experiencing higher drag while swimming, swam faster and had straighter swimming paths (Table 4-5). Swimming appendage length (SA) was hypothesized to be positively correlated with speed and vertical velocity. This was partially true, as longer swimming appendages were positively correlated vertical velocity and path straightness and resulted in zoeae spending more time swimming upward and in motion, but SA was not related to absolute speed. Larger zoeae (higher RDL) also had higher vertical velocities, spent more time swimming upward (higher *P*), and spent

more time in motion (higher *M*). The hypothesis that s_{max} and w_{max} would be positively correlated with A_B was not supported by these results. Interestingly, *s* was negatively correlated with A_B, where even though zoeae could produce more thrust from abdominal contractions, they moved more slowly on average. Though only some of our hypotheses were confirmed by this analysis, morphological differences provide a partial explanation for behavioral differences between broods.

Table 4-5: Results of multiple regression of swimming metrics as a function of morphological metrics (RDL, SA, A_D, and A_B). Columns with morphological metrics show the regression coefficients of the metrics used in each model. Swimming metrics marked with an asterisks (*) denote that a beta regression was used. Values in parentheses denote coefficients for the precision parameter of the beta regressions. P values are adjusted with a Bonferroni correction.

Swimming Metric	Intercept	RDL	SA	A_D	A_B	Model R^2	Model p-value
s	-1.4	-	-	29.3	-86.9	0.67	0.15
s_{max}	-18.5	-	-	77.0	-	0.83	<0.001
w	-23.84	9.0	36.7	-	-	0.65	0.018
w_{max}	-17.4	-	30.5	11.0	-	0.61	0.024
NGDR*	-3.5 (-29.9)	-	-	8.7 -	- 111.2	0.42	<0.001
$NGDR_y$*	-6.1 (-39.7)	-	15.0 -	- 140.3	-	0.49	<0.001
P*	-21.8 (-131.6)	14.4 (42.7)	21.8 (222.0)	-	-	0.63	<0.001
M*	-12.8 (-47.8)	18.3 -	11.8 -	-	-68.8 (778.5)	0.27	<0.001

4.4 Discussion

4.4.2 Swimming Behavior

The swimming behavior of *C. sapidus* zoeae under various laboratory conditions has been well-documented. Sulkin et al. (1980) found that first stage *C. sapidus* zoeae show a strong negative geotaxis and high barokinesis at pressures greater than 1 atm. While

Sulkin et al. observes generally positive phototaxis in zoeae, Forward and Buswell (1989) show that phototaxis can be modulated by light intensity, where at high intensities more zoeae are negatively phototactic. However it is difficult to directly compare these studies, as the light intensity used by Sulkin et al. was an order of magnitude higher than that used by Forward and Buswell. First stage *C. sapidus* zoeae also respond to rapid decreases in pressure by swimming downward. The combinations of these behaviors facilitate export from estuaries and explain the near-surface distribution of *C. sapidus* zoeae (Epifanio and Cohen 2016).

In this study, about 80% zoeae exhibited a hovering behavior, with a near-zero vertical velocity, and nearly 20% showed no net vertical displacement. Given that in field observations, *C. sapidus* larvae are almost exclusively found in near-surface waters (Epifanio 1995), it makes sense that a substantial fraction of larvae did not show any net movement. This hovering behavior may also be the result of the shallow depth of aquarium being insufficient to induce a strong barokinetic response (Sulkin et al. 1980). However, it is worth noting that a lack of vertical displacement does not equate to a lack of activity or energy expenditure. Zoeae are still moving horizontally, and the lack of a near-zero component for speed metrics confirms this. Additionally, even without net displacement, hovering still necessitates an energetic cost to counter their negative buoyancy.

The bimodal distribution of zoeal orientation was somewhat unexpected. Near-surface field observations (Epifanio 1995) and the consistent upward swimming in other studies (Sulkin et al. 1980), would suggest that zoeae should not exhibit downward swimming, especially at the lower portion of the aquarium. Though negative vertical velocity could be attributed to passive sinking, negative vertical velocities often exceeded

a zoeae's terminal sinking velocity. Since the depth of the observation container was shallow (10 cm) and zoeae were not observed to aggregate on the bottom in any trial, presumably the downward swimming zoeae were returning to the surface out of the camera's frame. This potential vertical oscillation would be on a small scale (~10 cm), and is thus not necessarily inconsistent with field observations (Provenzano 1983; Epifanio 1995). Additionally, the bimodal distribution of swimming directions is similar to that observed by Forward and Buswell (1989) in dark conditions.

First stage *C. sapidus* zoeae must be able to swim enough to overcome passive sinking and turbulent mixing in near-surface waters, while also minimizing the energetic expenditure of locomotion. We propose a hypothetical optimized vertical swimming behavior, where optimally swimming zoeae should then be those swimming upwards with a high NGDR and oriented close to 90° upward. By this definition, zoeae meeting these criteria would be minimizing their energetic expenditure for vertical displacement. Not all zoeae observed in this study would be considered optimal swimmers by this definition. Mixture model results showed that for each behavior metric, component distribution could be categorized into optimal and non-optimal modes of behavior (upward versus downward swimming, slow versus fast swimming, less-directional versus straight paths). By this definition, 26% of all zoeae observed would meet these optimal swimming criteria. In contrast, for individual broods this proportion varies from 6% to 42%, showing that brood-level differences in behavior may influence swimming ability. Optimized vertical swimming is not the only consideration for larval behavior, and while this experiment was not designed to address the energetics and efficiency of swimming, the persistence of

brood-level variation in behavior suggests that energetic considerations may vary between broods.

Zoeae are highly sensitive to a variety of environmental conditions (Epifanio and Cohen 2016), and thus the swimming behaviors observed in this study should not be interpreted as entirely representative of wild behavior. Differences between experimental and natural conditions, as well as the influence of experimental artefacts, do not allow a definitive assessment of optimal swimming behavior or the presence of behavioral modes in the wild from this study. Collapsing three-dimensional swimming behavior into two dimensions results in an underestimate of velocities. Additionally, because of the practical need to observe multiple larvae in a single video, zoeae may interact with each other prior to coming within the camera's field of view. Zoeae may also be influenced by the proximity to the outer walls of the observation aquarium. Some of these wall effects should be mitigated as the camera was focused on the center of the tank (4 cm from the side walls and) and the aquarium size was comparable to those used in similar studies (Ford et al., 2005; Forward and Buswell, 1989; Sulkin et al., 1980). However, the camera was fixed fairly close (1 cm) from the bottom, which may have excluded behaviors near the surface and introduced interactions with the bottom.

Other environmental conditions can also cause our results to differ from natural behavioral responses. Zoeae are very sensitive to light parameters, specifically the wavelength, intensity, and angular distribution of the light source (Epifanio and Cohen 2016). Collimated light used in this experiment does not accurately represent the natural light distribution in shallow water, and has been shown to change the phototactic response in *Rhithropanopeus harrisii* (Forward et al. 1984; Forward and Buswell 1989). Coastal

oceans are turbulent environments, and several studies have demonstrated that small-scale turbulence can influence zooplankton swimming behavior in bivalves (Fuchs and Dibacco, 2011), gastropods (Fuchs et al. 2018), enchinoderms (Roy et al. 2012), and copepods (Saiz and Alcaraz 1992). Since this study was conducted in still water, potential behavioral changes in response to turbulence would not be present. Lastly, zoeae were not fed prior to observations, and the presence of food can alter swimming behavior in zoeae (Cronin and Forward 1980). Regardless of the inaccuracies in simulating natural conditions, all observed zoeae still experienced similar environmental parameters, and thus, comparisons of behavior among and between groups of zoeae are still valid.

4.4.2 Morphology and Behavior

Theoretically, morphological characteristics of zoeae should have some impact on swimming ability. Carapace spines are thought to stabilize zoeae while in motion, and to decrease passive sinking rates (Smith and Jensen 2015). It is also possible that swimming stabilization would result in straighter swimming trajectories (high NGDR). Zoeae produce thrust via rapid oscillations of their maxillipeds, where thrust is proportional to the morphology and movements of maxillipeds and setae (Chia et al. 1984). The angular velocity and spread of setae also influence thrust and were not able to be measured in this study. By contracting their abdomens, zoeae are able to quickly change direction and create a burst of speed (Foxon 1934), which is dependent on both the speed of the contraction and the cross-sectional area of their abdomens. The overall size and shape of zoea, particularly that of the carapace, relates to the drag induced while swimming (Chia et al. 1984). As larvae become larger or have carapaces with a disproportionately larger dorsal cross-

sectional area (A_D), more drag is experienced while swimming and thus more thrust must be produced to move at a given velocity.

Some of the theoretical relationships noted above between morphology and swimming ability were not observed in this study. This is especially evident in the fact that dorsal cross-sectional area was not negatively correlated with any speed or velocity metrics, despite the notion that larvae experiencing more drag would swim more slowly. It is possible that there are mechanistic changes in how zoeae swim (e.g. increasing the angular velocity or beat frequency of swimming appendages) that overcompensate for the increase in drag. Also unexpectedly, swimming appendage length (SA) was only positively correlated with median vertical velocity (*w*) but not swimming speed (*s*). This may be due to the fact that swimming vertically requires more force to counteract negative buoyancy, and thus the increased thrust from longer swimming appendages is more important for swimming upward. Interestingly, abdominal cross-sectional area (A_B) was only negatively correlated to speed but not velocity. This indicates that abdominal contractions may play a smaller role in determining swimming velocity than hypothesized.

Regarding the swimming path straightness (NGDR and $NGDR_y$), zoea with larger dorsal areas (A_D) and swimming appendages (SA) swam in straighter trajectories. The reason for this is unknown, but increased drag and longer appendages may cause rapid changes in direction energetically disadvantageous. Zoeae with larger swimming appendages might also rely more on cruise rather than burst swimming, as abdominal contractions would cause more erratic motion with a lower NGDR.

Zoeae that swam upwards more often (higher *P*) could produce more propulsive thrust (higher SA), which is consistent with our hypotheses, but zoeae that have longer spines (higher RDL) are also more likely to swim upward. Carapace spines have been demonstrated to increase the hydrodynamic stabilization of zoeae while swimming and prevent tumbling (Smith and Jensen 2015), which could help keep zoeae oriented upward, especially given their negative geotaxis. The proportion of time spent in motion (*M*) was negatively correlated with abdominal area (A_B), possibly because zoeae that can travel in shorter, faster bursts do not need to spend as much time swimming.

A caveat for this type of analysis, though, is that it was not possible to directly compare the morphology and behavior for individuals, and so we are only able to highlight the trends of groups of individuals on the level of larval broods. Additionally, while some of the variation in swimming ability and efficiency can be explained by differences in morphology, there are likely other factors that influence swimming that were not addressed in this study. These included variation in environmental responses and swimming mechanics. It is possible that how zoeae respond to their environment (temperature, salinity, light, etc.) differs between broods. Observations in this study were performed just after hatching, and differences in the energetic content of eggs between broods may vary the amount of energy reserves zoeae can spend on swimming. Modeling studies have demonstrated the effect of differing appendage morphology and kinematics on the swimming efficiency of copepods (Morris et al. 1985; Williams 1994). However, there have been no studies testing sensitivity of swimming behavior to changes in morphology in zoeae. Our results indicate that morphology can influence zoeal swimming behavior, but

a more complete mechanistic model of swimming may be required to determine the precise relationships between morphology and swimming behaviors.

4.5 Conclusion

Our study has demonstrated that for early *Callinectes sapidus* zoeae, swimming behavior is highly variable, not only for swimming velocity, but also for orientation and path efficiency. This variation is partially explained by brood-level differences in morphology, but substantial variation exists within broods as well, irrespective of morphology. Mixture model results showed that both among all zoeae sampled and among zoea from individual broods, there exist two main modes of behavior for each metric that could be described as hovering versus swimming, orienting upward versus downward, and low versus high path straightness. When assessing metrics individually, a majority of zoeae hover, orient upward, and swim in straighter paths. Generally, morphology explains some of the variation in swimming behavior. Although some hypothetical relationships were not confirmed. For example, zoeae that would seemingly experience more drag swim at higher velocities and with straighter paths. Additionally maxilliped size appears to be more related to vertical velocity than abdomen size. Future studies modelling *C. sapidus* kinematics or larval dispersal should incorporate behavioral and morphological variability that may differ among subsections of the population.

4.6 Literature Cited

Benaglia T, Chauveau D, Hunter DR, Young D (2009) Mixtools: An R package for analyzing finite mixture Models. J Stat Softw 32:1–29.

Buskey EJ (1984) Swimming pattern as an indicator of the roles of copepod sensory systems in the recognition of food. Mar Biol 79:165–175.

Caracappa JC, Munroe DM (2018) Morphological variability among broods of first-stage blue crab (*Callinectes sapidus*) zoeae. Biol Bull 235:123–133.

Charmant J (2018) Kinovea.

Chia F-S, Buckland-Nicks J, Young CM (1984) Locomotion of marine invertebrate larvae: a review. Can J Zool 62:1205–1222.

Cribari-Neto F, Zeileis A (2010) Beta regression in R. J Stat Softw 34:1–24.

Cronin TW, Forward RB (1980) The effects of starvation on phototaxis and swimming of larvae of the crab *Rhithropanopeus Harrisii*. Biol Bull 158:283–294. doi: 10.2307/1540855

DiBacco C, Fuchs HL, Pineda J, Helfrich K (2011) Swimming behavior and velocities of barnacle cyprids in a downwelling flume. Mar Ecol Prog Ser 433:131–148. doi: 10.3354/meps09186

Doall MH, Colin SP, Strickler JR, Yen J (1998) Locating a mate in 3D : The case of *Temora longicornis*. Philos Trans R Soc London B 353:681–689.

Epifanio CE (1988) Dispersal strategies of two species of swimming crab on the continental shelf adjacent to Delaware Bay. Mar Ecol Prog Ser 49:243–248.

Epifanio CE (1995) Transport of blue crab (*Callinectes sapidus*) larvae in the waters off Mid-Atlantic states. Bull Mar Sci 57:713–725.

Epifanio CE, Cohen JH (2016) Behavioral adaptations in larvae of brachyuran crabs: A review. J Exp Mar Bio Ecol 482:85–105. doi: 10.1016/j.jembe.2016.05.006

Epifanio CE, Tilburg CE (2008) Transport of blue crab larvae in the Middle Atlantic Bight: A wet and windy journey. J Mar Res 66:723–749.

Ferrari S, Cribari-Neto F (2008) Beta regression for modelling rates and proportions. J Appl Stat 35:407–419.

Ford MD, Schuegraf MJ, Elkink MS, Edwin DeMont M (2005) A comparison of swimming structures and kinematics in three species of crustacean larvae. Mar Freshw Behav Physiol 38:79–94. doi: 10.1080/10236240500148934

Forward RB, Cronin TW, Stearns DE (1984) Control of diel vertical migration : photoresponses of a larval crustacean '. 29:146–154.

Forward RJB, Buswell CU (1989) A comparative study of behavioral responses of larval decapod crustaceans to light and pressure. Mar Behav Physiol 16:43–56.

Foxon GEH (1934) Notes on the swimming methods and habits of certain crustacean larvae. J Mar Biol Assoc United Kingdom 19:829–850. doi: 10.1017/S0025315400046816

Fuchs HL, Dibacco C (2011) Mussel larval responses to turbulence are unaltered by larval age or light conditions. Limnol Oceanogr Fluids Environ 1:120–134. doi: 10.1215/21573698-1444613

Fuchs HL, Mullineaux LS, Solow AR (2004) Sinking behavior of gastropod larvae (*Ilyanassa obsoleta*) in turbulence. Limnol Oceanogr 49:1937–1948. doi: 10.4319/lo.2004.49.6.1937

Fuchs HL, Gerbi GP, Hunter EJ, Christman AJ (2018) Waves cue distinct behaviors and differentiate transport of congeneric snail larvae from sheltered versus wavy habitats. 115:7532–7540. doi: 10.1073/pnas.1804558115

Johnson DF, Hess KW (1990) Numerical simulations of blue crab larval dispersal and recruitment. Bull Mar Sci 46:195–213.

Levine DM, Sulkin SD (1979) Partitioning and utilization of energy during the larval development of the Xanthid crab, *Rhithropanopeus harrisii* (Gould). J Exp Mar Bio Ecol 40:247–257.

López-Duarte PC, Tankersley R a. (2007) Circatidal swimming behavior of brachyuran crab zoea larvae: Implications for ebb-tide transport. Mar Biol 151:2037–2051. doi: 10.1007/s00227-007-0614-3

Mootz CA, Epifanio CE (1974) An energy budget for *Menippe mercenaria* Larvae fed Artemia Nauplii. Biol Bull 146:44–55.

Morgan SG (1987) Morphological and behavioral antipredatory adaptations of decapod zoeae. Oecologia 73:393–400.

Morris MJ, Gust G, Torres JJ (1985) Propulsion efficiency and cost of transport for copepods: a hydromechanical model of crustacean swimming. Mar Biol 86:283–295.

Ogburn MB, Hall M, Forward RB, Forward Jr. RB (2012) Blue crab (*Callinectes sapidus*) larval settlement in North Carolina: Environmental forcing, recruit-stock relationships, and numerical modeling. Fish Oceanogr 21:20–32. doi: 10.1111/j.1365-2419.2011.00606.x

Provenzano A (1983) Vertical distribution of first stage larvae of the blue crab, *Callinectes sapidus*, at the mouth of Chesapeake Bay. Estuar Coast Shelf Sci 16:489–499.

R Core Team (2015) R: A language and environment for statistical computing.

Rhodes A, Lipton D, Shabman L (2001) A socio-economic profile of the Chesapeake Bay commercial blue crab fishery.

Roy A, Metaxas A, Ross T (2012) Swimming patterns of larval *Strongylocentrotus droebachiensis* in turbulence in the laboratory. Mar Ecol Prog Ser 453:117–127. doi: 10.3354/meps09662

Saiz E, Alcaraz M (1992) Free-swimming behaviour of *Acartia clausi* (Copepoda: Calanoida) under turbulent water movement. Mar Ecol Prog Ser 80:229–236.

Smith AE, Jensen GC (2015) The role of carapace spines in the swimming behavior of porcelain crab zoeae (Crustacea: Decapoda: Porcellanidae). J Exp Mar Bio Ecol 471:175–179. doi: 10.1016/j.jembe.2015.06.007

Sulkin S (1984) Behavioral basis of depth regulation in the larvae of brachyuran crabs. Mar Ecol Prog Ser 15:181–205. doi: 10.3354/meps015181

Sulkin SD, van Heukelem W, Kelly P, van Heukelem L (1980) The behavioral basis of larval recruitment in the crab *Callinectes sapidus* Rathbun: A laboratory investigation of ontogenetic changes in geotaxis and barokinesis. Biol Bull 159:402–417.

Tamura H, Landeira JM, Goshima S (2017) Morphological and morphometric variability in the zoea I larvae of *Pugettia quadridens* (De Haan, 1839): Looking for reliable characters for taxonomic studies on the genus *Pugettia* Dana, 1851 (Majoidea: Epialtidae). Zootaxa 4226:264–272.

Torres JJ (1984) Relationship of oxygen consumption to swimming speed in *Euphausia pacifica* - II. Drag, efficiency and a comparison with other swimming organisms. Mar Biol 78:231–237. doi: 10.1007/BF00393008

Velazquez CCS (2016) The kinematics and particle image velocimetry of the shore crab larvae *Carcinus maenas*. California State University, Fresno

Villanueva R, Nozais C, Boletzky S V. (1996) Swimming behaviour and food searching in planktonic octopus *Vulgaris cuvier* from hatching to settlement. J Exp Mar Bio Ecol 208:169–184. doi: 10.1016/S0022-0981(96)02670-6

Wilkin JL, Jeffs AG (2011) Energetics of swimming to shore in the puerulus stage of a spiny lobster: Can a postlarval lobster afford the cost of crossing the continental shelf? Limnol Oceanogr Fluids Environ 1:163–175. doi: 10.1215/21573698-1504363

Williams TA (1994) Locomotion in developing *Artemia* larvae: Mechanical analysis of antennal propulsors based on large-scale physical models. Biol Bull 187:156–163. doi: 10.2307/1542238

Zeileis A (2002) Diagnostic checking in regression relationships. R News 2:7–10.

Chapter 5: Implications of Brood-Dependent Larval Transport for Blue Crabs *Callinectes sapidus*

Abstract

Blue crabs (*Callinectes sapidus*) support valuable fisheries in the US mid-Atlantic, and their unpredictable and variable recruitment suggests that a better understanding of larval development and dispersal is needed. Blue crab larval dispersal involves export to the continental shelf followed by re-entry of estuaries. Transport is facilitated by wind and buoyancy-driven surface currents, and zoeae generally maintain a near-surface distribution. Though several studies have investigated larval dispersal, none have evaluated the effects of varying individual swimming behavior on transport. This study simulates larvae with observed swimming and sinking velocities, as well as observed brood-dependent behavior, within an idealized wind-driven estuarine plume. Model results showed that larval transport was predominately influenced by wind speed, but transport was significantly modified by behavioral characteristics. Faster swimming larvae were more able to maintain a near-surface position despite vertical diffusivity, such that in all model scenarios larvae travelled further and held different vertical distributions than passive particles. Model results show up to a 1.7 fold difference in transport between broods and up to a 4.9 fold difference in transport across all larvae. These results indicate that behavior and its variability may be an important factor in *C. sapidus* larval dispersal and should be better defined empirically, and incorporated into future models.

5.1 Introduction

Blue crab (*Callinectes sapidus*) larval dispersal has been a topic of research over the past 50 years. High inter-annual variability in recruitment creates challenges for long-term management, and prediction of recruitment has not been achieved; therefore, critical gaps in the understanding of early life stage processes still remain. While models of *C. sapidus* larval dispersal exist for the mid-Atlantic (a thorough review can be found in Epifanio and Cohen, 2016), it is not yet possible to accurately predict the spatio-temporal patterns of recruitment. Studies have identified the potential for larval behavior to influence dispersal dynamics (Shanks 2009); however, to our knowledge, there have been no models of *C. sapidus* larval dispersal that incorporate behavior explicitly. Several laboratory studies have identified complex swimming behavior with many environmental triggers (Sulkin et al. 1980; Forward and Buswell 1989; Epifanio and Cohen 2016), yet models typically treat larvae as passive particles moving within the upper few meters of the water column (Johnson and Hess 1990; Garvine et al. 1997; Tilburg et al. 2009).

After hatching near the mouths of estuaries, blue crab larvae (zoeae) swim to the surface and are exported onto the continental shelf, where they undergo 7 to 8 molt stages (over a 30-40 day duration) before metamorphosis (Costlow and Bookhout 1959). Current understanding of larval dispersal in the mid-Atlantic (Epifanio and Tilburg 2008) has larvae carried southward via a near-shore buoyancy-driven surface current. Recruitment back to their parental estuary can occur when upwelling drives larvae offshore where a counter-current carries them northward, eventually reentering estuaries during wind-driven downwelling events. This hypothetical pathway for larvae necessitates that they remain in these surface currents.

Though it is generally understood that blue crab zoeae maintain a near-surface distribution (Epifanio 1995), field sampling shows their vertical position can extend several meters below the surface (Smyth 1980; Provenzano 1983). There is no indication whether or not this is caused by behavior or is due to vertical mixing. Laboratory studies have demonstrated swimming responses of *C. sapidus* zoeae to temperature, salinity, light, gravity, and pressure (Sulkin et al. 1980; Forward and Buswell 1989). Together, the contemporary understanding of zoeal depth-regulation has early stage larvae exhibiting negative geotaxis and high barokinesis, resulting in continual upward swimming (Sulkin 1984). Once at the surface, zoeae must presumably stop swimming for some time and resume swimming once triggered by depth or time-dependent cues. Additionally, the presence of a mixed layer with variable degrees of turbulence means that zoeae may not always be able to stay within the neuston.

Swimming ability for *C. sapidus* zoeae is a function of both behavior and morphology. Larvae swim predominantly by oscillating their maxillipeds. The attached setae are fanned during their power stroke and are retracted on the recovery stroke to produce net thrust (Velazquez 2016). The amount of thrust they can produce is proportional to length and cross-sectional area of these appendages as well as the angular velocity and period of oscillations. The overall size and shape of the larval carapace can influence the drag larvae experience, with more drag occurring for larvae with a larger cross-sectional area (dorsal while swimming and anterior while sinking; Figure 1-2). Early zoeal stages exhibit negative geotaxis, high barokinesis, and positive phototaxis at high light intensities (Sulkin et al. 1980), explaining their near-surface vertical distribution. However, there is no evidence for diel or tidal vertical migrations (López-Duarte and Tankersley 2007).

Recent studies have shown that blue crab larvae exhibit substantial variability in morphological (Caracappa and Munroe 2018) and behavioral (Caracappa and Munroe 2019) characteristics. This variability particularly relates to the size of larvae (Caracappa and Munroe 2019). In addition to population-level variability, individual broods of larvae can be morphologically and behaviorally distinct (Caracappa and Munroe 2018, 2019). A 3-fold difference in swimming velocity has been observed between broods, which is partially explained by morphological variation (Caracappa and Munroe 2019). This degree of brood-level variation, when applied to physical processes during dispersal, may potentially result in differences among brood-level larval transport. If larvae from some broods are dispersed differently than others, a better understand population-level dynamics in blue crab dispersal and recruitment may be possible.

Circulation on the inner continental shelf, where mid-Atlantic *C. sapidus* larvae develop, is governed primarily by the buoyant outflow of large riverine estuaries and wind-driven Ekman dynamics (Garvine et al. 1997). Buoyancy gradients created by estuarine plumes drive a southward inshore current (Yankovsky et al. 2000). Episodic and seasonal changes in wind direction can cause offshore or inshore transport of near-surface waters, where a northward countercurrent can occur (Johnson et al. 1984). Additionally, sheared currents can be generated by wind-stress and friction between water layers (Richman et al. 1987; Craig 1996). Wind stress and breaking waves can result in vertical diffusivity that increases with until some intermediate depth (Visser 1997), resulting in turbulent motion influencing larvae's vertical position.

The goal of this study was to investigate the potential for behavioral-physical interactions to alter the dispersal of *C. sapidus* larvae, based on observational and

experimental data. This was done through model simulations in an idealized estuarine plume over the continental shelf. Specifically, our objectives were to (1) determine the degree to which blue crab larval behavior influences larval transport, (2) identify if variation in behavioral traits significantly alters dispersal trajectories, and (3) determine whether brood-level behavioral differences may result in differences in transport.

5.2 Methods

5.2.1 Model Design

Larval transport was simulated in a two-layer idealized estuarine plume over a continental shelf with an unbounded horizontal plane and 50 m depth. Horizontal movement was driven entirely by a wind-driven Ekman current profile under constant northward wind-stress. Simulations were set to be in the northern hemisphere with positive x (U velocity) as eastward, and positive y (V velocity) as northward. No vertical velocity was present, except for that generated from vertical diffusivity.

The depth of the estuarine plume (z_p) was determined based on a model by Fong and Geyer (Fong and Geyer 2001).

$$z_p = \left[\frac{4\left(\frac{\tau}{\rho_0}\right)^2}{g\left(\frac{\Delta\rho}{\rho}\right)}\right]^{\frac{1}{3}} \quad \textbf{(5.1)}$$

where ρ_0 is the mean density of seawater within the plume, ρ is the density of the bottom layer (1023 kg m^{-3}), $\Delta\rho$ is the difference in average density between both layers, g is the gravitation acceleration (9.8 m s^{-2}), and τ is the wind stress, which was estimated from free-stream wind speed using an empirical relationship (Large and Pond 1980).

Current profiles were then defined using a steady-state Ekman system with a constant northward wind (Pond and Pickard 1983)

$$U(z) = \frac{\sqrt{2}\pi\tau}{z_p\rho_0|f|}\cos\left(\frac{\pi}{4}+\frac{\pi}{z_p}z\right)e^{\frac{\pi}{z_p}z} \quad \textbf{(5.2)}$$

$$V(z) = \frac{\sqrt{2}\pi\tau}{z_p\rho_0|f|}\sin\left(\frac{\pi}{4}+\frac{\pi}{z_p}z\right)e^{\frac{\pi}{z_p}z} \quad \textbf{(5.3)}$$

where f is the Coriolis parameter (10^{-4} s^{-1}), z is the depth in meters. In all model scenarios, a constant wind was applied at one of 3 levels (5 ms^{-1}, 10 ms^{-1}, 15 ms^{-1}), which encompasses the range in wind speed seen from the NOAA NDBC CMAN4 station in the mouth of Delaware Bay, USA. Two different plume configurations were also used. The first was a shallower plume with a ρ_0 of 1019 kg m^{-3}, and the second was a deeper plume with a ρ_0 of 1020 kg m^{-3}. Plume configurations are hereafter referred to as plume types. These densities were based on observations from Whitney and Garvin (2005), from vertical salinity profiles made during the time *C. sapidus* zoeae hatch. Together these wind speeds and plume depths made six different velocity profiles (Figure 5-1) each with a different plume depth (Table 5-1).

Table 5-1: Plume depth (z_p) for each configuration of plume type and wind speed.

Plume Type	**Wind Speed (ms^{-1})**	**z_p (m)**
Deeper	5	2.52
Deeper	10	6.36
Deeper	15	12.91
Shallower	5	2.29
Shallower	10	5.78
Shallower	15	11.73

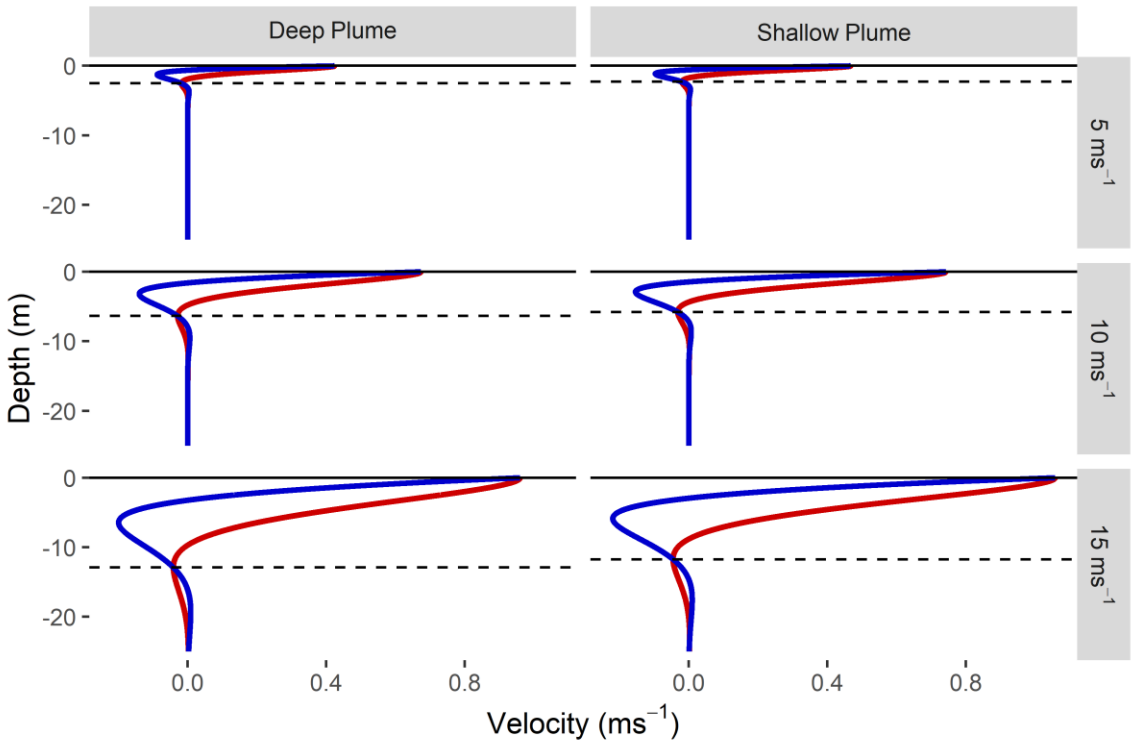

Figure 5-1: *Vertical profiles from combinations of plume densities (columns) and wind speeds (rows). Horizontal velocity in the x (red) and y (blue) directions are shown by solid lines. Plume depth (z_p) is denoted by the black dashed line.*

A vertical diffusivity (A_v) profile was also specified by

$$\boldsymbol{A_v} = \begin{cases} \boldsymbol{u_* \mathrm{K} z \left(\frac{H - z}{H}\right)} & \boldsymbol{-z_p \leq z \leq 0} \\ \boldsymbol{5 \times 10\text{^} - 6} & \boldsymbol{z < -z_p} \end{cases} \tag{5.4}$$

where κ is the Von Kármán constant (0.4), H is the water column depth (50 m), and u_* is the shear velocity defined by

$$\boldsymbol{u_*} = \sqrt{\frac{\boldsymbol{\tau}}{\boldsymbol{\rho_0}}} \tag{5.5}$$

The value for the background diffusivity (5×10^{-6} m^2s^{-1}) was based on Fong and Geyer's model (2001). This produced a profile that was dependent on wind speed with a maximum A_v at one half the plume depth. A cubic spline was used to create a differentiable A_v profile at the bottom of the plume (i.e. pycnocline), as well as the first derivative of the profile. Different A_v profiles were also generated for each combination of wind speed and plume density (Figure 5-2).

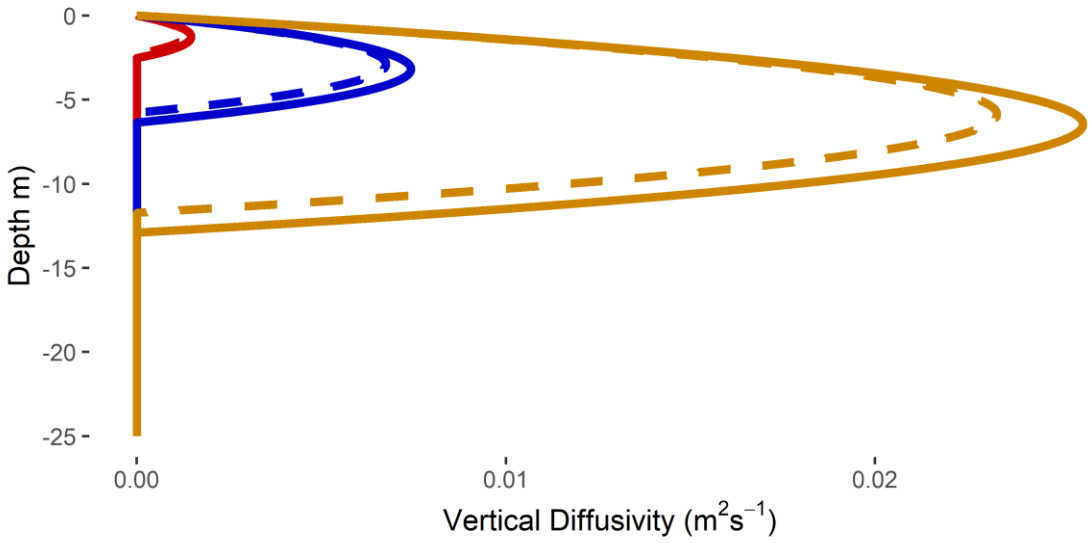

Figure 5-2: *Vertical diffusivity profiles over the top half of the model depth. Profiles are shown for 5 ms^{-1} (red), 10 ms^{-1} (blue), and 15 ms^{-1} (yellow), as well as the shallower (dashed lines) and deeper (solid lines) plume configurations.*

5.2.2 Larval Behavior

Swimming behavior in this model has larvae swim upward and, once near the surface, passively sink until they reach a pre-determined depth trigger (D_{max}). Since the precise nature of this depth trigger is unknown, D_{max} was given three possible values (0, 1.5, and 3m). When larvae have a nonzero D_{max}, they vertically oscillate between the surface and their D_{max} in a sawtooth pattern when diffusivity is absent. This behavior differs from depth tracking, as there is no evidence that larvae aggregate at any non-surface depths,

but it does represent a type of depth-regulation. A D_{max} of 0m results in constant upward swimming regardless of depth, and the others are within the vertical distribution observed in field studies (Provenzano 1983).

It is now understood that first stage *C. sapidus* zoeae exhibit significant brood-dependent morphology and swimming velocities (Caracappa and Munroe 2018, 2019); therefore, I incorporated this known variation in our model, using empirical relationships between swimming velocity and morphology. This approach was taken because there is no available data on paired swimming and sinking behavior for individual larvae on the basis of larval broods.

A full description of the methods used to generate swimming and sinking velocity can be found in Appendix C. Four larval broods (A through D) were selected from Caracappa & Munroe (2019), such that between broods, significant differences in both morphology and swimming velocity were present (Figure 5-3). It is important to note that these brood names do not correspond to the ones used in Chapter 3. The overall distribution of all larvae measured in that study was also used (O), making 5 larval groups in total. Since paired observations of individual zoeal swimming and sinking velocities are not available, individual swimming and sinking velocities were generated from empirical relationships to a strongly correlated morphometric, the dorsal cross-sectional area (A_D). Upward swimming velocity (W_{swim}) was best approximated by the exponential function $W_{swim} = 0.04\, e^{1.06 \times 10^7 A_D + \varepsilon}$ ($p \ll 0.001$, $R^2 = 0.41$; Figure 5-4), where ε is a normally distributed error term with a mean of 0 and a standard deviation equal to that of the residuals of the regression. An exponential function was used to prevent negative W_{swim}

for smaller larvae. Random values of A_D were drawn from observed distributions within each larval group, and a corresponding W_{swim} was generated.

Sinking velocity (W_{sink}) was estimated based on morphology according balance of drag and buoyancy and by the equation:

$$W_{sink} = \sqrt{\frac{2gV_L(\rho_L - \rho_f)}{\rho_f A_A C_D}} \quad \textbf{(5.6)}$$

Where g is the gravitation acceleration (9.8 m s^{-2}), ρ_L is the density of larvae (1066 kg m^{-3}: Fuchs and Low, unpublished data.), and A_A is the anterior cross-sectional area of larvae (in their sinking orientation). C_D is the drag coefficient of larvae (White, 1974):

$$C_D = \frac{24}{Re} + \frac{6}{1 + \sqrt{Re}} + 0.4 \quad \textbf{(5.7)}$$

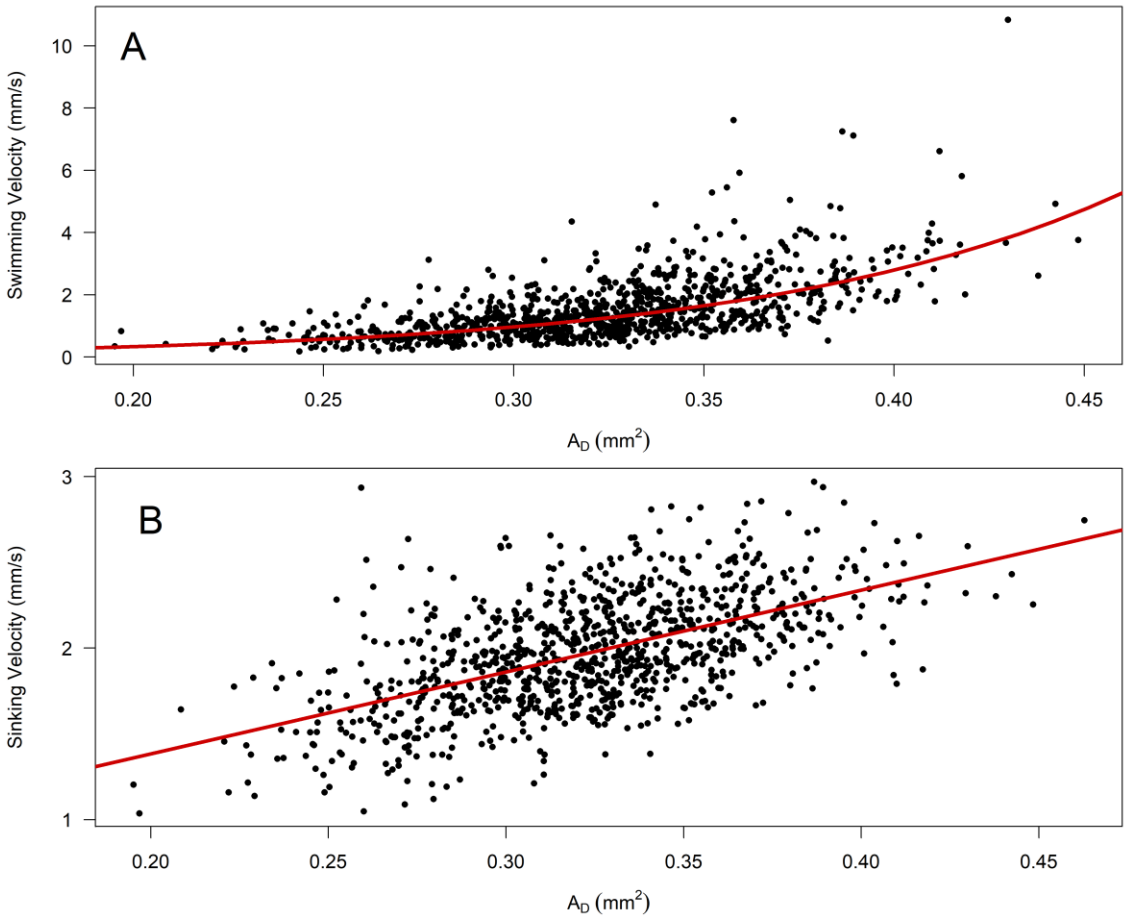

Figure 5-3: *Relationship between dorsal cross-sectional area (A_D) and larval swimming (A) and sinking (B) velocity. Red lines shows the results of the log-linear regression for swimming velocity (R^2 = 0.39, $p < 0.001$) and the linear regression for sinking velocity (R^2 = 0.30, $p \ll 0.001$). Both show larvae from the overall distribution (group O).*

Re is the Reynolds number, defined by $\frac{CL \times W_{sink}}{\nu}$ where CL is the carapace length (the characteristic length) of larvae, and ν is the kinematic viscosity of seawater (0.001 kg $m^{-1}s^{-1}$). This formulation of C_D is valid for objects with Re from 1 to 2×10^5 (White, 1974) and encompasses the typical range of zoeal Re. W_{sink} was solved for numerically. Linear regressions were used to generate A_A, CL, and V_T from A_D. For A_A the equation was

$$A_A = 0.58A_D + 4.32 \times 10^{-8} + \varepsilon \textbf{ (p} \ll \textbf{0.001, R}^2\textbf{=0.68)} \quad \textbf{(5.8)}$$

Similarly,

$$CL = 534A_D + 2.04 \times 10^{-4} + \varepsilon \textbf{ (p} \ll \textbf{0.001, R}^2\textbf{=0.46)} \quad \textbf{(5.9)}$$

and

$$V_T = 1.57 \times 10^{-4}A_D - 1.08 \times 10^{-11} + \varepsilon \textbf{ (p} \ll \textbf{0.001, R}^2\textbf{=0.70)} \quad \textbf{(5.10)}$$

Together, this allowed empirically-based distributions of W_{swim} and W_{sink} to be generated for individual larval broods (Table 5-2) while also enabling individual-level variation.

Table 5-2: Median swimming (W_{swim}) and sinking (W_{sink}) velocity and median absolute deviation for each larval group.

Larval Group	W_{swim} (mm s^{-1})	W_{sink} (mm s^{-1})
O	1.25 ± 0.77	1.97 ± 0.34
A	2.56 ± 1.39	2.27 ± 0.30
B	1.74 ± 0.93	2.11 ± 0.30
C	1.16 ± 0.61	1.93 ± 0.31
D	0.98 ± 0.52	1.86 ± 0.32

5.2.3 Inclusion of Turbulent Motion

Turbulence was incorporated into the vertical motion of particles using Ross & Sharples' (2004) method whereby the vertical position of larvae (z) was determined by the discrete-time process:

$$z_{n+1} = z_n + \frac{\delta A_v(z_n)}{\delta z}\Delta t + R\left[\frac{2}{r}A_v\left(z_n + \frac{1}{2}\frac{\delta A_v(z_n)}{\delta z}\Delta t\right)\Delta t\right]^{1/2} + W_p\Delta t \quad \textbf{(5.11)}$$

Where n is the time step index, Δt is the discrete time increment (1s), R is a uniformly distributed random number between -1 and 1, r is the variance of the uniform distribution

(1/3), and W_p is the directed particle velocity (W_{swim} or W_{sink}) depending on the orientation. The second term is deterministic and moves particles towards depths of increased diffusivity. The third term is random motion that increases nonlinearly with depth. The final term represents the directed motion of larvae.

A simple reflective boundary was used such that deviations above or below the top and bottom boundary were redirected proportionally inwards

$$z_{n+1}\begin{cases} -z_n & z_{n+1} > 0 \\ 2H + z_{n+1} & z_{n+1} < -H \end{cases} \quad \textbf{(5.12)}$$

5.2.4 Model Scenarios

All models were implemented in R (R Core Team 2015). In all model configurations, 10,000 particles were released. This number exceeds that needed to reach less than 5% unexplained variance described by Simons et al. (2013) and allows for a smooth distribution of particle positions. A timestep of 1s was used, which meets criteria specified by Ross and Sharples (2004). For each timestep, horizontal and vertical displacements were applied based on the vertical velocity and diffusivity profiles specified for each model configuration. When behavior was present, particles would swim upwards until reaching the surface then begin sinking until they reached their D_{max}. All particles were released at 1m depth for 4 days simulated time, with position output saved every 10 minutes.

Two distinct model scenarios were constructed. In the first scenario (*behavior model*), larval behavior was present, and configurations included all combinations of wind speed (3), plume density (2), D_{max} (3), and larval group (5), for a total of 90 model

configurations. The second scenario was a passive control simulation (*passive model*) where particles were neutrally buoyant and no behavior was present (W_{swim} = 0 ms^{-1} and W_{sink} = 0 ms^{-1}). Particle trajectories were simulated for all combinations of wind speed (3) and plume density (2), for a total of 6 configurations.

5.2.5 Statistical Analysis

All statistical analyses were performed in R (R Core Team 2015). For each model configuration, the final position of particles was vectorized in the x-y plane to obtain the net transport distance (*S*). The net-transport in the x (along-plume) and y (cross-plume) directions were also calculated, X_{net} and Y_{net}, respectively. Since the distributions of *S* were sometimes skewed or irregular, medians were used as the central statistic with the median absolute deviation (MAD) as a measure of dispersion. For each scenario, an ANOVA was performed to determine whether *S* changes with physical (wind and plume density) and behavioral parameters (D_{max} and larval group). Then Kolmogorov-Smirnov (K-S) tests were used to determine whether the distribution of *S* from the *behavior model* differed from the *passive model*. Additionally, the depth of particles was calculated after 4 days for all configurations in both the *passive model* and the *behavior model*. An ANOVA was used to determine whether model parameters influence vertical position. Additionally, K-S tests were used to evaluate whether mean particle depth from the *behavior model* differed from analogous configurations of the *passive model*.

In order to investigate the relationship between larval swimming velocity and net transport, the maximum possible transport was calculated for each model configuration as a reference point. This was done by calculating the magnitude of the current produced by each wind speed (eq 5.2 and 5.3) at the average depth zoeae should occupy at a given D_{max}

and with no diffusivity. This average depth is approximately one half of $D_{max,}$ as their behavior aims to keep them above D_{max} at all times. Assuming this constant horizontal velocity, the maximum transport distance over the 4 day simulation time was calculated.

For each wind configuration the Péclet number (Pe) was calculated for all larval swimming velocities. Pe is a dimensionless measure of the balance between diffusive and advective forces, and it can be used as a general indicator of the dominant forces acting on swimming plankton (Karp-Boss et al. 1996). Pe is defined in this case by

$$Pe = \frac{z_p W_{swim}}{\overline{A_v}} \quad \textbf{(5.13)}$$

Where $\overline{A_v}$ is the mean A_v across the plume. The fraction of simulated larvae above or below Pe=1 was calculated to evaluate those model configurations for which swimming behavior dominated particle motion.

5.3 Results

5.3.1 Behavior Model

For the *behavior model* a 4-factor ANOVA was performed (*S* = Wind × Plume Type × D_{max} × Larval Group; Table 5-3). Wind speed was the dominant factor, where generally, an increase in wind speed resulted in further transport (Figure 5-4). However, in the case of D_{max} = 0m, particles were able to maintain a near-surface position at low wind speeds, increasing their transport relative to particles with a deeper D_{max} (Figure 5-5). This effect explains the relatively strong interaction between wind and D_{max}. Typically,

differences in D_{max} alone were more important during low wind conditions where larvae had more control over their vertical position. Larval group also had a relatively large effect on *S*, specifically when D_{max} was 0m. Here, faster swimming broods were able to stay closer to the surface and transport further. For deeper D_{max} configurations, particles were more evenly mixed throughout the plume, and the brood effect is diminished. When wind speed increases with a corresponding increase in A_v, the difference between broods' transport increases. While unintuitive, this effect is due to slower swimming broods being mixed deeper with reduced transport, whereas faster swimming broods are still able to hold a higher vertical position. The two plume types resulted in differences in *S*, but with a relatively small effect size compared to other factors.

The relative frequency of *S* for each larval group was also calculated (Figure 5-6). Distributions were unimodal and more symmetrical for particles with a D_{max} of 1.5m and 3m. Particles with a D_{max} of 0m had more skewed distributions where the most frequent transport distance differing between larval groups. Notably, the fasting swimming brood (A) is transported significantly further than all other broods (K-S test, $p \ll 0.001$). As wind speed increases, distributions of *S* become narrower because the larvae become more uniformly mixed throughout the plume layer. When more evenly mixed, larvae experience almost a depth-averaged current and thus over time are transported somewhat similarly, despite increased diffusivity.

When separating net transport into along- (X_{net}) and across- (Y_{net}) plume components, X_{net} followed the same response to model configurations as *S* (Figure 5-7). However, when particles were positioned at an intermediate depth within the plume they experienced a reversal in flow, driving them more southward than those closer to the

surface. This is evident through the interaction of wind speed and D_{max} on Y_{net} (Figure 5-7). When D_{max} is 0m, Y_{net} decreases when wind speed increases since particles are mixed deeper and average current velocity experienced by larvae decreases. When D_{max} increases and wind speed remains low, larvae are mixed more uniformly across the plume and their average V velocity trends towards zero. However, when wind speed is increased, larvae are still more deeply mixed but V also increases, resulting in a greater Y_{net}. The increase in Y_{net} with D_{max} and wind is also evident when looking at the x-y trajectories of particles (Figure 5-8).

Table 5-3: Results of 4-way ANOVA on net transport distance in the *Behavior Model* scenario. P values are adjusted using a Bonferroni correction (90 comparisons).

	Df	Mean Square	F	p	Effect Size
Wind	2	5.15×10^8	5.70×10^5	$\ll 0.001$	0.385
Plume Type	1	2.49×10^7	2.76×10^4	$\ll 0.001$	0.009
D_{max}	2	1.84×10^8	2.04×10^5	$\ll 0.001$	0.138
Larval Group	4	4.88×10^7	5.41×10^4	$\ll 0.001$	0.073
Wind × Plume Type	2	1.88×10^6	2,086	$\ll 0.001$	0.001
Wind × D_{max}	4	4.25×10^7	4.70×10^4	$\ll 0.001$	0.064
Plume Type × D_{max}	2	9.76×10^5	1,081	$\ll 0.001$	0.001
Wind × Larval Group	8	1.72×10^6	1,911	$\ll 0.001$	0.005
Plume Type × Larval Group	4	6.45×10^4	71	$\ll 0.001$	<0.001
D_{max} × Larval Group	8	5.37×10^6	5,953	$\ll 0.001$	0.016
Wind × Plume Type × D_{max}	4	1.89×10^5	210	$\ll 0.001$	<0.001
Wind × Plume Type × Larval Group	8	3,514	4	$\ll 0.001$	<0.001
Wind × D_{max}× Larval Group	16	4.13×10^5	457	$\ll 0.001$	0.002
Plume Type × D_{max} × Larval Group	8	1.92×10^4	21	$\ll 0.001$	<0.001
Wind × Plume Type × D_{max} × Larval Group	16	1,573	2	0.033	<0.001
Residuals	899910	902			

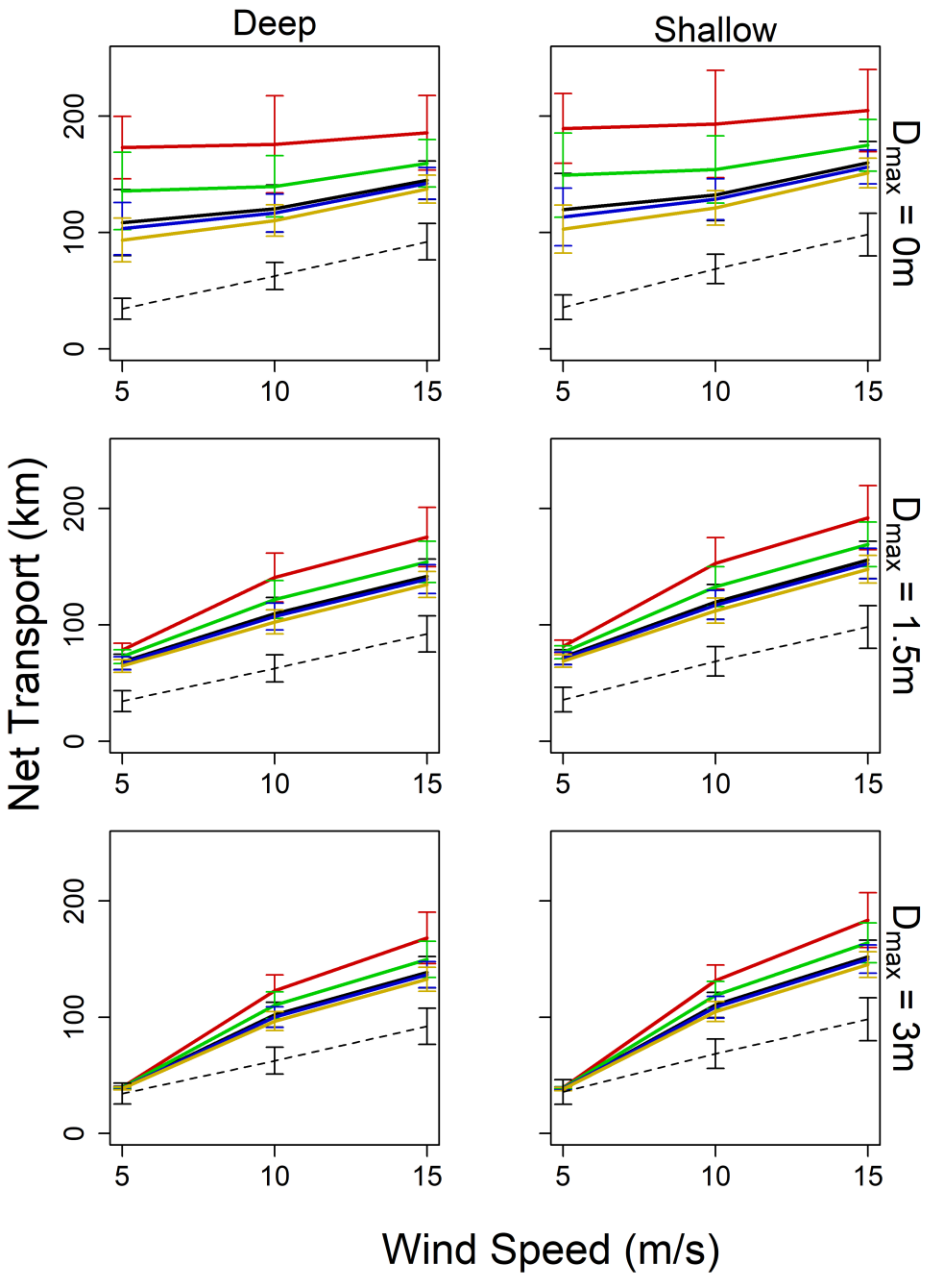

Figure 5-4: *Net particle transport was calculated for each configuration of the behavior model. Larval groups are represented by solid lines (A, red; B, green; C, blue; D, yellow; O, black). Dashed lines show the transport from the passive model for the corresponding wind speed and plume type. Transport is separated by plume type (columns) and* D_{max} *(rows). Error bars represent the median absolute deviation of net transport for all particles (N = 10,000).*

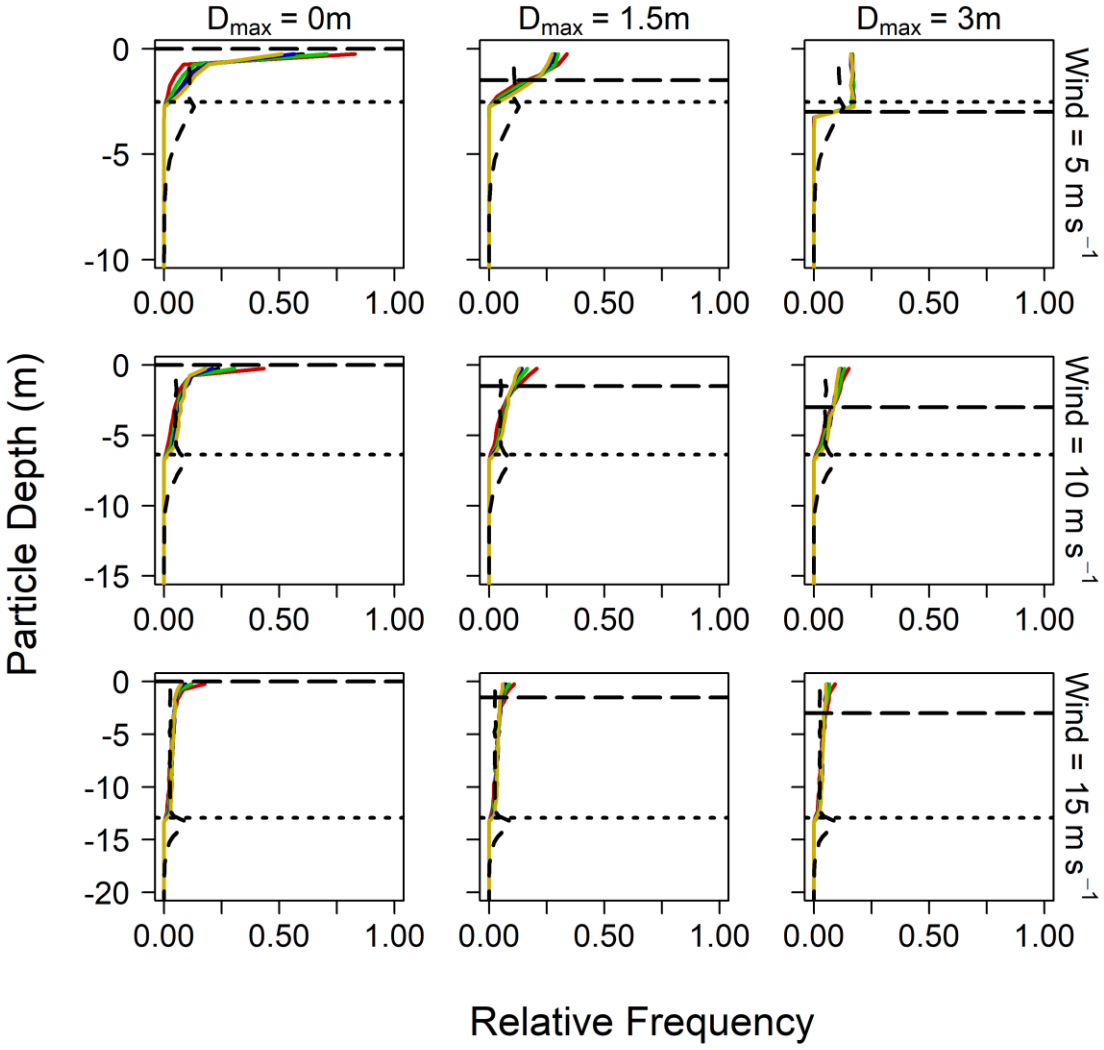

Figure 5-5: *The relative frequency of the vertical position of particles was calculated using 1m bins. Solid lines denote each larval group lines (A, red; B, green; C, blue; D, yellow; O, black), and dashed lines denote vertical distribution of passive particles. Horizontal dotted lines show the plume depth at each configuration. Horizontal dashed lines show D_{max} depth. Only the depths from the deeper plume are shown here (shallow plume distributions follow the same pattern). D_{max} values are shown in columns and wind speeds are shown by rows.*

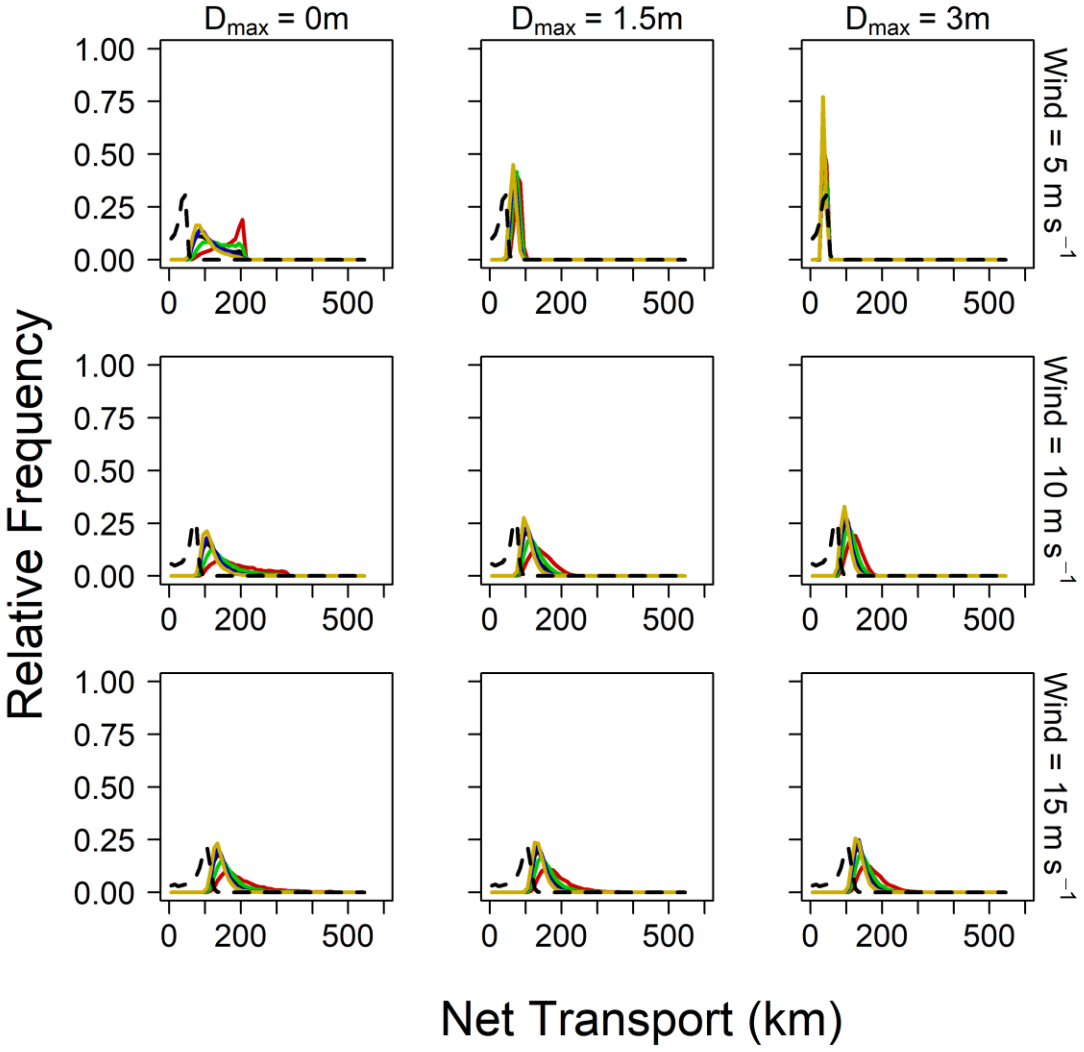

Figure 5-6: *Relative frequency of net transport was calculated using 10 km bins. Solid lines denote each larval group lines (A, red; B, green; C, blue; D, yellow; O, black), and dashed lines denote distribution of net transport for passive particles. Rows and columns show results for different configurations of wind speed and D_{max}, respectively. Only data from the deeper plume configuration is shown here.*

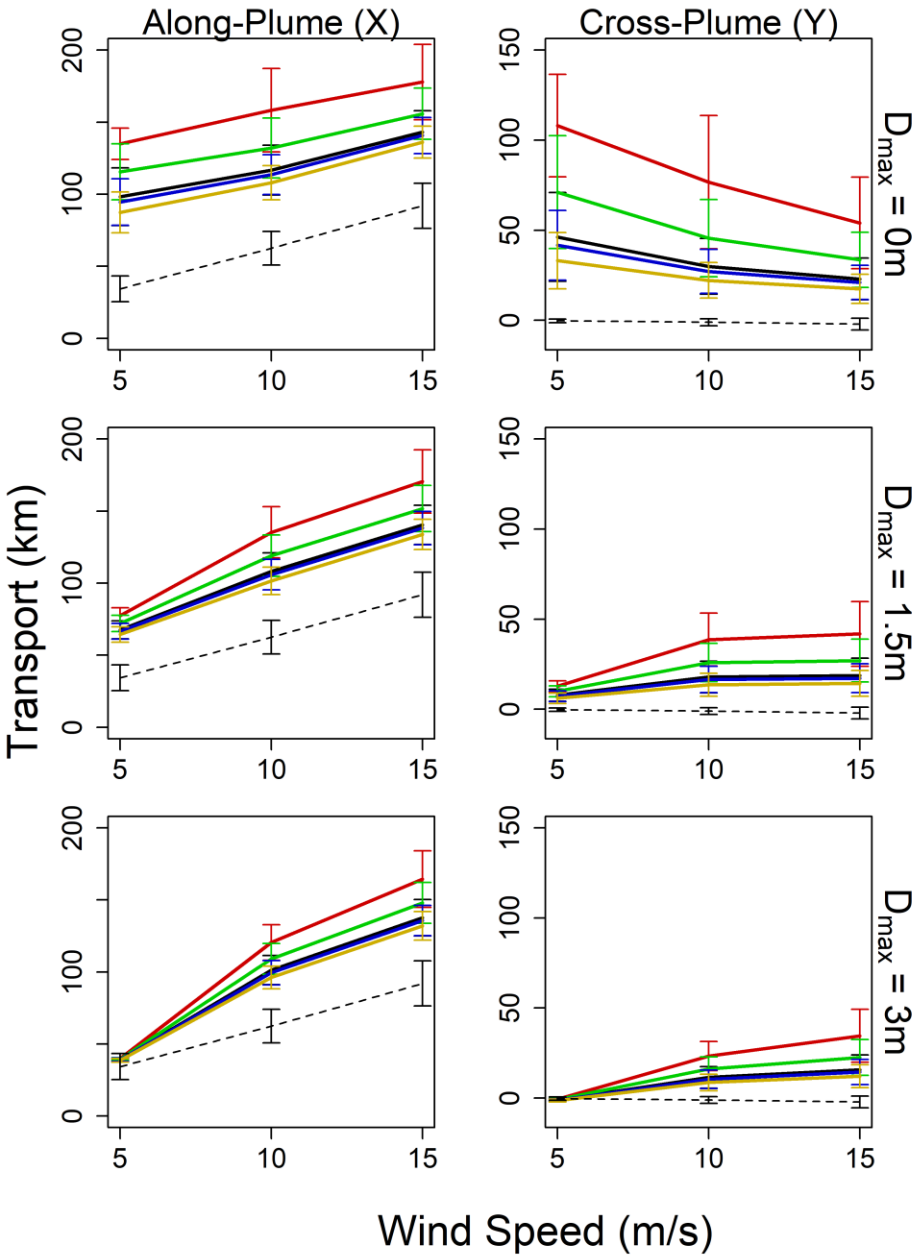

Figure 5-7: *Particle transport was calculated in the along-plume (x) direction (left column) and the cross-plume (y) direction (right column) as a function of wind speed. Larval groups are represented by solid lines (A, red; B, green; C, blue; D, yellow; O, black). Dashed lines show the transport from the passive model for the corresponding wind speed. Rows show transport for each* D_{max} *value. Error bars represent the median absolute deviation of net transport for all particles (N = 10,000).*

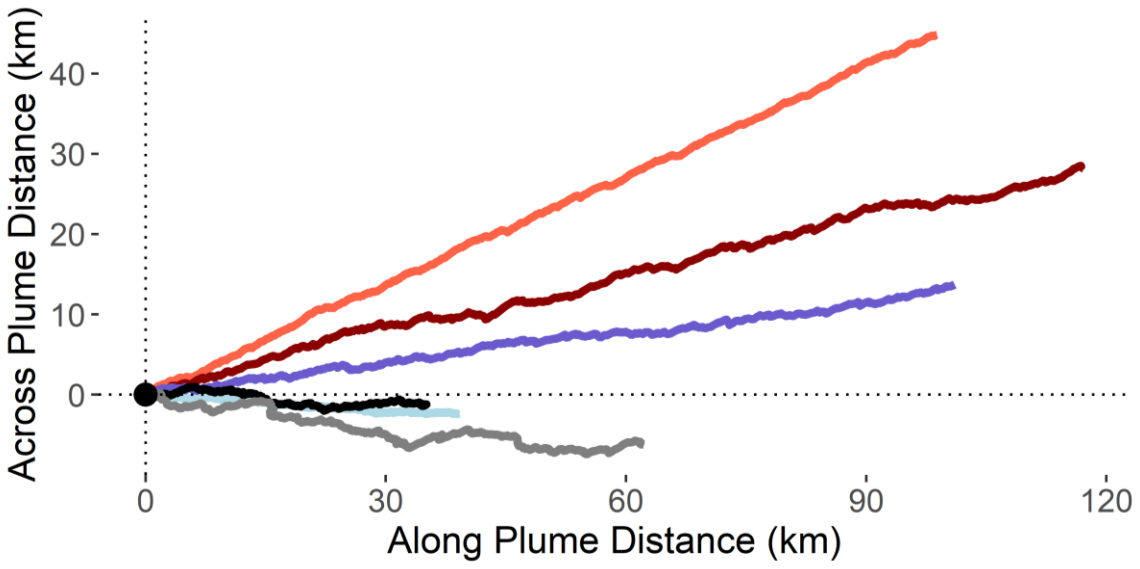

Figure 5-8: *Example 2-dimensional trajectories of particles representative of median net transport from various model configurations. Particles with a* D_{max} *of 0m (red) and 3m (blue) are shown for both a 5* ms^{-1} *(light shade) and 10* ms^{-1} *(dark shade) wind. Two passive particle trajectories are also shown for 5* ms^{-1} *(black) and 10* ms^{-1} *(grey) wind speeds.*

5.3.1 Passive Model

A 2-way ANOVA was performed for the *passive model* (*S* = wind × plume type; Table 5-3), and both factors as well as their interaction resulted in different transport distances. Similar to the *behavior model*, *S* increases with wind speed (Figure 5-4) and plume type has a significant but relatively weak effect on *S*. Particles in the *passive model* became uniformly distributed across the plume within 1 to 2 hours. There was a slight aggregation at the pycnoline (Figure 5-5), caused by the rapid decrease in A_v to the background diffusivity in the lower layer. Over the course of the 4 days simulation, particles began to mix deeper into the lower layer, but did not reach a uniform distribution there.

Two-sampled K-S tests were used to assess whether *S* differed between larval groups in the *behavior model* and passive particles. In all 90 configurations of the *behavior*

model the distribution of S and vertical position differed from that of passive particles (K-S, $p \ll 0.001$). Furthermore, the median *S* for all larval groups was greater than that of passive particles in the same physical conditions. The difference between both models was the smallest at the slowest wind speed and highest D_{max} (Figure 5-4). When D_{max} is closer to the plume depth, larvae spent more time sinking and thus were mixed more thoroughly throughout the plume resulting in trajectories more like passive particles (Figure 5-5; Figure 5-8).

Table 5-3: Results of 2-way ANOVA on net transport distance in the *passive model* scenario. P values are adjusted with a Bonferroni correction (6 comparisons).

	Df	**Mean Square**	**F**	**p**	**Effect Size**
Wind	2	7.04×10^8	3.53×10^8	$\ll 0.001$	0.38
Plume Type	1	1.94×10^6	1.94×10^6	$\ll 0.001$	0.001
Wind × Plume Type	2	1.39×10^6	6.94×10^5	$\ll 0.001$	0.001
Residuals	119994	1.14×10^9	9,524		

5.3.2 Swimming Velocity and Transport

The presence brood-dependent larval transport observed in the *behavior model* suggested that transport should be related to larval swimming velocity. When plotting *S* as a function of W_{swim} there was a positive non-linear relationship whereby faster swimming larvae travel further, but this relationship asymptotes to some maximum transport distance (Figure 5-9). This distance appears to be close to the maximum distance particles can be transported over the model duration when fixed at one half of D_{max}, as it is roughly the mean depth larvae occupy in the absence of vertical diffusivity. This point is reached at slower W_{swim} when wind speed is lower. The majority of larvae swam too slowly to reach this maximum

transport distance in most model configurations, with the exception of those at the slowest wind speeds that were able to achieve maximum transport.

To help illustrate the source of brood-dependent transport and its relationship to W_{swim}, the fraction of all simulated larvae whose Péclet number exceeded one was calculated (Table 5-4). At a wind speed of 5 ms^{-1} in the deeper plume scenario, at least 95% of zoeae from all larval groups had a Pe > 1. Thus, almost all zoeae have control over their vertical position when wind speeds are low. However, as wind speed increases the proportion of larvae whose Pe>1 decreases and the differences in Pe between broods is more apparent. When winds are 15 ms^{-1}, the fastest swimming brood (A) swimming dominates vertical transport for 88% of larvae, but for the slowest swimming brood (D), only 30% of larvae have a Pe>1. This disparity between broods explains why there is an increase in brood-level differences in transport at higher wind speeds despite an increase in diffusivity. In no model configuration do all larvae have a Pe <1, resulting in broods never entirely like passive particles.

Table 5-4: The proportion of larvae with a Péclet number greater than 1 for each wind speed within the deeper plume configurations.

Wind Speed (ms^{-1})	O	A	B	C	D
5	0.97	1.00	1.00	0.97	0.95
10	0.77	0.98	0.93	0.77	0.66
15	0.47	0.88	0.69	0.41	0.30

5.4 Discussion

5.4.1 Larval Behavior and Transport

The results of this study suggest that observed variation in *Callinectes sapidus* larval behavior can result in differences in larval transport within wind-driven estuarine plumes. Though the idealized plume structure and Ekman dynamics in this model exclude other important physical processes, wind-driven systems can produce vertically sheared currents (Richman et al. 1987; Craig 1996). The simplicity of this model allowed for a clearer investigation on the interaction between physical conditions and different behaviors. Though wind speed was the dominant factor in determining net transport, larval swimming velocity and depth-regulating behaviors significantly influenced the vertical position and net transport of simulated larvae. Specifically, zoeae simulated from different larval broods differed in their transport, predominantly due to differences in swimming velocity. Furthermore, in all model configurations, larvae with behavior were transported differently than passive particles. Together, these results indicate that brood effects on *C. sapidus* zoeal swimming behavior observed by Caracappa and Munroe (2019) may result in brood-dependent larval transport.

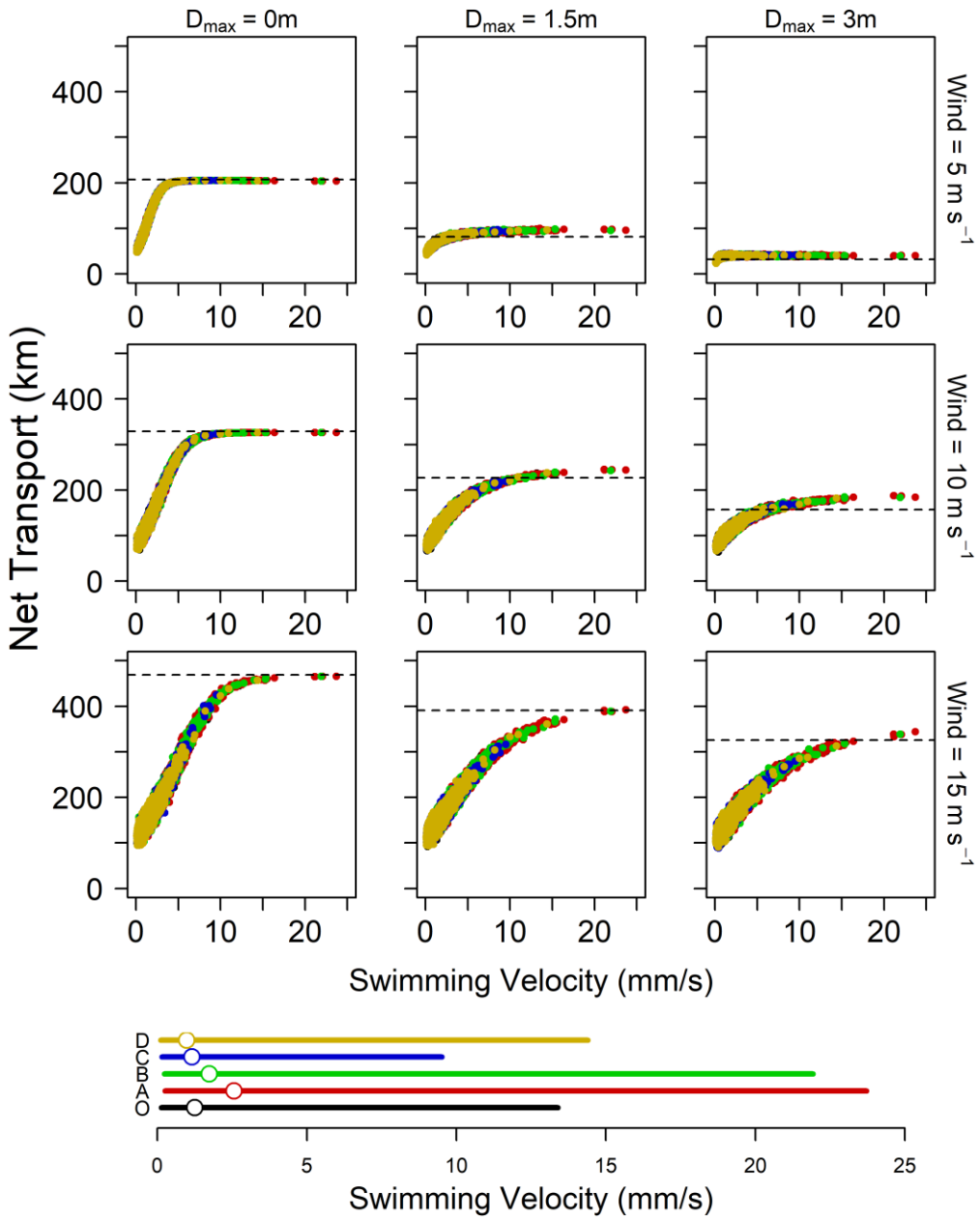

Figure 5-9: The net transport for all particles in the behavior model as a function of larval swimming velocity. Data is divided by Dmax (columns) and wind speed (rows). Dashed horizontal lines show the maximum transport possible for particles fixed at one half Dmax for a given wind speed. Bottom panel shows the range of swimming velocities for each larval group with open circles denoting the median. *Larval groups are separated by color* (A, red; B, green; C, blue; D, yellow; O, black).

Several studies have modeled *Callinectes sapidus* larval dispersal in the mid-Atlantic, but to my knowledge none have incorporated individual larval behavior or behavioral variability. Johnson et al. (1984) utilized a two-layer wind-driven circulation model to investigate the dynamics of larval dispersal for blue crabs in coastal waters. They identified the presence of a southward nearshore current with an offshore counter-current, hypothesized to be responsible for the return of larvae to the estuary. In a follow-up study, Johnson (1985) utilized the same model but applied to the geography of the Chesapeake Bay mouth, wherein the importance of wind-stress and seasonality in determining trajectories was noted. A later model (Johnson and Hess 1990) incorporated more accurate environmental data as well as estuarine circulation dynamics to simulate larval transport within and offshore of Chesapeake Bay. This study identified reinvasion of the estuary as the primary source of recruitment rather than retention of larvae within the bay. Garvine et al. (1997) used an idealized Delaware Bay mouth and inner continental shelf to simulate *C. sapidus* dispersal. That model included both wind-driven and buoyancy driven circulation and was able to replicate one recruitment event. More recently, models (Tilburg et al. 2005, 2006, 2009) have used more refined spatial boundaries and general circulation to investigate mesoscale processes underlying dispersal dynamics and the spatial cohesion of larvae, but they also treated larvae as passive particles. While advancements in computational power and our understanding of coastal circulation have greatly improved during this period, none of these models included elements of individual and varying larval behavior beyond surface retention. Instead, larvae were either simulated as pure Lagrangian drifters (i.e. passive particles) or passive particles travelling with the mean surface (upper 2 m) circulation.

Though most zooplankton do not have the ability to swim against horizontal currents, many are able to exert control over their vertical position. Since horizontal advection can vary substantially with depth (i.e. sheared flow), swimming behavior can potentially alter the trajectories of larvae in ways different than those predicted by passive transport alone (Shanks 1995, 2009; Metaxas 2001). Behavior-driven differences in larval transport have been simulated in models of larval bivalves (North et al. 2008; Munroe et al. 2018), corals (Szmant and Meadows 2006), and other decapod crustaceans (Katz et al. 1994; Moksnes et al. 2014). *C. sapidus* larvae maintain a position near the surface, and a constant effort is required to counter their negative buoyancy. The results of this model align with field observations, where under relatively calm conditions, zoeae are heavily skewed towards the surface. However, to my knowledge, there are no published data on the vertical distribution of zoeae as a function of wind speed or vertical diffusivity. Due to the nature of wind-driving mixing, zoeae should be more deeply mixed when winds are stronger, but the how behavior and other processes influence their vertical distributions in the field remains unknown.

While behaviors encompassed observed variability, they were based on experiments done under controlled and static conditions (Caracappa and Munroe 2019), and *C. sapidus* larval behavior can vary with environmental conditions (Forward and Cronin 1980; Sulkin et al. 1980) or molt stage (Sulkin et al. 1980). However, behavioral responses to some important environmental conditions (e.g. turbulence, salinity, temperature, light, food) have either not been published or not in enough detail to create a distribution of possible behaviors. These data gaps make an individual-based model with larval behavior that aim to simulate larval transport in real space, difficult to parameterize

accurately, and more experimental or monitoring work is needed to fully understand the complete range of *C. sapidus* larval behaviors and how they influence dispersal processes.

5.4.2 Behavioral Variation

While the model used in this study was not intented to accurately simulate the full dynamics of inner-shelf or estuarine circulation, it does illustrate how observed variation in basic behaviors can influence the trajectories of larvae. Larval morphology has been shown to differ between broods in both *C. sapidus* (Caracappa and Munroe 2018) and *Pugettia quadridens* (Tamura et al. 2017), and these differences have been shown to correlate with differences in swimming behavior (Caracappa and Munroe 2019). Brood-level variation results in a 2.5 fold difference in W_{swim} in these simulations, which caused up to a 1.7 fold difference in brood transport. However, when ignoring larval groups, variation in W_{swim} caused over a 2-fold difference in net transport in some cases. The highly-skewed distributions of swimming velocity result in similarly skewed transport distances, such that the faster-swimming half of the larvae can be transported a wider range of distances than the slower-swimmign half. Though net transport differed statistically between larval broods, the differences between broods can become quite small, especially for slower wind speeds and deeper D_{max}.

While the behaviors of the larval broods chosen for this study do form a continuous, overlapping distribution of behaviors, there is no certainty that they are sufficient or entirely representative of the reproducing population, nor across multiple populations. Regardless, the presence of outlier broods, such as brood A, suggest that there could be a small subset of the reproducing population that is capable of producing larvae that can swim fast enough to be transported much further than others. It may be the larvae within

the long tails of the velocity distributions that end up dispersing to further distant habitats (founder individuals).

Across the population, successful recruitment of *C. sapidus* larvae is a relatively rare event, with estimates of over 99% mortality during larval development and dispersal (McConaugha 1992). Past modelling efforts have identified that loss to advection (i.e. larval wastage) may be the largest component of mortality (Garvine et al. 1997). It is worth stressing that transport distance is in no way a metric of successful dispersal. For instance, larvae exported too far south along the mid-Atlantic shelf may be advected outside suitable settlement habitat via the Gulf Stream. Clearly, more complex models of shelf dynamics are needed to predict realistic dispersal trajectories and evaluate success rates across the population. However, with the knowledge of how larval behavior interacts with sheared flow and diffusivity to influence transport, coupled with observed behavioral variaiblity in *C. sapidus* larvae, it stands to reason that a better understanding is needed of how larval behavior and its variability can influence dispersal and recruitment.

5.5 Literature Cited

Caracappa JC, Munroe DM (2018) Morphological variability among broods of first-stage blue crab (*Callinectes sapidus*) zoeae. Biol Bull 235:123–133.

Caracappa JC, Munroe DM (2019) Variability in swimming behavior among broods of blue crab (*Callinectes sapidus*) zoeae. J Exp Mar Bio Ecol 518:151176. doi: 10.1016/j.jembe.2019.151176

Costlow JDJ, Bookhout CG (1959) The larval development of *Callinectes Sapidus* Rathbun reared in the laboratory. Biol Bull 116:373–396.

Craig PD (1996) Velocity profiles and surface roughness under breaking. J Geophys Res 101:1265–1277.

Epifanio CE (1995) Transport of blue crab (*Callinectes sapidus*) larvae in the waters off Mid-Atlantic states. Bull Mar Sci 57:713–725.

Epifanio CE, Cohen JH (2016) Behavioral adaptations in larvae of brachyuran crabs: A review. J Exp Mar Bio Ecol 482:85–105. doi: 10.1016/j.jembe.2016.05.006

Epifanio CE, Tilburg CE (2008) Transport of blue crab larvae in the Middle Atlantic Bight: A wet and windy journey. J Mar Res 66:723–749.

Fong DA, Geyer RW (2001) Response of a river plume during an upwelling favorable wind event. J Geophys Res Ocean 106:1067–1084. doi: 10.1029/2000JC900134

Forward RB, Cronin TW (1980) Tidal rhythms of activity and phototaxis of an estuarine crab larvae. Biol Bull 158:295–303.

Forward RJB, Buswell CU (1989) A comparative study of behavioral responses of larval decapod crustaceans to light and pressure. Mar Behav Physiol 16:43–56.

Garvine RW, Epifanio CE, Epifanio CC, Wong K-C (1997) Transport and recruitment of blue crab larvae: A model with advection and mortality. Estuar Coast Shelf Sci 45:99–111. doi: 10.1006/ecss.1996.0161

Johnson DF, Hess KW (1990) Numerical simulations of blue crab larval dispersal and recruitment. Bull Mar Sci 46:195–213. doi: 10.1111/j.1365-294X.2005.02538.x

Johnson DR (1985) Wind-forced dispersion of blue crab larvae in the Middle Atlantic Bight. Cont Shelf Res 4:733–745. doi: 10.1016/0278-4343(85)90039-1

Johnson DR, Hester BS, Mcconaugha JR (1984) Studies of a wind mechanism influencing the recruitment of blue crabs in the Middle Atlantie Bight. 3:425–437.

Karp-Boss L, Boss E, Jumars PA (1996) Nutrient fluexes to planktonic osmotrophs in the presence of fluid motion. Oceanogr Mar Biol An Annu Rev 34:71–107.

Katz CH, Cobb JS, Spaulding M (1994) Larval behavior, hydrodynamic transport, and potential offshore-to-inshore recruitment in the American lobster *Homarus americanus*. Mar Ecol Prog Ser 103:265–274. doi: 10.3354/meps104265

Large WG, Pond S (1980) Open ocean momentum flux measurements in moderate to strong winds. J Phys Oceanogr 11:324–336.

López-Duarte PC, Tankersley R a. (2007) Circatidal swimming behavior of brachyuran crab zoea larvae: Implications for ebb-tide transport. Mar Biol 151:2037–2051. doi: 10.1007/s00227-007-0614-3

McConaugha J (1992) Decapod larvae: Dispersal, mortality, and ecology. A working hypothesis. Am Zool 32:512–523.

Metaxas A (2001) Behaviour in flow: Perspectives on the distribution and dispersion of meroplanktonic larvae in the water column. Can J Fish Aquat Sci 58:86–98. doi: 10.1139/f00-159

Moksnes P-O, Corell H, Tryman K, Hordoir R, Jonsson PR (2014) Larval behavior and dispersal mechanisms in shore crab larvae (*Carcinus maenas*): Local adaptations to different tidal environments? Limnol Oceanogr 59:588–602. doi: 10.4319/lo.2014.59.2.0588

Munroe DM, Haidvogel D, Caracappa JC, Klinck JM, Powell EN, Hofmann EE, Shank B V, Hart DR (2018) Modeling larval dispersal and connectivity for Atlantic sea scallop (*Placopecten magellanicus*) in the Middle Atlantic Bight. Fish Res 208:7–15. doi: 10.1016/j.fishres.2018.06.020

North EW, Schlag Z, Hood RR, Li M, Zhong L, Gross T, Kennedy VS (2008) Vertical swimming behavior influences the dispersal of simulated oyster larvae in a coupled particle-tracking and hydrodynamic model of Chesapeake Bay. Mar Ecol Prog Ser 359:99–115. doi: 10.3354/meps07317

Pond S, Pickard GL (1983) Introductory Dynamical Oceanography. Pergamon Press

Provenzano A (1983) Vertical distribution of first stage larvae of the blue crab, *Callinectes sapidus*, at the mouth of Chesapeake Bay. Estuar Coast Shelf Sci 16:489–499.

R Core Team (2015) R: A language and environment for statistical computing.

Richman JG, de Szoeke RA, Davis RE (1987) Measurements of near-surface shear in the ocean. J Geophys Res 92:2851–2858.

Ross ON, Sharples J (2004) Recipe for 1-D Lagrangian particle tracking models in space-varying diffusivity. Limnol Oceanogr Methods 2:289–302.

Shanks AL (1995) Mechanisms of cross-shelf dispersal of larval invertebrates. In: McEdward LR (ed) Ecology of Marine Invertebrate Larvae. CRC Press, New York, pp 323–368

Shanks AL (2009) Pelagic larval duration and dispersal distance revisited. Biol Bull 216:373–385. doi: 10.2307/25548167

Simons RD, Siegel DA, Brown KS (2013) Model sensitivity and robustness in the estimation of larval transport: A study of particle tracking parameters. J Mar Syst 119–120:19–29. doi: 10.1016/j.jmarsys.2013.03.004

Smyth PO (1980) *Callinectes* (decapoda: portunidae) larvae in the Middle Atlantic Bight, 1975-77. Fish Bull 78:251–265.

Sulkin SD (1984) Behavioral basis of depth regulation in the larvae of brachyuran crabs. Mar Ecol Prog Ser 15:181–205. doi: 10.3354/meps015181

Sulkin SD, van Heukelem W, Kelly P, van Heukelem L (1980) The behavioral basis of larval recruitment in the crab *Callinectes sapidus* Rathbun: A laboratory investigation of ontogenetic changes in geotaxis and barokinesis. Biol Bull 159:402–417.

Szmant AM, Meadows MG (2006) Developmental changes in coral larval buoyancy and vertical swimming behavior : Implications for dispersal and connectivity. Proc 10th Int Coral Reef Symp 431–437.

Tamura H, Landeira JM, Goshima S (2017) Morphological and morphometric variability in the zoea I larvae of *Pugettia quadridens* (De Haan, 1839): looking for reliable characters for taxonomic studies on the genus *Pugettia* Dana, 1851 (Majoidea: Epialtidae). Zootaxa 4226:264–272.

Tilburg CE, Reager JT, Whitney MM (2005) The physics of blue crab larval recruitment in Delaware Bay: A model study. J Mar Res 63:471–495. doi: 10.1357/0022240053693699

Tilburg CE, Houser LT, Steppe CN, Garvine RW, Epifanio CE (2006) Effects of coastal transport on larval patches: Models and observations. Estuar Coast Shelf Sci 67:145–160. doi: 10.1016/j.ecss.2005.11.019

Tilburg CE, Dittel AI, Epifanio CE (2009) High concentrations of blue crab (*Callinectes sapidus*) larvae along the offshore edge of a coastal current: Effects of convergent circulation. Fish Oceanogr 18:135–146. doi: 10.1111/j.1365-2419.2009.00502.x

Velazquez CCS (2016) The kinematics and particle image velocimetry of the shore crab larvae *Carcinus maenas*. California State University, Fresno

Visser AW (1997) Using random walk models to simulate the vertical distribution of particles in a turbulent water column. Mar Ecol Prog Ser 158:275–281.

White FM (1974) Viscous Fluid Flow. McGraw-Hill, New Yor

Whitney MM, Garvine RW (2005) Wind influence on a coastal buoyant outflow. J Geophys Res 110:1–15. doi: 10.1029/2003JC002261

Yankovsky AE, Garvine RW, Münchow A (2000) Mesoscale currents on the inner New Jersey shelf driven by the interaction of buoyancy and wind forcing. J Phys Oceanogr 30:2214–2230.

Chapter 6: Concluding Remarks

My objectives for this dissertation were to investigate how morphological variation in *Callinectes sapidus* zoeae influences aspects of behavior and transport. I also sought to characterize brood-level differences in these traits and attempt to quantify their impacts on larger-scale processes. In Chapter 2, I determined that not only was morphology more variable than previously indicated, but larval broods could contain distinct morphological features. However, it was not evident under further work in Chapter 3 whether these brood differences persist further into development. Though not enough zoeae were able to be reared through the entirety of larval development, I was able to confirm that brood-dependent morphology was still present for older zoeae. Furthermore, the degree of morphological differences among broods increases, indicating some degree of divergent morphology.

Simple models of swimming efficiency in Chapters 2 and 3 suggested that morphological differences between broods could translate to behavioral differences. In Chapter 4, I was able to identify that swimming behavior also differs between broods, as well as modes of behavior that are conserved between broods. Finally, in Chapter 5, I sought to simulate how potential interactions between brood-dependent swimming behavior and hydrology could influence larval transport. This model idealized dominant processes in coastal circulation, but it did not include all physical processes. However, it was useful in highlighting how the combination of swimming velocity, vertical diffusivity, and sheared currents could affect how *C. sapidus* larvae are transported. In all, this dissertation has established the presence and implications of brood and population-level

trait variability in *C. sapidus*. It also provides a framework for investigating similar questions for other species.

Crab zoeae have complex morphological features, and in addition to various spines and appendages, have general body shapes that are not entirely smooth or geometric in nature. A functional view of morphology necessitates an understanding of the nature of the interaction between these features, the organism, and their environment (Koehl 1996). Based on observations made across dozens of larval broods and hundreds of zoeae, it is clear that the means and standard deviations of one or two morphological features (typically carapace length and rostro-dorsal length; Appendix E) do not sufficiently characterize morphology. In fact, due to interactions with their fluid environment, zoeal carapace length alone does not enable inferences of drag or Reynold number due to their dorsal swimming orientation. Additionally, the non-spherical shape of their carapace require multiple body measurements to make such calculations. Since a complete morphological analysis of zoeae can be resource intensive, researchers should carefully consider which morphological features are necessary in order to understand their focus processes.

Beyond requiring a suite of morphometrics, a more complete characterization of trait variability is necessary in understanding morphological function across populations. Many of my morphological analyses required non-parametric tests due to the significant non-normality of metric distributions. The effects of these distribution shapes not only make the mean an insufficient summary, but individuals' whose traits lie far outside the mean may have quite different interactions with their environment. For instance, the distribution of the dorsal cross-sectional area, which is directly proportional to drag, varies

by nearly a factor of 6. When estimates of survival for zoeal development are so low, individuals on the tails of distributions can't necessarily be ignored, especially if those traits may potentially aid in their survival, locomotion, energetics, or dispersal potential.

Similar patterns of complexity and variability can be seen when observing zoeal swimming behavior. Unlike some other marine invertebrate larvae (e.g. bivalves; Cragg 1980 or echinoderms Chia et al. 1984), zoeae swim in seemingly erratic motions on short time scales. While other studies have typically focused on environmental responses amongst groups of zoeae (Cohen et al. 2015; Forward and Buswell 1989; Hamasaki et al. 2013; Sulkin et al. 1980; review Epifanio and Cohen 2016), Chapter 4 highlights the complex trajectories of individual *C. sapidus* zoeae. Even under still-water conditions, zoeae rarely travel in straight lines and can exhibit rapid accelerations and changes in direction. Though it would be reasonable to assume these temporal variations would be smoothed by longer observation times, the distribution of individuals' swimming velocity is highly skewed, with zoeae capable of swimming an order of magnitude higher than the median. Furthermore, additional analyses in Chapter 4 show that distinct modes of behavior exist for *C. sapidus* zoeae, and while it is not clear whether these are different behaviors over time or between individuals, they suggest that swimming behavior is variable in ways that a mean velocity and orientation is not capable of describing. These levels of variability also indicate that for *C. sapidus* zoeae, and possibly other species, behavioral responses to environments may differ among individuals of the same species. It is likely that such variable responses could result in a range of beneficial to detrimental effects.

One of the key findings of this dissertation was the presence of brood-level difference in morphology and swimming behavior in *C. sapidus* zoeae. These differences suggest that individuals' trait differences are not uniformly distributed throughout the population, and that larval broods are a significant component to the structure of population variability. I show that brood differences are present in a variety of traits including unidimensional morphometrics (i.e. lengths), higher-dimensional morphological characteristics (e.g. cross-sectional area, volume), swimming velocity, orientation, trajectory characteristics, and the timing of behaviors. One ecological implication of such differences is that, if one accepts that these morphological and behavior traits serve important functions for zoeal development and success, then maternal influences on offspring traits may be an important factor in zoeal success. This arises a potential for successful recruits to exhibit predominately beneficial traits and originate from only a subset of reproducing females, as opposed to an entirely random subset of the population.

The cause of these brood-dependent morphological differences is still unknown. While their origin was the not the focus of this dissertation, I was able to determine that maternal size (carapace width) and fecundity (brood volume) were not correlated to brood-level morphology. However, there are a number of other potential sources that have not been evaluated. All of the zoeae that I reared were obtained through the wild capture of ovigerous females in various stages of egg development. Thus it was not possible to determine the environmental conditions eggs were incubated, indicators of maternal nutrition prior to egg laying, or whether this was the crab's first clutch or not, all of which could be potential sources of maternal influence. Incubation environment has been shown to influence the timing and successful hatching in *C. sapidus* eggs (Costlow and Bookhout

1959), and crab zoeae are generally sensitive to temperature and salinity conditions (Costlow et al. 1961; Anger 1991; Schuh and Diesel 1995). There is some evidence of differences in larval characteristics between subsequent *C. sapidus* clutches (Darnell et al. 2009), but there is no data on their effects on morphology. Additionally, trait differences may also originate in genetic differences between broods, which I was not able to test for but has been suggested as a cause in similar effects in other species (Tamura et al. 2017). The cause of brood-level differences may not be important in some applications. One case that could prove useful were if biometrics from adult surveys or environmental conditions could be used to provide indicators of larval condition or predictors of recruitment. In this scenario, these indicators could be used to understand ecological questions, such as which portions of the population are supplying the most successful larvae, as well as fisheries management questions, such as do population or environmental characteristics improve the chances of successful larval development. However, since morphology and behavior are not the only factors in determining larval success, such a discovery would likely only inform trends rather than make firm predictions of recruitment.

The interaction between the observed morphological and behavioral variation with the physical environment zoeae develop in suggest some important considerations regarding larval transport. With an understanding that the physical model used in Chapter 5 was idealized and does not sufficiently replicate the complex hydrology of inshore waters, the concept that individual and brood-level differences in swimming behavior can influence transport should be a serious consideration in future models of *C. sapidus* larval dispersal. If successful dispersal was entirely stochastic, modeling all zoeae similarly should give reasonably accurate results. However, the findings of this dissertation have

shown that zoeal traits are variable, such that some groups of larvae may be more capable than others to maintain a near-surface position. Depending on vertical structure of the circulation, vertical diffusivity, and near-surface velocity gradients (e.g. from breaking waves or Stoke's drift), zoeae that can counter passive sinking and vertical mixing may be transported much further than others. When combined with brood-dependent swimming behavior, some larval broods may in fact be transported differently than others. These differences can have implications for meta-population connectivity, in that there can be maternal influences on the destination of their offspring. However, the zoeae observed in this study do not necessarily represent the extent of population-level variation in traits, and more observation would be needed to determine how these larval traits are distributed across the population. Regardless of brood effects, it is clear that *C. sapidus* larval behavior varies considerably, and despite the notion that *C. sapidus* zoeae maintain an entirely neustonic distribution (Epifanio and Tilburg 2008), assuming zoeae maintain a fixed depth or even that they move entirely with the mean flow of a water layer (Tilburg et al. 2005) may not accurately predict dispersal trajectories.

6.1 Literature Cited

Anger K (1991) Effects of temperature and salinity on the larval development of the Chinese mitten crab *Eriocheir sinensis* (Decapoda: Grapsidae). Mar Ecol Prog Ser 72:103–110. doi: 10.3354/meps072103

Chia F-S, Buckland-Nicks J, Young CM (1984) Locomotion of marine invertebrate larvae: A review. Can J Zool 62:1205–1222.

Cohen JH, Hanson CK, Dittel AI, Miller DC, Tilburg CE (2015) The ontogeny of larval swimming behavior in the crab *Hemigrapsus sanguineus*: Implications for larval transport. J Exp Mar Bio Ecol 462:20–28. doi: 10.1016/j.jembe.2014.10.003

Costlow JDJ, Bookhout CG (1959) The larval development of Callinectes Sapidus Rathbun reared in the laboratory. Biol Bull 116:373–396.

Costlow JDJ, Bookhout CG, Munroe R (1961) Salinity-temperature effects on the larval development of the crab, *Panopeus herbstii* Milne-Edwards, reared in the laboratory. Physiol Zool 35:79–93.

Cragg SM (1980) Swimming behaviour of the larvae of *Pecten maximus* (L .) (Bivalvia). J Mar Biol Assoc United Kingdom 60:551–564.

Darnell MZ, Rittschof D, Darnell KM, McDowell RE (2009) Lifetime reproductive potential of female blue crabs *Callinectes sapidus* in North Carolina, USA. Mar Ecol Prog Ser 394:153–163. doi: 10.3354/meps08295

Epifanio CE, Cohen JH (2016) Behavioral adaptations in larvae of brachyuran crabs: A review. J Exp Mar Bio Ecol 482:85–105. doi: 10.1016/j.jembe.2016.05.006

Epifanio CE, Tilburg CE (2008) Transport of blue crab larvae in the Middle Atlantic Bight: A wet and windy journey. J Mar Res 66:723–749.

Forward RJB, Buswell CU (1989) A comparative study of behavioral responses of larval decapod crustaceans to light and pressure. Mar Behav Physiol 16:43–56.

Hamasaki K, Sugimoto A, Sugizaki M, Murakami Y, Kitada S (2013) Ontogeny of sinking velocity, body density, and phototactic behaviour in larvae of the coconut crab *Birgus latro*: Implications for larval dispersal and recruitment in the sea. J Exp Mar Bio Ecol 442:58–65. doi: 10.1016/j.jembe.2013.02.001

Koehl MAR (1996) When does morphology matter? Annu Rev Ecol Syst 27:501–542. doi: 10.1146/annurev.ecolsys.27.1.501

Schuh M, Diesel R (1995) Effects of salinity, temperature, and starvation on the larval development of *Armases* (=*Sesarma*) *miersii* (rathbun, 1897), a semiterrestrial crab with abbreviated development (Decapoda: Grapsidae). J Crustac Biol 15:205–213.

Sulkin SD, van Heukelem W, Kelly P, van Heukelem L (1980) The behavioral basis of larval recruitment in the crab *Callinectes sapidus* Rathbun: A laboratory investigation of ontogenetic changes in geotaxis and barokinesis. Biol Bull 159:402–417.

Tamura H, Landeira JM, Goshima S (2017) Morphological and morphometric variability in the zoea I larvae of *Pugettia quadridens* (De Haan, 1839): looking for reliable characters for taxonomic studies on the genus *Pugettia* Dana, 1851 (Majoidea: Epialtidae). Zootaxa 4226:264–272.

Tilburg CE, Reager JT, Whitney MM (2005) The physics of blue crab larval recruitment in Delaware Bay: A model study. J Mar Res 63:471–495. doi: 10.1357/0022240053693699

Appendix A: Morphological Data

Figure A-1: *Distribution of newly-hatched (1 day old) Callinectes sapidus zoeal morphometrics. Bars represent observational frequencies for N=448 zoeae across all observed larval broods. Black lines show kernel density estimates scaled to frequency. Morphometrics (A-R) are defined in Table 2-2. Bar colors are coded as: tan, carapace dimensions; purple, abdomen dimensions; grey, total length; orange, spine lengths; brown, maxilliped dimensions; green, cross-sectional areas; red, volumes.*

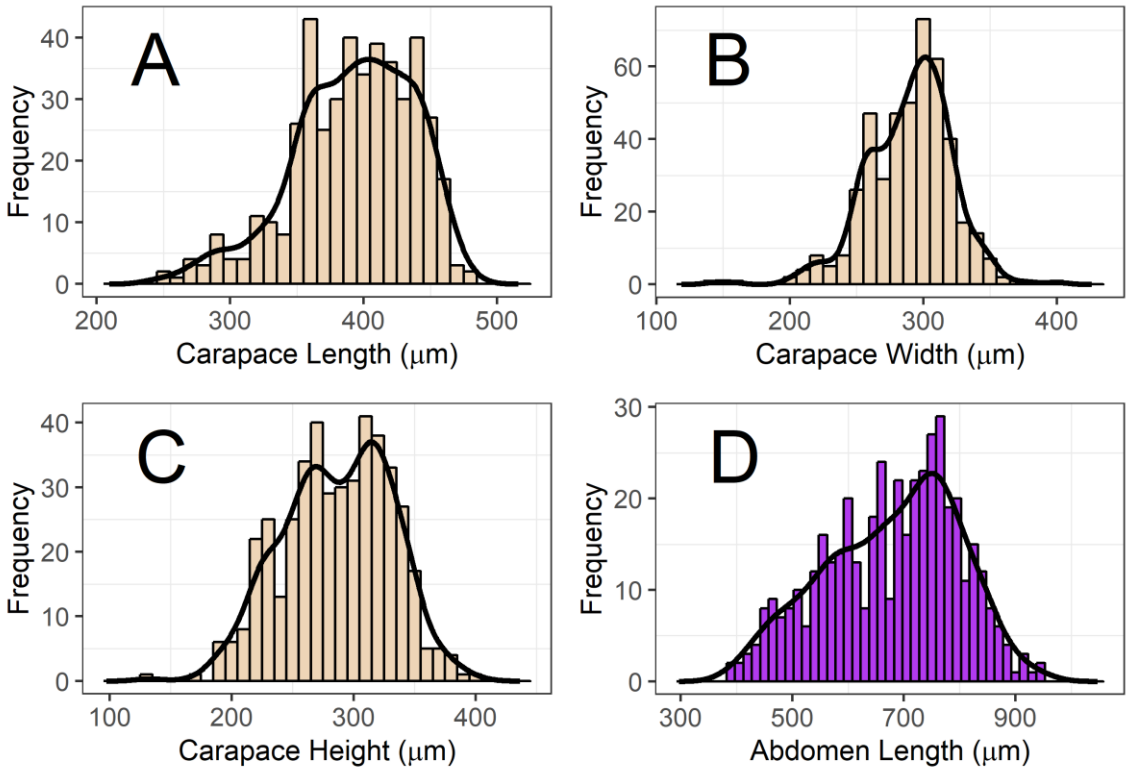

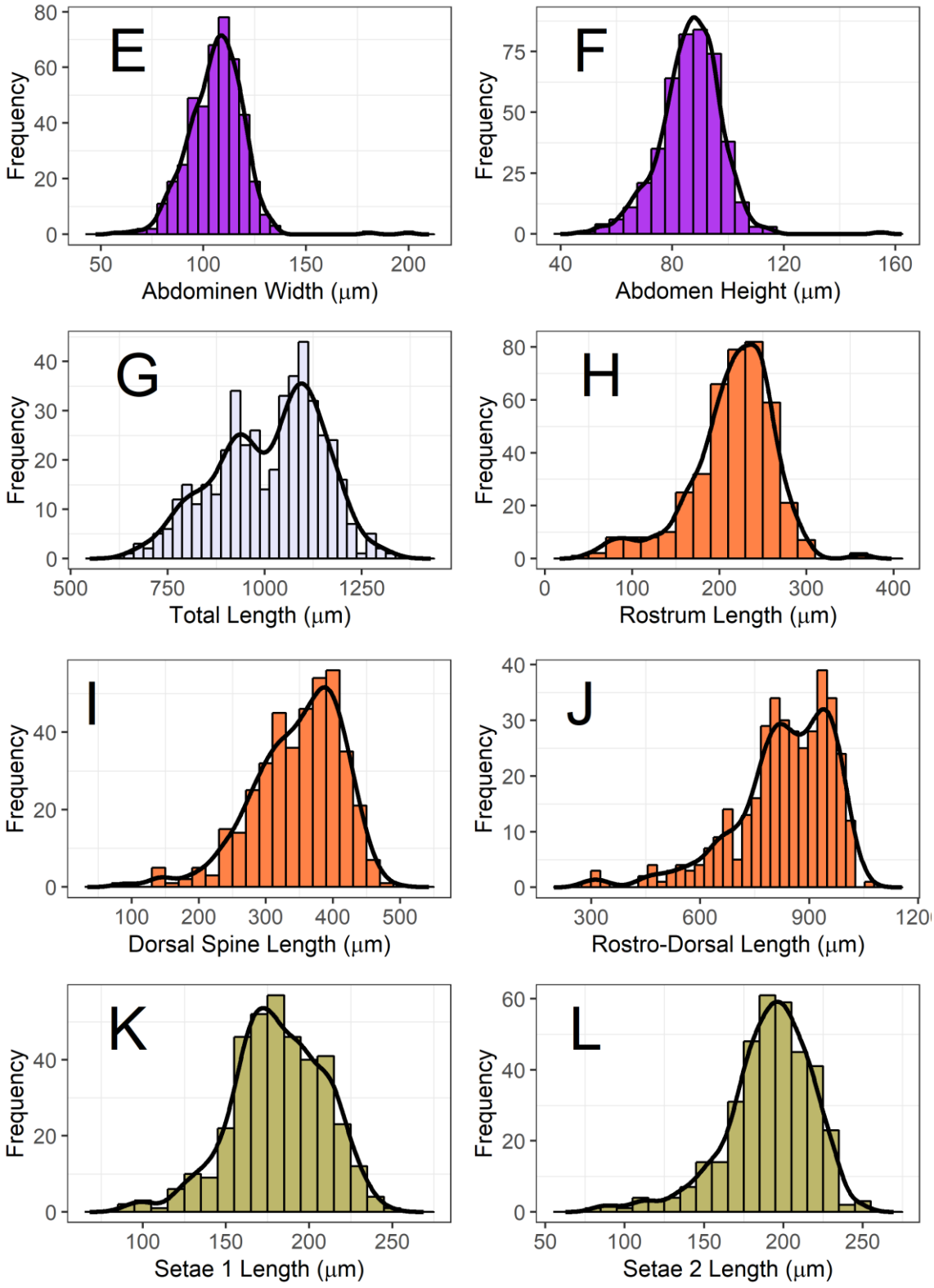
E
Frequency
Abdominen Width (μm)
F
Frequency
Abdomen Height (μm)
G
Frequency
Total Length (μm)
H
Frequency
Rostrum Length (μm)
I
Frequency
Dorsal Spine Length (μm)
J
Frequency
Rostro-Dorsal Length (μm)
K
Frequency
Setae 1 Length (μm)
L
Frequency
Setae 2 Length (μm)

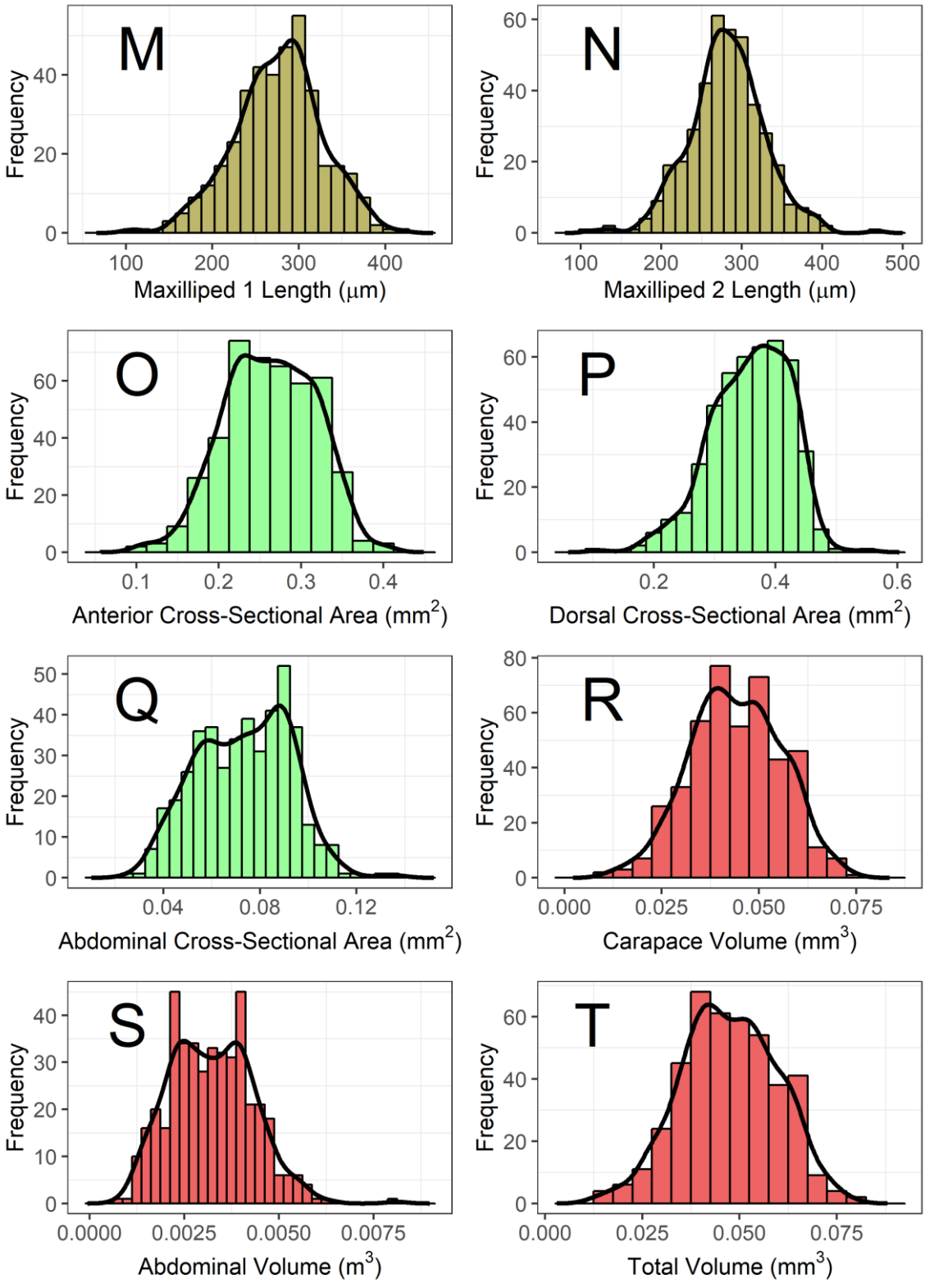
M
Frequency
Maxilliped 1 Length (μm)
N
Maxilliped 2 Length (μm)
O
Anterior Cross-Sectional Area (mm²)
P
Dorsal Cross-Sectional Area (mm²)
Q
Abdominal Cross-Sectional Area (mm²)
R
Carapace Volume (mm³)
S
Abdominal Volume (m³)
T
Total Volume (mm³)

Appendix B: Behavioral Data

Part of the mixture model analysis in Chapter 4 involved identifying the relationship between modes of behavior within individual broods and those of the overall distribution of behaviors. Though a bootstrapping analysis did confirm the presence of two component distributions for each of the focal behavioral metrics, a qualitative analysis of behavior distributions within each brood was insightful (Figure B-1). These distributions highlight some trends, such as the bimodal nature of swimming direction, as well as how velocity distributions are shifted for some broods. The results of bootstrapped mixture models for individual broods (Table B-2), was also helpful in quantifying the similarities and differences in modes of behavior among broods. Of particular note is the high divergence in sign for vertical velocity between some broods and the changes in dominant swimming direction.

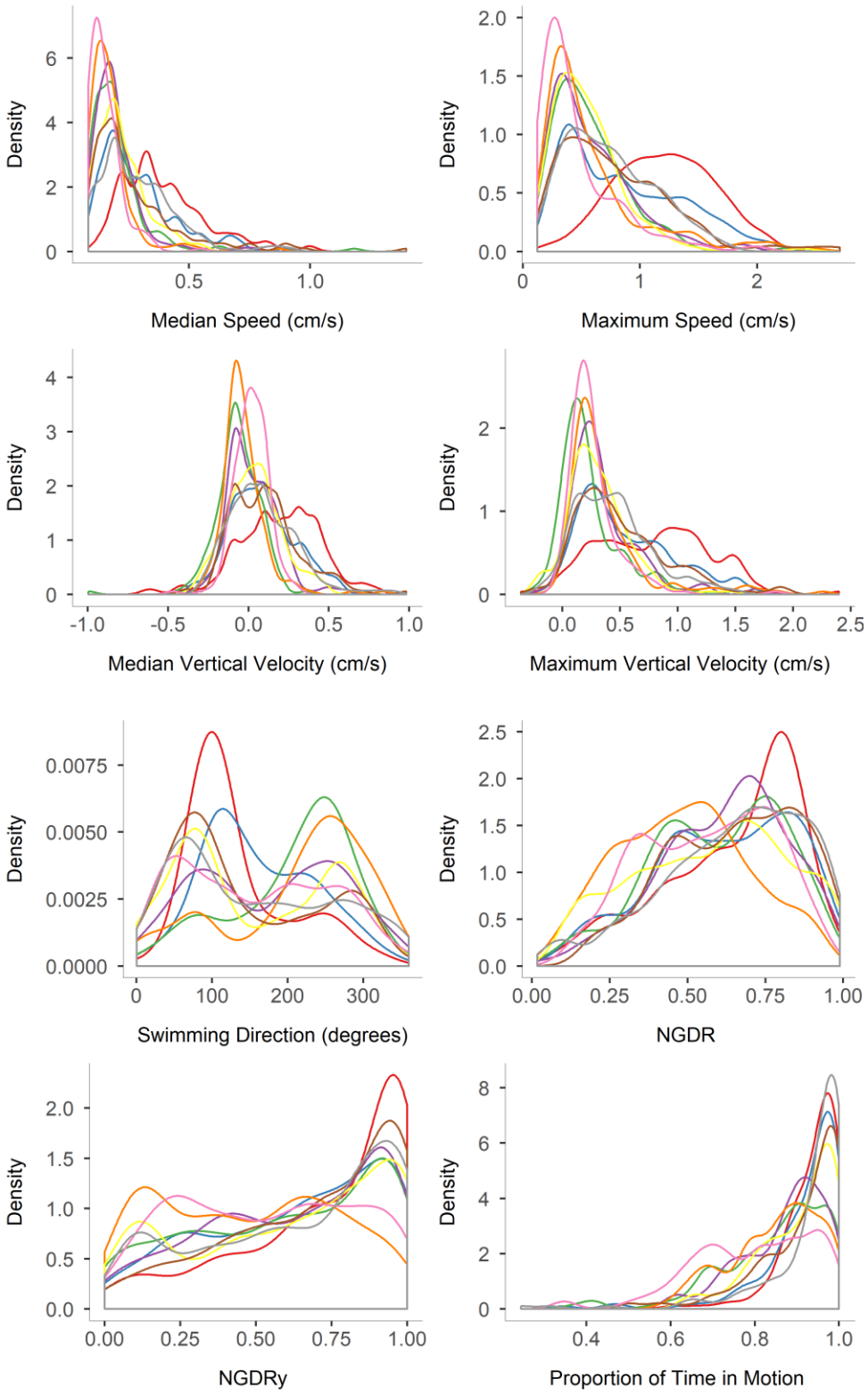

Figure B-1: *Summary of the distributions of behavioral metrics. Curves represent kernel density estimates and colors denote larvae of the same brood.*

Table B-1: Summary of brood-level results from mixture models in Chapter 4. For each brood (A-F), there were two component normal distributions that signify modes of behavior. Each component has an associated proportion of observations (λ) and mean (μ). Swimming direction is measured in decrease from horizontal (right is 0°).

Behavior	Parameter	A	B	C	D
Swimming Direction (deg)	λ_1	0.78	0.64	0.24	0.46
	λ_2	0.22	0.36	0.76	0.54
	μ_1	102.06	117.33	88.65	87.58
	μ_2	247.61	241.35	243.85	253.63
Proportion of Time Upward	λ_1	0.28	0.46	0.84	0.59
	λ_2	0.72	0.54	0.16	0.41
	μ_1	0.22	0.21	0.13	0.18
	μ_2	0.85	0.79	0.7	0.81
NGDR	λ_1	0.27	0.39	0.41	0.29
	λ_2	0.73	0.61	0.59	0.71
	μ_1	0.35	0.4	0.4	0.39
	μ_2	0.75	0.76	0.74	0.71
NGDRy	λ_1	0.23	0.35	0.39	0.4
	λ_2	0.77	0.65	0.61	0.6
	μ_1	0.3	0.29	0.26	0.32
	μ_2	0.86	0.81	0.8	0.82
Median Vertical Velocity (cm/s)	λ_1	0.13	0.74	0.89	0.96
	λ_2	0.87	0.26	0.11	0.04
	μ_1	-2.97	0.05	-0.48	0.09
	μ_2	2.37	3.31	-6.87	4.82
Median Speed (cm/s)	λ_1	0.86	0.86	0.97	0.96
	λ_2	0.14	0.14	0.03	0.04
	μ_1	3.45	2.42	1.87	1.84
	μ_2	7.18	5.87	7.78	5.83

Table B-1: Cont.

Behavior	Parameter	E	F	G	H	I
Swimming Direction (deg)	λ_1	0.24	0.55	0.65	0.53	0.6
	λ_2	0.76	0.45	0.35	0.47	0.4
	μ_1	68.4	74.1	80.39	78.52	83.59
	μ_2	259.89	258.33	263.9	246.08	267.55
Proportion of Time Upward	λ_1	0.82	0.56	0.48	0.75	0.53
	λ_2	0.18	0.44	0.52	0.25	0.47
	μ_1	0.19	0.22	0.24	0.23	0.22
	μ_2	0.71	0.77	0.85	0.73	0.85
NGDR	λ_1	0.54	0.41	0.4	0.44	0.24
	λ_2	0.46	0.59	0.6	0.56	0.76
	μ_1	0.35	0.34	0.44	0.37	0.35
	μ_2	0.65	0.74	0.79	0.72	0.75
NGDRy	λ_1	0.5	0.36	0.31	0.49	0.35
	λ_2	0.5	0.64	0.69	0.51	0.65
	μ_1	0.23	0.24	0.33	0.28	0.27
	μ_2	0.73	0.82	0.84	0.78	0.83
Median Vertical Velocity (cm/s)	λ_1	0.98	0.83	0.88	0.95	0.95
	λ_2	0.02	0.17	0.12	0.05	0.05
	μ_1	-0.41	-0.08	0.51	0.25	0.58
	μ_2	6.4	2.8	5.02	-3.07	6.43
Median Speed (cm/s)	λ_1	0.95	0.87	0.92	0.92	0.96
	λ_2	0.05	0.13	0.08	0.08	0.04
	μ_1	1.59	1.91	2.32	1.38	2.68
	μ_2	5.62	4.15	8.2	3.25	7.85

Appendix C: Morphological Predictors of Swimming and Sinking

One of the objectives of Chapter 5 was to determine potential influences of brood-level behavior on *Callinectes sapidus* larval transport. The parameterization of larval swimming behavior requires each particle to have an upward swimming and passive sinking velocity that is related to the observed brood-level differences in Chapters 2 and 4. However, due to practical considerations for Chapter 4, I was not able to have paired behavioral and morphological observations for individual zoeae; rather, all data collected was summarized on the level of larval broods. This required me to make inferences of behavioral terms based on individual-based morphological observations. The aim of this part of the analysis was to identify the fewest number of morphometrics that could predict both upward swimming velocity (W_{swim}) and passive sinking velocity (W_{sink}).

Though vertical swimming velocity observed in Chapter 4 could either be oriented upward or downward, for the purposes of the model in Chapter 5, I was only concerned with positive (upward) values. Thus, the median positive vertical velocity from Chapter 4's broods was used in this analysis.

The model I used for W_{sink} from Chapter 2 was

$$\boldsymbol{W_{sink} = \sqrt{\frac{2g(V_A + V_C)(\rho_z - \rho_f)}{\rho_f A_A C_D}}} \qquad \textbf{(C.1)}$$

where g is gravitation acceleration (9.8 m s^{-1}), ρ_f is the fluid density (1024 kg m^{-3}), ρ_z is larval density (1066 kg m^{-3}), A_A is the abdominal cross-sectional area, and V_A and V_C are

the abdominal and carapace volume, respectively. The total larval volume (V_T) is the sum of V_A and V_C. C_D is the drag coefficient defined by

$$C_D = \frac{24}{Re} + \frac{6}{1+\sqrt{Re}} + 0.4 \quad \textbf{(C.2)}$$

where Re is the Reynolds number defined by

$$Re = \frac{CL * W_{sink}}{\nu} \quad \textbf{(C.3)}$$

where CL is the zoeal carapace length, and ν is the kinematic viscosity of seawater (9.5×10^{-7} m^2s^{-1}). In total V_T, A_A, and CL, based on zoeae observed in Chapter 4, were used to calculate W_{sink}.

Although it would be possible to calculate estimates of W_{sink} from measured morphometrics alone, I wanted to be able to draw large numbers random values from the observed trait distributions. If only observed larvae were drawn from, this would either limit the number of unique simulated larvae or require complex criteria to ensure that the observed relationships among variables was held during simulations. The regression analysis in Chapter 4 identified dorsal cross-sectional area (A_D) to be a metric that correlates well across multiple measurements of swimming. It is also a general indicator of zoeal size, and thus should correlate well with V_T, A_A, and CL.

A strictly linear regression between W_{sink} and A_D could result in negative velocities for smaller larvae. I instead fit an exponential curve of the form

$$W_{swim} = ae^{bA_D+\varepsilon} \quad \textbf{(C.4)}$$

to the data, where a and b are constants. ε is a normally distributed error term with a mean of 0 and a standard deviation equal to the standard deviation of the model residuals, Due

to the lack of paired observations of morphology and swimming velocity, means of larvae from each video were used for both variables, weighted by the reciprocal of video-level standard deviations of W_{swim}. This resulted in a significant correlation where a=0.04 and b=1.06 × 10^7 ($p \ll 0.001$, $R^2 = 0.41$; Figure B-1), when A_D is in m^2 and W_{swim} is in mm s^{-1}.

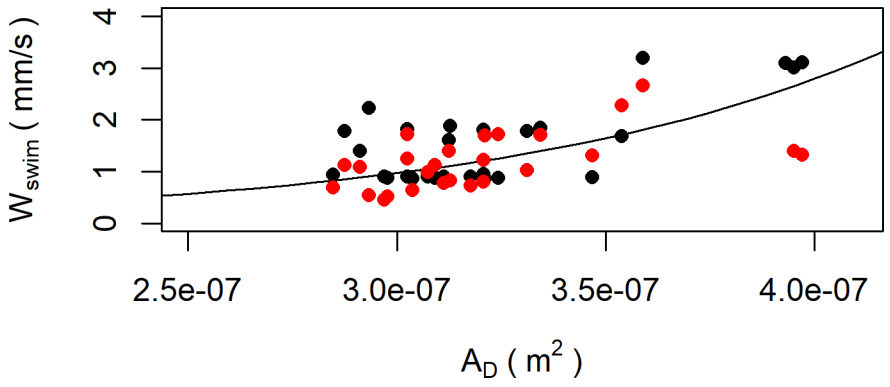

Figure C-1: *Dorsal cross-sectional area (A_D) was used to predict the mean upward swimming velocity (W_{swim}) from each video observation. The line shows the fitted exponential curve (eq B.4). W_{swim} values generated by the model are shown in red.*

For V_T, A_A, and CL the processes was simplified due to complete morphological observation sets of individual zoeae. Thus linear regression were used for all zoeae regardless of brood identify. V_T (Figure B-2), A_A (Figure B-3), and CL (Figure B-4) all had statistically significant regressions. Together, these analyses allowed for W_{swim} and W_{sink} values to be generated for larvae based solely on a distribution of A_D. A description of those analysis can be found in section 5.5.2.

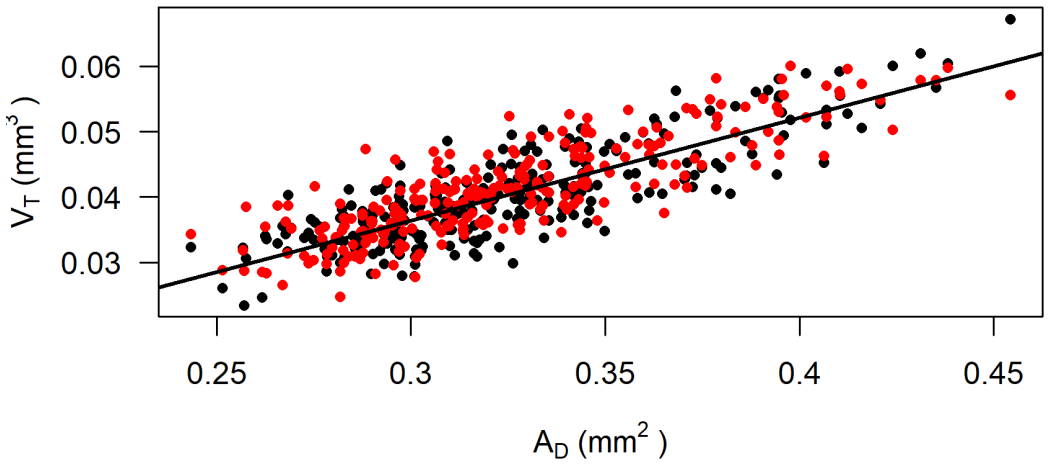

Figure C-2: *Results of linear regression between dorsal cross-sectional area (A_D) and total volume (V_T). Original observations (black) and simulated ones (red) are shown. The solid line shows the model fit of the form $A_D = 0.157V_T - 0.011$ for V_T in mm^3 and A_D in mm^2 ($p \ll 0.001$, $R^2=0.69$).*

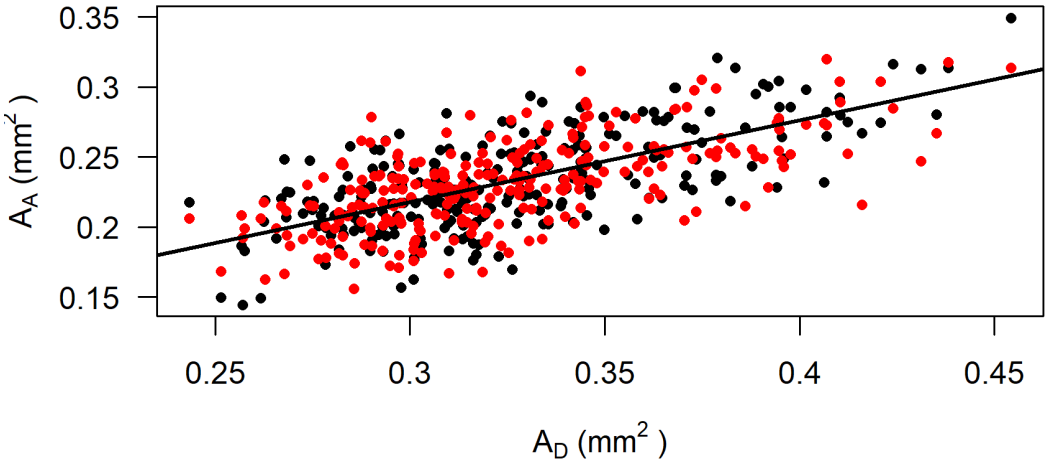

Figure C-3: *Results of linear regression between dorsal cross-sectional area (A_D) and anterior cross-sectional area (A_A). Original observations (black) and simulated ones (red) are shown. The solid line shows the model fit of the form $A_D = 0.58V_T - 0.043$ for A_A and A_D in mm^2 ($p \ll 0.001$, $R^2=0.46$).*

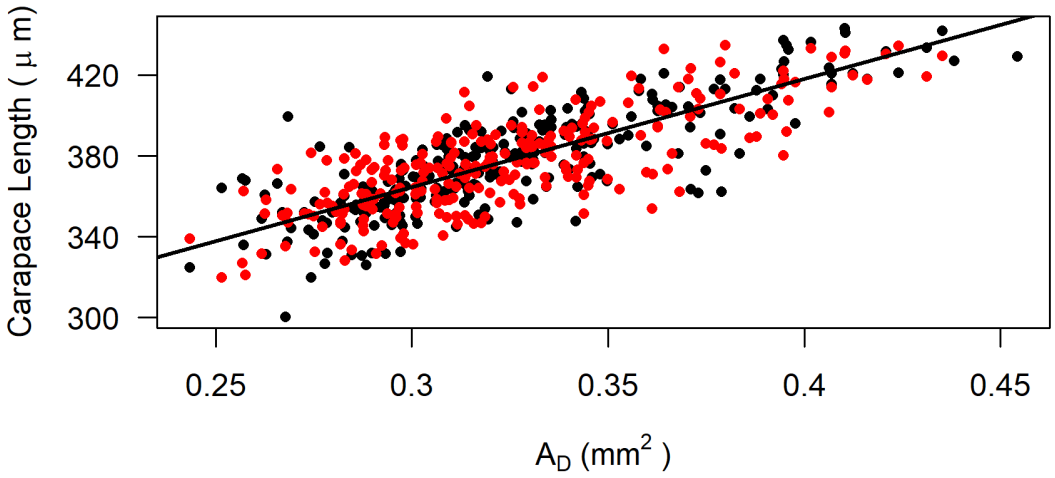

Figure C-4: *Results of linear regression between dorsal cross-sectional area (A_D) and carapace length (CL). Original observations (black) and simulated ones (red) are shown. The solid line shows the model fit of the form $A_D = 534CL+204.4$ for CL in μm and A_D in mm^2 ($p \ll 0.001$, $R^2=0.64$).*

Appendix D: Implications of Morphology and Swimming on Energetics

In several instances in this dissertation there is mention of the interactions between morphology, behavior, and fluid environments having the potential to influence zoeal energetics while swimming. This section aims to illustrate how the energetic costs of swimming might be estimated based on behavior, morphology, and first principals. The following model is not meant to provide precise predictions of actual energetic expenditure, as it makes some larger simplifications of swimming behavior and associated physical processes. Rather, it should be used to provide semi-quantitative comparisons between different behavioral and morphological traits. Though, for the context of my research this model is meant to address questions regarding *Callinectes sapidus* zoeae, in principle, it should apply to actively swimming zoeae in general.

Though larvae often swim in complex trajectories, on short time-scales, their movements can be simplified in two-dimensions (Figure D-1), with some up-and-down and some side-to-side component. The objective here is to determine the minimum amount of thrust F_T larvae must produce in order to swim.

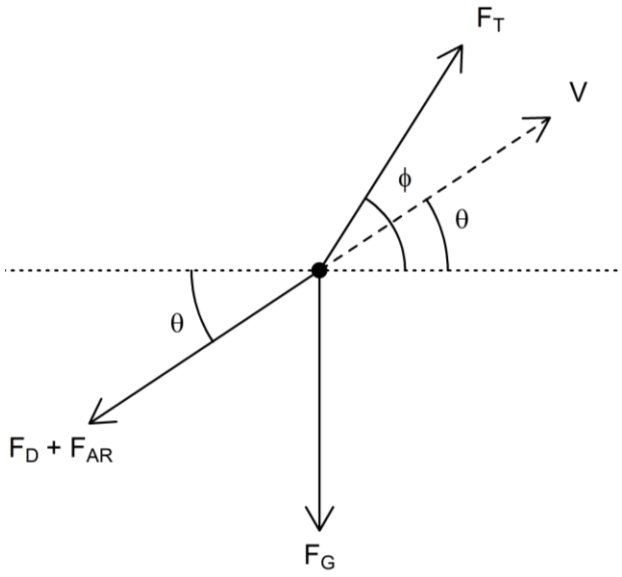

Figure D-1: Force diagram of swimming larvae in the vertical plane. Direction of F_{AR} is not fixed.

Larvae swimming at some velocity (V) at an angle (θ) will need to produce a thrust (F_T) at a different angle (ϕ). F_T and ϕ must be such that they balance they balance resistive drag forces (F_D), an acceleration reaction (F_{AR}), as well as buoyant forces (F_B), where

$$\boldsymbol{F_D = \frac{1}{2}\rho_f C_D A V^2} \qquad \textbf{(D.1)}$$

ρ_f is the fluid density, A is the cross-sectional area in the direction of motion, and C_D is the drag coefficient (Vogel 1994). F_g is defined by

$$\boldsymbol{F_g = (\rho_z - \rho_f) V_z g} \qquad \textbf{(D.2)}$$

where g is the gravitational acceleration, and ρ_z and V_z are the density and volumes of larvae, respectively (Vogel 1994). F_{AR} is defined by

$$F_{AR} = \rho_f \mathrm{K} V_z \left(\frac{\delta V}{\delta t}\right) \quad \textbf{(D.3)}$$

where K is an added-mass coefficient (Williams 1994a).

F_D acts in the opposite direction of motion (i.e. 180° from V), F_{AR} acts opposite to direction, and F_B will act downwards. Thus by balances forces in the horizontal (x) and vertical (y) directions, we get:

$$x: F_T cos\phi = (F_D + F_{AR}) cos\theta \quad \textbf{(D.4)}$$

$$y: F_T cos\phi = F_g + (F_D + F_{AR}) sin\theta \quad \textbf{(D.5)}$$

By solving for ϕ we get

$$\phi = \cos^{-1}\left(\frac{(F_D + F_{AR})\cos\theta}{F_T}\right) \quad \textbf{(D.6)}$$

And similarly for F_T

$$F_T = \frac{F_g + (F_D + F_{AR}) sin\theta}{sin\phi} \quad \textbf{(D.7)}$$

Then by substituting ϕ in D.4 and simplifying, we obtain

$$F_T = -\sqrt{F_g^2 + (F_D + F_{AR})^2 + 2(F_D + F_{AR}) F_g sin\theta} \quad \textbf{(D.8)}$$

In order to estimate the work performed on the larvae (W), F_T can be integrated along a larva's path of motion. Alternatively, a discrete-time model can be used to incrementally calculate F_T over short distances and then summing over all increments. This estimate of W is not quite equivalent to the energy required by the larvae to swim, however it is a lower bound. W would likely need to be scaled by some factor relating to the mechanical efficiency of larvae (i.e. the proportion of energy spent that goes into the directed motion) as well as a muscular efficiency (i.e. the additional energy required to carry out swimming motions by the musculature). However, with a very generous assumption that these efficiency terms do not vary considerably by larvae, W provides a baseline for comparisons between individuals of differing swimming velocities, swimming trajectories, and morphological characteristics.

A sensitivity analysis was then done, exploring how behavioral and morphological parameters seen in *C. sapidus* zoeae influence this model. For these tests unless otherwise indicated calculations were made with all variables held constant. Table D-1 shows constants used. Particle length, area, and volume were based on first-stage *C. sapidus* zoeal carapace height, dorsal cross-sectional area, and volume, respectively. Parameter ranges for sensitivity analysis were based on observations made in Chapters 2 and 4. I also assumed that particles were moving at a constant velocity, and thus F_{AR} was neglected.

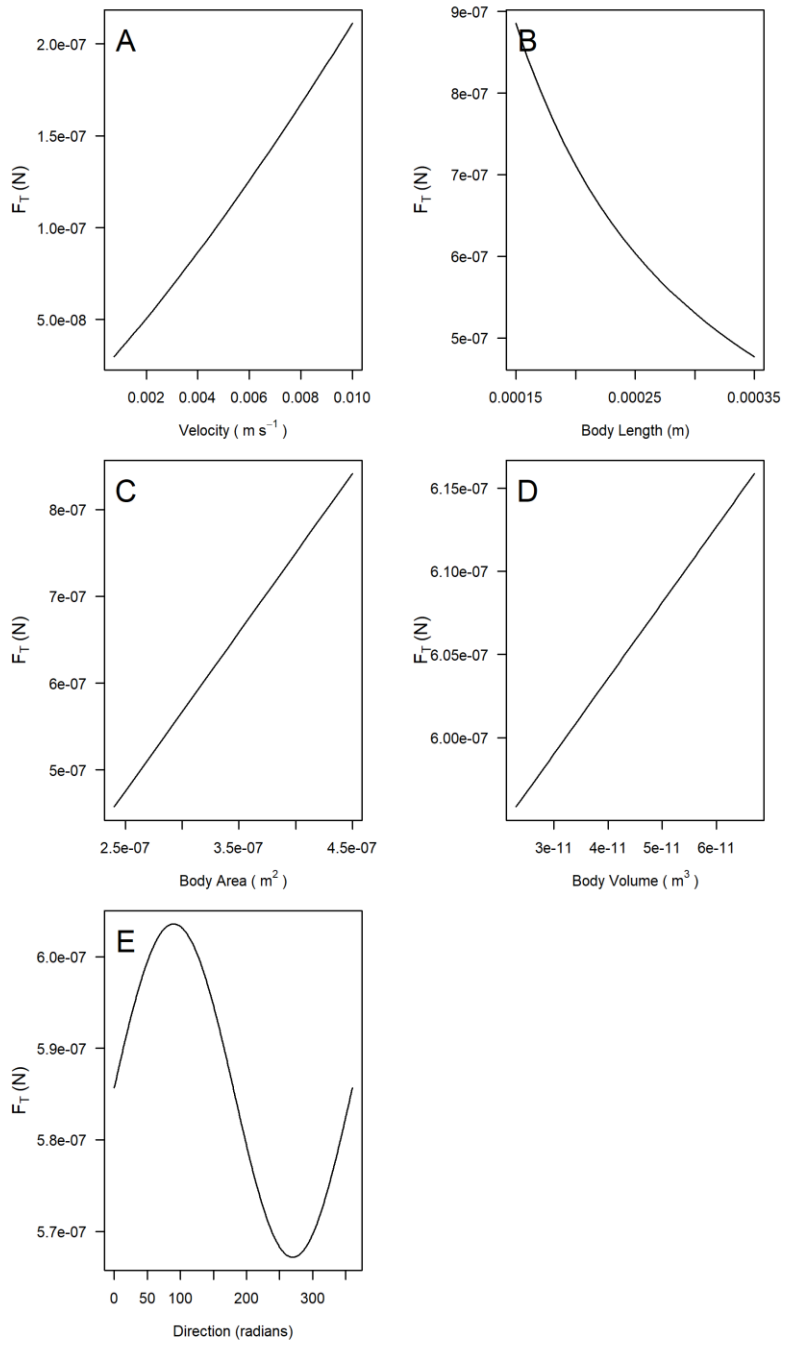

Figure D-1: *Sensitivity of thrust to larval velocity (A), body length (B), cross-sectional area (C), body volume (D), and swimming direction (E).*

As velocity increases (Figure D-1A), there is a slightly nonlinear increase in F_T. Increases in body length (Figure D-1B) result in a nonlinear decrease in F_T. Both body area (Figure D-1C) and volume (Figure D-1D) result in a somewhat linear increase in F_T. F_T also changes sinusoidally with swimming direction (Figure D-1E), whereby downward swimming is aided by gravity and reduces required thrust.

In this analysis observed ranges in zoeal characteristics can result in substantial differences in required thrust. Over possible swimming velocities, F_T increased by over a factor of 7. F_T differed by a factor of 1.9 for body length, and 1.8 for body area. Despite the increase in F_T with volume, the relative increase was minor when compared to other variables.

This energetics model was not explicitly incorporated into the analyses in this dissertation. However, my aim was to use it to provide context for how morphology and behavior can have additional effects, specifically, the energetics of swimming. This model is also helpful in translating models of F_D in Chapters 2 and 3 into something more tangible. Though this model does make some major simplifications, it is versatile enough to be used alongside behavioral observations (such as in Chapter 4) to make relative comparisons of swimming energetics.

Table D-1: Summary of constants used in thrust sensitivity analysis

Parameter	Value
Salinity	30 ppt
Temperature	25°
Velocity	0.025 m s^{-1}
Length	2.5×10^{-4} m
Cross-Sectional Area	3.2×10^{-7} m^2
Volume	4.0×10^{-11} m^3
Direction	90°
g	9.8 m s^{-2}
ρ_z	1066 kg m^{-3}

D.1 Literature Cited

Vogel S (1994) Life in Moving Fluids: The Physical Biology of Flow, 2nd edn. Princeton University Press

Williams T a (1994) A model of rowing propulsion and the ontogeny of locomotion in *Artemia* larvae. Biol Bull 187:164–173. doi: 10.2307/1542239

Appendix E: Meta-Analysis of Brachyuran Zoeal Morphology

In order to provide context for the morphological observations made in this dissertation, a meta-analysis was performed aiming to compare *Callinectes sapidus* zoeal morphology to other species. A literature review was performed searching for studies that provide quantitative morphological descriptions. One complication was the lack of standardized reporting of morphological features. Many studies only provide qualitative descriptions of broader morphological features (e.g. spine locations, appendage setation, etc.), which while useful for species identification and staging, do not allow for quantitative comparisons. For each study, means and standard deviations of all reported morphometrics were recorded. The original intent was to perform an ordination analysis (i.e. principal component analysis) on morphological data determine what morphological characteristics define different taxonomic groups. However, additional inconsistencies in which morphometrics are recorded made it impossible to perform this type of analysis without estimating missing metrics. A full description of morphological features obtained from this review can be found in Table E-1.

Zoeal carapace length (CL) and rostro-dorsal length (RDL) were the two most commonly reported morphometrics, and thus, they were the only ones used for comparisons (Figure E-1). The ratio RDL:CL from brood-level morphological data of *C. sapidus* zoeae from Chapter 2 was used for comparisons. Significant differences in RDL:CL between first stage *C. sapidus* zoeae and other Portunid species was observed (T-test: $p \ll 0.001$), but there were no significant differences between *C. sapidus* and Grapsid

species (T-test: p = 0.12). Considerable variation is present in RDL:CL across *C. sapidus* broods, but I was not able to find enough brood-level analyses in the literature to make comparisons on that level. Despite significant differences with other Portunids, *C. sapidus* have more similar RDL:CL to Portunids than to Grapsoidea, Majoidea, and Ocypodoidea species. However, there were not enough examples to test these relationships. Due to complex morphological characteristics, RDL:CL is not sufficient on its own to make proper taxonomic comparisons. A more complete anlaysis would require multivariate analyses that incorporate differences across a number of morphometrics.

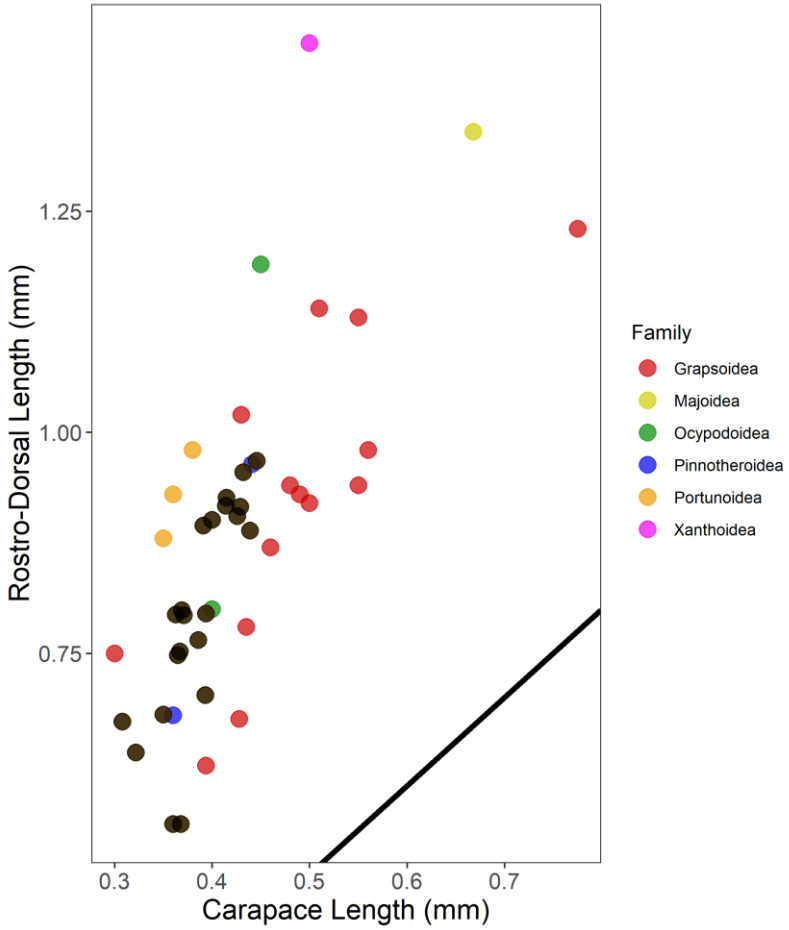

Figure E-1: *Comparison between carapace length and rostro-dorsal length of different first stage Brachuyan zoeae. Solid line denotes 1:1 relationship. Black points show C. sapidus larval broods from Chapter 2.*

Table E-1: Summary of literature review of Brachyuran first stage zoeal morphology. Metrics include carapace length (CL), rostrum length (RL), dorsal spine length (DL), and rostro-dorsal length (RDL). All morphometrics are recorded as means in mm with standard deviations (if provided).

Super Family	Genus	Species	CL	RL	DL	RDL	Source
Calappoidea	*Calappa*	*gallus*	-	-	-	1.35	Taishaku and Konishi, 1995
Calappoidea	*Calappa*	*japonica*	-	-	-	1.68	Taishaku and Konishi, 1995
Grapsoidea	*Aratus*	*pacificus*	0.39 ± 0.01	0.16 ± 0.01	0.17 ± 0.01	0.62 ± 0.02	Rebolledo et al., 2015
Grapsoidea	*Aratus*	*pisonni*	0.43 ± 0.02	0.16 ± 0.01	0.19 ± 0.01	0.68 ± 0.03	Rebolledo et al., 2015
Grapsoidea	*Eriocheir*	*japonicus*	0.55 ± 0.03	-	-	1.13 ± 0.08	Kornienko et al., 2008
Grapsoidea	*Eriocheir*	*sinensis*	0.43 ± 0.02	0.29 ± 0.02	0.36 ± 0.02	1.02 ± 0.02	Kim and Hwang, 1995
Grapsoidea	*Geograpsus*	*lividus*	0.42 ± 0.02	0.22 ± 0.02	0.16 ± 0.01	0.75 ± 0.03	Cuesta and Schubart, 1999
Grapsoidea	*Geograpsus*	*lividus*	0.45 ± 0.01	-	-	0.81 ± 0.02	Guerao et al., 2001
Grapsoidea	*Goniopsis*	*pulchra*	0.3 ± 0.01	0.21 ± 0.01	0.22 ± 0.01	0.75 ± 0.02	Cuesta and Schubart, 1999
Grapsoidea	*Grapsus*	*grapsus*	0.5 ± 0.01	-	-	0.92 ± 0.02	Guerao et al., 2001
Grapsoidea	*Hemigrapsus*	*longitarsis*	0.46 ± 0.02	-	-	0.87 ± 0.03	Kornienko et al., 2008
Grapsoidea	*Hemigrapsus*	*penicillatus*	0.48 ± 0.01	-	-	0.94 ± 0.03	Kornienko et al., 2008
Grapsoidea	*Hemigrapsus*	*sanguineus*	0.56 ± 0.01	-	-	0.98 ± 0.03	Kornienko et al., 2008
Grapsoidea	*Pachygrapsus*	*transversus*	-	-	-	0.95 ± 0.06	Cuesta and Schubart, 1998
Grapsoidea	*Sesarma*	*aequatoriale*	0.49 ± 0.03	-	-	0.93 ± 0.02	Schubart and Cuesta, 1998
Grapsoidea	*Sesarma*	*catenata*	0.23	0.24	0.16	0.44	Lago, 1987

Table E-1: Cont

Super Family	Genus	Species	CL	RL	DL	RDL	Source
Grapsoidea	*Sesarma*	*curacaoense*	0.81 ± 0.04	-	-	-	Anger et al., 1995
Grapsoidea	*Sesarma*	*curacaoense*	0.74 ± 0.02	-	-	1.23 ± 0.03	Schubart and Cuesta, 1998
Grapsoidea	*Sesarma*	*rhizophorae*	0.55 ± 0.02	-	-	0.94 ± 0.03	Schubart and Cuesta, 1998
Grapsoidea	*Sesarma*	*rubinofforum*	0.51 ± 0.01	-	-	1.14 ± 0.02	Schubart and Cuesta, 1998
Majoidea	*Hyas*	*araneus*	1.02	-	1.85	4.01	Christiansen, 1973
Majoidea	*Hyas*	*coarctatus*	0.88	-	1.43	3.34	Christiansen, 1973
Majoidea	*Pugettia*	*quadridens*	0.67 ± 0.03	-	-	1.34 ± 0.05	Tamura et al., 2017
Ocypodoidea	*Heloecius*	*cordiformis*	0.45 ± 0.02	0.36 ± 0.04	0.56 ± 0.06	1.19 ± 0.06	Fielder and Greenwood, 1985
Ocypodoidea	*Uca*	*tangeri*	0.4 ± 0.02	-	-	0.8 ± 0.02	Rodriguez and Jones, 1993
Pilumnoidea	*Benthopanope*	*indica*	0.71	-	-	0.82	Ko, 1995
Pinnotheroidea	*Dissodactylus*	*crinitichelis*	0.44 ± 0.01	0.34 ± 0.01	0.27 ± 0.01	0.96 ± 0.02	Pohle and Telford, 1981
Pinnotheroidea	*Dissodactylus*	*nitidus*	0.36 ± 0.01	0.24 ± 0.02	0.12 ± 0.01	0.68 ± 0.02	Pohle, 1989
Portunoidea	*Callinectes*	*bocourti*	0.38 ± 0.03	0.26 ± 0.02	0.42 ± 0.03	0.98 ± 0.03	Mantelatto et al., 2014.
Portunoidea	*Callinectes*	*dane*	0.36 ± 0.04	0.24 ± 0.03	0.41 ± 0.03	0.93 ± 0.03	Mantelatto et al., 2014.

Table E-1: Cont.

Super Family	Genus	Species	CL	RL	DL	RDL	Source
Portunoidea	*Callinectes*	*exasperatus*	0.35 ± 0.02	0.23 ± 0.02	0.38 ± 0.04	0.88 ± 0.03	Mantelatto et al., 2014.
Portunoidea	*Callinectes*	*sapidus*	0.39 ± 0.03	0.26 ± 0.03	0.4 ± 0.02	0.96 ± 0.04	Mantelatto et al., 2014.
Xanthoidea	*Xantho*	*poressa*	0.5 ± 0.18	-	-	1.44 ± 0.19	Rodriguez and Martin, 1997

E.1 Literature Cited

Anger K, Schreiber D, Montu M (1995) Abbreviated larval development of *Sesarma curacaoense* (Rathbun, 1897) (Decapoda: Grapsidae) reared in the laboratory. Nauplius 3:127–154.

Christiansen ME (1973) The complete larval development of *Hyas araneus* (Linnaeus) and *Hyas coarctatus* Leach (Decapoda, Brachyura, Majidae) reared in the laboratory. Nor Jouranl Zool 21:63–89.

Cuesta J a, Schubart CD (1998) Morphological and molecular differentiation between three allopatric populations of the littoral crab *Pachygrapsus transversus* (Gibbes, 1850) (Brachyura: Grapsidae). J Nat Hist 32:1499–1508. doi: 10.1080/00222939800771031

Cuesta JA, Schubart CD (1999) First zoeal stages of *Geograpsus lividus* and G*goniopsis pulchra* from Panama confirm consistent larval characters for the subfamily Grapsinae (Crustacea: Brachyura: Grapsidae). Ophelia 51:163–176.

Fielder DR, Greenwood JR (1985) The systematic position of *Heloecius cordiformis* (H. Milne Edwards, 1837) (Decapoda, Ocypodidae) as revealed by larval morphology. Crustaceana 48:244–248.

Guerao G, Schubart CD, Cuesta JA (2001) The first zoeal stages of *Grapsus grapsus* (Linnaeus) and *Geograpsus lividus* (H. Milne Edwards) (Decapoda, Brachyura, Grapsidae) from the Western Atlantic. Nauplius 9:111–121.

Kim CH, Hwang SG (1995) The Complete Larval development of the mitten crab *Eriocheir sinensis* H. Milne Edwards, 1853 (Decapoda, Brachyura, Grapsidae) reared

in the laboratory and a key to the known zoeae of the Varuninae. Crustaceana 68:793–812.

Ko HS (1995) Larval development of *Benthopanope indica* (de Man, 1887) (Decapoda: Brachyura: Pilumnidae) in the Laboratory. J Crustac Biol 15:280–290.

Kornienko ES, Korn OM, Kashenko SD (2008) Comparative morphology of larvae of coastal crabs (Crustacea: Decapoda: Varunidae). Russ J Mar Biol 34:77–93. doi: 10.1134/S1063074008020016

Lago RP (1987) Larval development of *Sesarma catenata* Ortmann (brachyura Grapsidae Sesarminae) reared in the laboratory. South African J Zool 22:200–212.

Mantelatto FL, Reigada ÁLD, Gatti ACR, Cuesta J a. (2014) Morphology of the first zoeal stages of five species of the P*ortunid* genus Callinectes (Decapoda, Brachyura) hatched at the laboratory. An Acad Bras Cienc 86:755–767. doi: 10.1590/0001-3765201420130030

Pohle (1989) Development and morphology of laboratory-rearedlLarvae of *Dissodactylus nitidus* Smith, 1840 (Decapoda: Brachyura), with a discussion of phylogenetic aspects in the Pinnotheridae. J Crustac Biol 9:278–296.

Pohle G, Telford M (1981) Morphology and classification of decapod crustacean larval setae: A scanning electron microscope study of *Dissodactylus crinitichelis* Moreira, 1901 (Brachyura: Pinnotheridae). Bull Mar Sci 31:736–752.

Rebolledo AP, Wehrtmann IS, Cuesta JA (2015) Morphological and morphometric comparison of the first zoeal stage of the mangrove crabs of the genus *Aratus* H. Milne Edwards, 1853 (Decapoda: Sesarmidae). Zootaxa 3949:217–228. doi: 10.11646/zootaxa.3949.2.4

Rodriguez A, Jones DA (1993) Larval development of *Uca tangeri* (Eydoux, 1835) (Decapoda: Ocypodidae) reared in the laboratory. J Crustac Biol 13:309–321.

Rodriguez A, Martin JW (1997) Larval development of the crab *Xantho Poressa* (Decapoda: Xanthidae) reared in the laboratory. J Crustac Biol 17:98–110.

Schubart CD, Cuesta J a (1998) First zoeal stages of four *Sesarma* species from Panama, with identification keys and remarks on the American Sesarminae (Crustacea: Brachyura: Grapsidae). J Plankton Res 20:61–84. doi: 10.1093/plankt/20.1.61

Taishaku H, Konishi K (1995) Zoeas of *Calappa* species with special reference to larval characteristics of the family Calappidae (Crustacea, Brachyura). Zoolog Sci 12:649–654.

Tamura H, Landeira JM, Goshima S (2017) Morphological and morphometric variability in the zoea I larvae of *Pugettia quadridens* (De Haan, 1839): Looking for reliable characters for taxonomic studies on the genus *Pugettia* Dana, 1851 (Majoidea: Epialtidae). Zootaxa 4226:264–272.